Forschungszentrum Karlsruhe
in der Helmholtz-Gemeinschaft

Wissenschaftliche Berichte
FZKA 6929

Instructions for Using the Numeric Code FZKPTR for the Design of Pulse Tube Coolers

A. Hofmann

Institut für Technische Physik

Dezember 2003

Forschungszentrum Karlsruhe

in der Helmholtz-Gemeinschaft

Wissenschaftliche Berichte

FZKA 6929

Instructions for Using the Numeric Code FZKPTR for the Design of Pulse Tube Coolers

Albert Hofmann

Institut für Technische Physik

Forschungszentrum Karlsruhe GmbH, Karlsruhe

2003

Impressum der Print-Ausgabe:

Als Manuskript gedruckt

Forschungszentrum Karlsruhe GmbH
Postfach 3640, 76021 Karlsruhe

Mitglied der Hermann von Helmholtz-Gemeinschaft
Deutscher Forschungszentren (HGF)

ISSN 0947-8620

Abstract

Pulse tube refrigerators (PTR) are most attractive devices for cooling at cryogenic temperatures (T<100 K). Such coolers are based on Stirling process gas cycles, but they are so designed that they have no mechanical components moving at low temperatures. By this fact, they will run very smoothly, and they become very reliable. Temperatures down to about 20 K can be achieved with single stage configurations and even less than 2 K with two-stage systems. Single stage systems are ranging typically from sizes lifting less than 1 W up to several 100 W from 80 K to ambient temperature, and typical two-stage systems will lift about 1 W from 4 K. Operational frequencies may range from about 1 Hz for two-stage systems and more than 50 Hz for single-stage coolers. The design of such coolers is a difficult task. But the present computer code FZKPTR proves to be a valuable tool for doing such work and for getting a profound understanding of the thermodynamic process going on in the whole system. The easy-to-handle code is based on the thermoacoustic theory. It has been written for a two-stage 4 K PTR. But is can also be used for many other configurations. The basic use and the installation to a PC platform is described in the first chapters. The theoretical background and the basic architecture of the code will be explained with respect to use the code for manifold applications. This is being explained on hand of different examples ranging from low frequency (2 Hz) 4 K coolers to high frequency (60 Hz) single stage coolers with inertance tube phase shifters. Moreover it is shown how this code can be used to describe simple configurations of thermoacoustic drivers. This report serves as a manual for solving user defined applications. A wide spectrum of such applications can be treated just by modification of a clearly organized list of input data. The compiled code will run on any PC. Most users will not need a Fortran compiler.

Anleitung zum Rechenprogramm FZKPTR für die Auslegung von Pulsrohrkühlern

Zusammenfassung

Pulsrohrkühler (Pulse Tube Refrigerator, PTR) gewinnen zunehmend an Bedeutung zur Kühlung im kryogenen Temperaturbereich (T<100K). Hierbei handelt es sich um Gaskältemaschinen mit einem Stirling-Prozess, der ohne Komponenten, die bei tiefen Temperaturen bewegt werden müssen, funktioniert. Dadurch werden extrem gute Laufruhe und hohe Zuverlässigkeit erzielt. Mit einstufigen Einrichtungen erreicht man Kühltemperaturen bis herab zu etwa 20 K und mit zweistufigen Anordnungen sogar weniger als 2 K. Die Kühlleistungen von einstufigen Systemen reichen von weniger als 1 W bis zu einigen 100 W bei 80 K, und typische zweistufige Pulsrohrkühlern werden eingesetzt um bei 4K eine Kühlleistung von etwa 1 W aufzubringen. Die Betriebsfrequenzen reichen von etwa 1 Hz bei zweistufigen Kühlern bis zu mehr als 50 Hz bei einstufigen. Trotz des sehr einfach wirkenden Aufbaus ist die Auslegung solcher Geräte noch eine große Herausforderung. Der hier beschriebene Rechencode FZKPTR erweist sich als sehr wertvolles Werkzeug für solche Arbeiten. Er vermittelt auch einen vertieften Einblick in die thermodynamischen Prozesse, die in einem solche solchen System ablaufen. Der leicht zu handhabende Code basiert auf der thermoakustischen Theorie. Er wurde primär für zweistufige 4K-Pulsrohrkühler konzipiert, aber er kann auch für vielfältige andere Konfigurationen genutzt werden. In den ersten Kapiteln werden grundlegende Dinge zur Handhabung und zur Installation des Rechenprogramms auf einen PC erklärt. Danach werden die theoretischen Grundlagen und der Aufbau des Rechenverfahrens beschrieben. Die unterschiedlichen Modifikationen werden anhand von Beispielen, die von niederfrequenten (2 Hz) 4K-Kühlern bis zu hochfrequenten (60 Hz) einstufigen Kühlern mit 'Trägheitsrohr-Phasenschiebern', reichen. Darüber hinaus wird auch gezeigt, wie der Code verwendet werden kann, um einfache thermoakustische Treiber zu behandeln. Dieser Bericht dient als Handbuch zur Lösung von nutzerspezifischen Anwendungen. Die spezifischen Vorgaben werden in einer übersichtlich aufgebauten Liste eingegeben. Die Ergebnisse werden in Tabellen ausgegeben und können leicht in Grafikprogramme übertragen werden. Die hier beschriebenen Anwendungen können mit dem compilierten Code, der auf jedem PC läuft, bearbeitet werden. Somit werden die meisten Nutzer keinen zusätzlichen Fortran-Compiler benötigen.

TABLE OF CONTENTS

1 Introduction 1

2 Organization of the manual 2

3 Working with the code FZKPTR 2
3.1 First steps 2
3.1.1 Running the code 2
3.1.2 Inspection of the results 7

4 Single stage PTR 8

5 Theoretical background 10
5.1 The basic model 10
5.2 Adaptation to real regenerator structures 12
5.2.1 Friction and heat transfer 12
5.2.2 Longitudinal heat conduction 15

6 The numeric procedure 15
6.1 The concept 15
6.1.1 Single stage PTR 18
6.1.2 Two-stage PTR 23
6.2 Numeric accuracy 23

7 Advices for handling the data 23
7.1 Inspection of the alpha-numeric list 23
7.2 Graphical presentation 24
7.2.1 Single-stage PTR 24
7.3 Phasor presentation 26
7.4 One cycle presentation 27

8 Special parameters of the input list 28
8.1 Liquefaction of Helium 28
8.2 Access to supplementary variables 29
8.3 The GM-type PTR 32
8.4 Stirling type PTR (50/60 Hz) coolers 32

9 Expanders 35
9.1 Inertance tube expander 35
9.2 Piston expander 42
9.3 Double-inlet expander 43

10 Valved GM-type two-stage PTR 44

11 Thermally actuated drivers 48

12 Parallel tube regenerators and heat exchangers 50

13 Further options 52

14 Conclusion 52

15 References 53
Appendix A Typical numeric output of a two-stage cooler 56
Appendix B Friction and heat transfer of porous beds 59
Appendix C List of materials to be selected by the parameter 'jmat' 68
Appendix D Comments to the File of Input Data 70

LIST OF FIGURES

Fig. 3-1 Scheme of a two-stage pulse tube cooler (The numbers 1 to 20 will be explained in Fig. 3-2) 3
Fig. 3-2 List of typical input data for a two-stage 4K-PTR 4
Fig. 3-3 Explanation for running the calculation 6
Fig. 4-1 Input file of a single-stage PTR with 116 W at 50 K refrigeration power 9
Fig. 5-1 Geometry of the sound channel. 10
Fig. 6-1 Scheme of iteration loops for solving a two-stage PTR problem 17
Fig. 6-2 Energy flows in single-stage PTR 22
Fig. 7-1 Graphical presentation of the reference data file. Upper field: Temperatures in regenerator and in pulse tube; lower field: Energy flows 25
Fig. 7-2 Phasor diagram of the two-stage PTR (with enlarged part on the right) 27
Fig. 7-3 Files in the folder 'Ptr-work' when the parameter 'One Cycle ' has been activated. 28
Fig. 8-1 Scheme of a PTR used to liquefy helium gas 29
Fig. 8-2 Example for display of supplementary variables V(15) and V(20) together with the temperature profile of a second stage regenerator composed of Pb and HoCu2 30
Fig. 9-1 Scheme of o single stage PTR with inertance tube phase shifter 35
Fig. 9-2 Input data file of a single-stage PTR with inertance tube phase shifter (The lower lines are not shown, but they must be filled with dummies). 36
Fig. 9-3 Phase angles of pressure and volume flow in the components of a single-stage PTR with inertance tube phase shifter 39
Fig. 9-4 Energy flows (work, heat, and enthalpy) in the components of a single-stage PTR with inertance tube phase shifter 39
Fig. 9-5 Pressure amplitude in the components of a single-stage PTR with inertance tube phase shifter 40
Fig. 9-6 Temperature in the components of a single-stage PTR with inertance tube phase shifter 40
Fig. 9-7 Ratio of turbulent (Blasius) to laminar flow friction factors 41
Fig. 9-8 Scheme of a single-stage PTR with piston expander 42
Fig. 9-9 Scheme of a single-stage PTR with double-inlet expander 43
Fig. 10-1 Scheme of a 'valved' two-stage PTR with sensors for pressures (H, L, Reg, Pt1, PT2), temperatures (T) and the mass flow (FM)) 45
Fig. 10-2 Traces of pressures and valve timing 46
Fig. 10-3 Volume flows at the hot end of first stage regenerator and of first and second stage pulse tubes. Measurement on a valved PTR, calculation of theroacoustic model. 47
Fig. 11-1 Scheme of a pulse tube cooler combined with a 'thermal work flow amplifier' 49
Fig. 11-2 Input data for calculation of a PTR combined with a 'thermal work flow amplifier' 49
Fig. 12-1 Scheme of a PTR with parallel tube heat exchangers and inertance tube expander 51
Fig. 12-2 Input data for a single stage PTR with parallel tube heat exchangers and inertance tube phase shifter. 51

1 Introduction

Over the last decade, pulse tube cooling has become one of the most important methods for small and medium scale cryogenic applications. Having no moving parts in the cold head, such kinds of coolers seem to be very simple devices. Their main function is based on the Stirling process, a gas cycle known since about 150 years. Many machines for transforming cyclic work flow of compressed gas into thermal energy and vice versa are being used in technology, and there is a broad basis on theoretical and experimental expertise in academic and industrial institutions. But surprisingly, not many of those data can be used directly for the design of pulse tube coolers. Partially this may be because of companies privacy, and because pulse tube refrigerators were first developed by people in academic institutions who had not access to those design codes. On the other hand, aspects which were not relevant for conventional Stirling and Gifford-McMahon coolers had to be considered for pulse tube designs. A third aspect is that new cooler applications tend to very low refrigeration temperatures, to improved efficiency, and to more compact design. This has demanded for better methods for calculations of such systems. Numeric codes for such calculations have been developed by different groups, but some of such codes are on rudimentary levels so that they can be used only by the author. The code (REGEN3.1) developed at NIST [Sto90],[Gar85],[Gar91] is limited to NASA applications. It has been developed for regenerator design and does not comprise the complete cooler. The Los Alamos code DELTAE has been developed for the design of very general low-amplitude thermoacoustic engines. It is now commercially available [War94]. But we do not know whether it can be used for the design of multi-stage cooler with refrigeration temperatures in the 4 K range The other commercial product SAGE [Ged95] results from a long period of work on conventional coolers, but it can also be applied to many different types of pulse tube coolers. All those numeric codes will be very useful, they are very comprehensive, but each will certainly have specific advantages and disadvantages. Users interested in specific applications will not become rid of elaborate learning processes. But those codes were not available when we started our activities on pulse tube coolers. So we had to develop our own methods. This code FZKPTR might be a valuable completion. It has been developed for the design of two-stage pulse tube cooler with 4 K refrigeration temperature. But the model can also be applied to simpler single stage systems. And also the inversed process as used for thermoacoustic drivers can be handled with the code. The physical base (linear thermacoustics) of our code, FZKPTR, is mainly the same as that of DELTAE developed in the Los Alamos National Lab. In contrast to it, real gas properties and temperature dependant properties of a commercial solid material data base are included in our code.

The executable code of FZKPTR may be obtained from the Marketing Department of Forschungszentrum Karlsruhe (FZK/MAP). More details may be obtained from the author (albert.hofmann@itp.fzk.de). Users should have licences to the embedded codes of material properties [CRYODAT].

2 Organization of the manual

We will first show (Chapter 3) how the most complex version of the code, a two-stage 4K-PTR can be set in operation, how it works, and how it can be modified for the calculation much simpler systems such as a single stage 50K-PTR. In this chapter we also describe the implementation to the PC platform, and we give a brief explanation on the handling of input and output data.

Thereafter (Chapter 5) we give the theoretical background of the code, and we give some details on the numeric procedures (Chapter 6). The design of a new cooler will require many shots and controls of the target. Some tips for handling those data in numeric lists and graphical outputs are given in Chapter 7. Some special features such as liquefaction of gases by using pulse tube coolers will be described in Chapter 8. Here we give also a series of examples which can be treated without modification of the source code. This includes high frequency (50 Hz) coolers and thermoacoustic drivers. Other configurations can be treated by simple modifications of the source code. Examples are given for pulse tube coolers with different types of expanders (Chapter 9). The code is based on small amplitude approximations, and it does not take account of non-linear effect caused by higher harmonics. So it should not be expected to give precise results for 'valved' GM type pulse tube coolers. The discrepancy between predictions and experimental results of such systems are being discussed in Chapter 10 . In Chapter 11 we give an example for applying the code to a thermally actuated driver, and some aspects on the design of parallel tube heat exchangers are given in Chapter 12

3 Working with the code FZKPTR

3.1 First steps

3.1.1 Running the code

When speaking of pulse tube coolers, we mainly mean the cold head. Compressor and expanders are taken into account only in so far that their requirements will result from the demand of the cold head. The two-stage system has to be designed so that refrigeration powers $\dot{Q}_1$ and $\dot{Q}_2$ are lifted from the temperatures T_1 and T_2, respectively. The calculation will give the parameters of gas flow supplied to and extracted from the ambient temperature parts of the cold head with given parameters of size and material. In many cases, those cold head parameters are to be optimised for obtaining a maximum of refrigeration power with a minimum of input power. The total number of real system parameters will be very great. Hence, a computer code making all necessary iterations automatically would become very complicated. The better choice, we believe, is to modify the parameters manually and check the results for reasonableness. This procedure requires a fast response (within a few seconds) and an good overview on input and output data. Fast response means that restrictions in accuracy must be accepted. Under those aspects, our code FZKPTR may be considered

as a good compromise. The system under consideration here is shown schematically in Fig. 3-1. This is a two-stage PTR composed of 20 sections with different sizes and internal structures. A typical list of input data is shown in Fig. 3-2 (**example 1**). This file is a part of the file e030916.txt stored in the folder PTR-Initials, where all examples of this report are listed. The meaning of the parameters in this list will be explained later. Short explanations are given in Appendix D

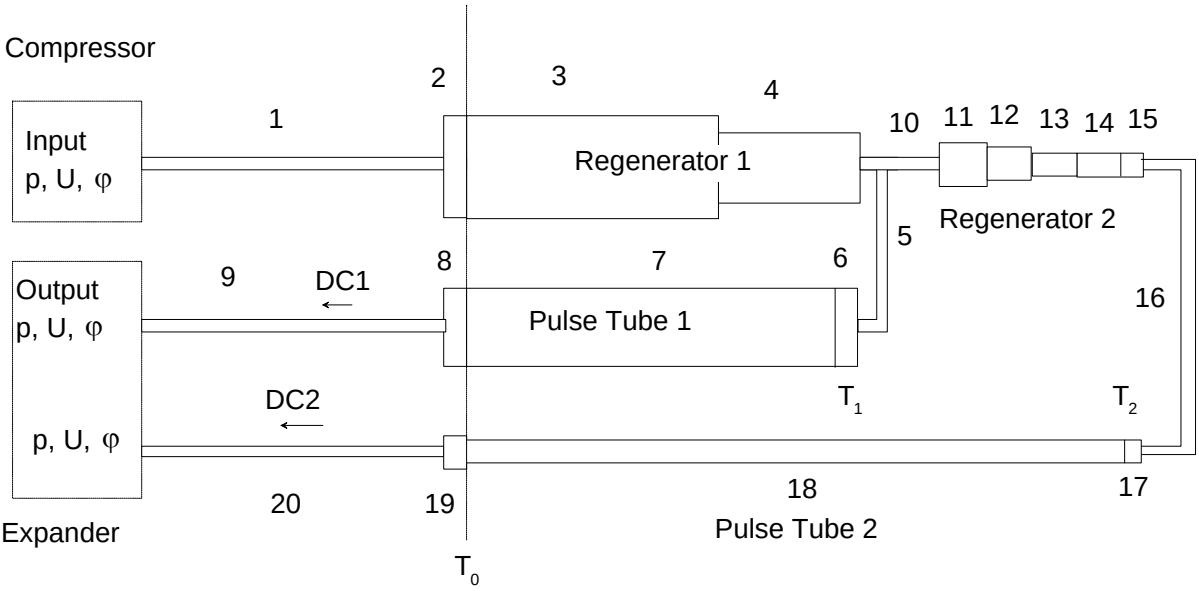

Fig. 3-1 Scheme of a two-stage pulse tube cooler (The numbers 1 to 20 will be explained in Fig. 3-2)

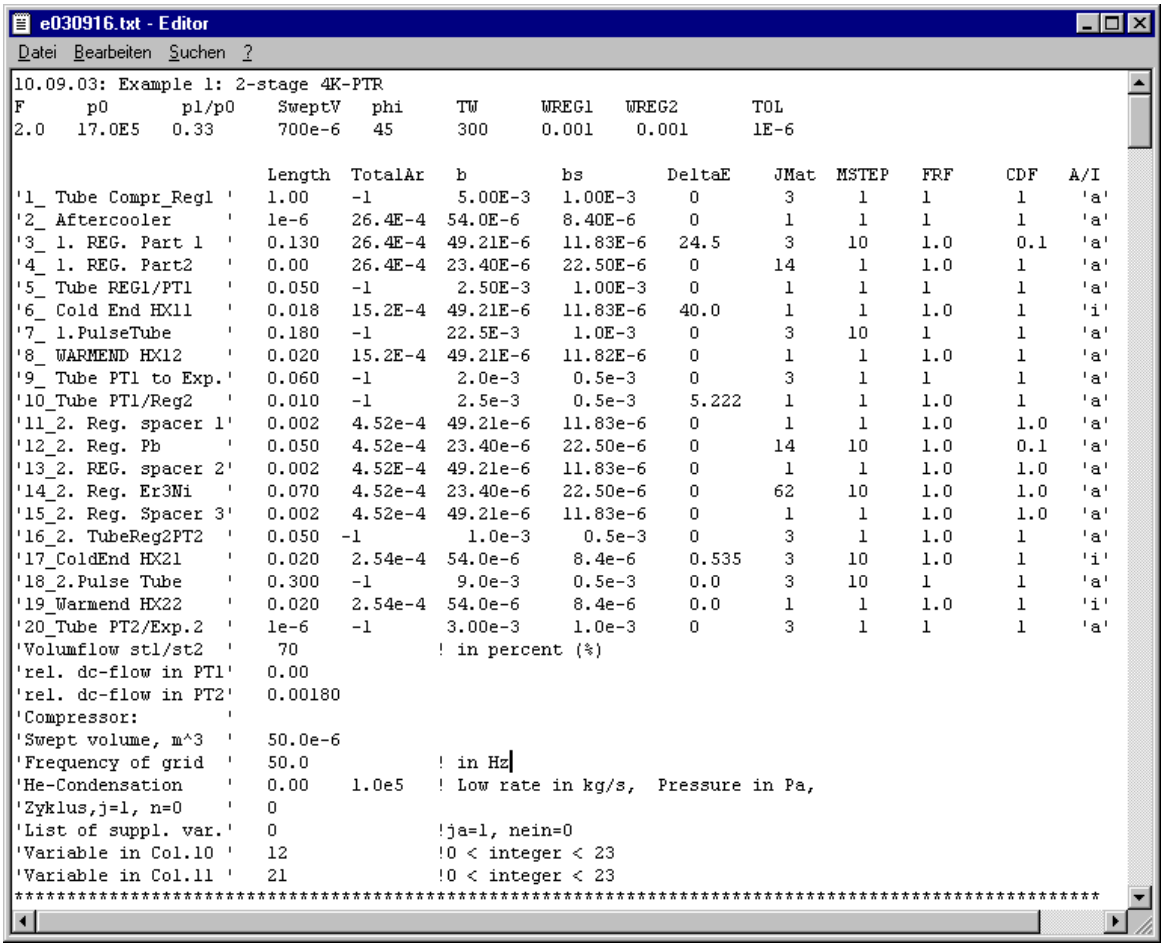

e030916.txt - Editor

Datei Bearbeiten Suchen ?

```
10.09.03: Example 1: 2-stage 4K-PTR
F       p0        p1/p0     SweptV   phi      TW       WREG1    WREG2        TOL
2.0    17.0E5    0.33       700e-6   45       300      0.001     0.001       1E-6

                          Length  TotalAr   b          bs         DeltaE    JMat  MSTEP   FRF      CDF    A/I
'1_ Tube Compr_Reg1 '     1.00    -1         5.00E-3    1.00E-3     0         3      1      1        1      'a'
'2_ Aftercooler     '     1e-6    26.4E-4   54.0E-6    8.40E-6     0         1      1      1        1      'a'
'3_ 1. REG. Part 1  '     0.130   26.4E-4   49.21E-6   11.83E-6    24.5      3     10      1.0      0.1    'a'
'4_ 1. REG. Part2   '     0.00    26.4E-4   23.40E-6   22.50E-6    0        14      1      1.0      1      'a'
'5_ Tube REG1/PT1   '     0.050   -1         2.50E-3    1.00E-3     0         1      1      1        1      'a'
'6_ Cold End HX11   '     0.018   15.2E-4   49.21E-6   11.83E-6    40.0      1      1      1.0      1      'i'
'7_ 1.PulseTube     '     0.180   -1        22.5E-3     1.0E-3      0         3     10      1        1      'a'
'8_ WARMEND HX12    '     0.020   15.2E-4   49.21E-6   11.82E-6    0         1      1      1.0      1      'a'
'9_ Tube PT1 to Exp.'     0.060   -1         2.0e-3     0.5e-3      0         3      1      1        1      'a'
'10_Tube PT1/Reg2   '     0.010   -1         2.5e-3     0.5e-3      5.222     1      1      1.0      1      'a'
'11_2. Reg. spacer 1'     0.002   4.52e-4   49.21e-6   11.83e-6    0         1      1      1.0      1.0    'a'
'12_2. Reg. Pb      '     0.050   4.52e-4   23.40e-6   22.50e-6    0        14     10      1.0      0.1    'a'
'13_2. REG. spacer 2'     0.002   4.52E-4   49.21e-6   11.83e-6    0         1      1      1.0      1.0    'a'
'14_2. Reg. Er3Ni   '     0.070   4.52e-4   23.40e-6   22.50e-6    0        62     10      1.0      1.0    'a'
'15_2. Reg. Spacer 3'     0.002   4.52e-4   49.21e-6   11.83e-6    0         1      1      1.0      1.0    'a'
'16_2. TubeReg2PT2  '     0.050  -1          1.0e-3     0.5e-3      0         3      1      1.0      1      'a'
'17_ColdEnd HX21    '     0.020   2.54e-4   54.0e-6     8.4e-6     0.535     3     10      1.0      1      'i'
'18_2.Pulse Tube    '     0.300   -1         9.0e-3     0.5e-3      0.0       3     10      1        1      'a'
'19_Warmend HX22    '     0.020   2.54e-4   54.0e-6     8.4e-6     0.0       1      1      1.0      1      'i'
'20_Tube PT2/Exp.2  '     1e-6    -1        3.00e-3     1.0e-3      0         3      1      1        1      'a'
'Volumflow stl/st2  '      70              ! in percent (%)
'rel. dc-flow in PT1'     0.00
'rel. dc-flow in PT2'     0.00180
'Compressor:        '
'Swept volume, m^3  '     50.0e-6
'Frequency of grid  '     50.0            ! in Hz
'He-Condensation    '     0.00    1.0e5   ! Low rate in kg/s,  Pressure in Pa,
'Zyklus,j=1, n=0    '     0
'List of suppl. var.'     0               !ja=1, nein=0
'Variable in Col.10 '     12              !0 < integer < 23
'Variable in Col.11 '     21              !0 < integer < 23
*****************************************************************************************************
```

Fig. 3-2 List of typical input data for a two-stage 4K-PTR

The code will calculate time averaged values of oscillating temperature, pressure, volume flow, work flow, and many other quantities at any position of the system. The output is listed in Appendix A. The form of the output file can be controlled by special parameters in the input file. Both input and output file are written as free format text files and can be edited under Windows just by a mouse click. The output is arranged so that a good information can be obtained from inspection of the different components. Alternatively parts of the data file can be plotted. For the following examples, we will use PlotIT [PlotIT], but any other graphic code may be used.

For explaining the meaning of the of the different parameters, we recommend to run the code in parallel to further reading of this report. For this purpose, you should copy all files of the enclosed disc into a folder PTR-INITIAL. All files in this folder should be made write protected. The numbers in some of the file names identify the date of last modification of the FORTRAN source code. All files with dates coded by 'yymmdd' should be renamed when the source code is modified. A brief description of all input parameters is given in Appendix D.

For abbreviations, the strings of the date codes will be omitted in the following text and we will use the expressions:

- Ptr.f for the source code ptryymmdd.f
- Ptr.exe for the compiled file ptryymmdd.exe

- e.txt for the file of input data eyymmdd.txt
- a.txt for the output file ayymmdd.txt

The present version with the code dated '030916' can be used for manifold application. It has been designed so that systems composed of up to 20 sections can be treated without modification of the source code. The respective 'run file', ptr.exe, will run on any PC. A fortran compiler is not required. More complex systems will need modifications of the source code, but this should be done by the author. The 'normal' user will only need a link to the ptr.exe file and a first sample of the input file. We recommend to copy the files ptr030916.exe and e030916.txt into a new folder PTR-work. The further handling is explained by Fig. 3-3. The calculation is started by a mouse click to the ptr.exe. This will read the data of the input file e.txt and produce the output a.txt. The progress of the calculation is displayed in auxiliary window which disappears when no errors have occurred. Otherwise the calculation will be interrupted, and the last lines in the auxiliary window will give information were the calculation has stopped. This will help to find improved parameters for the next run..

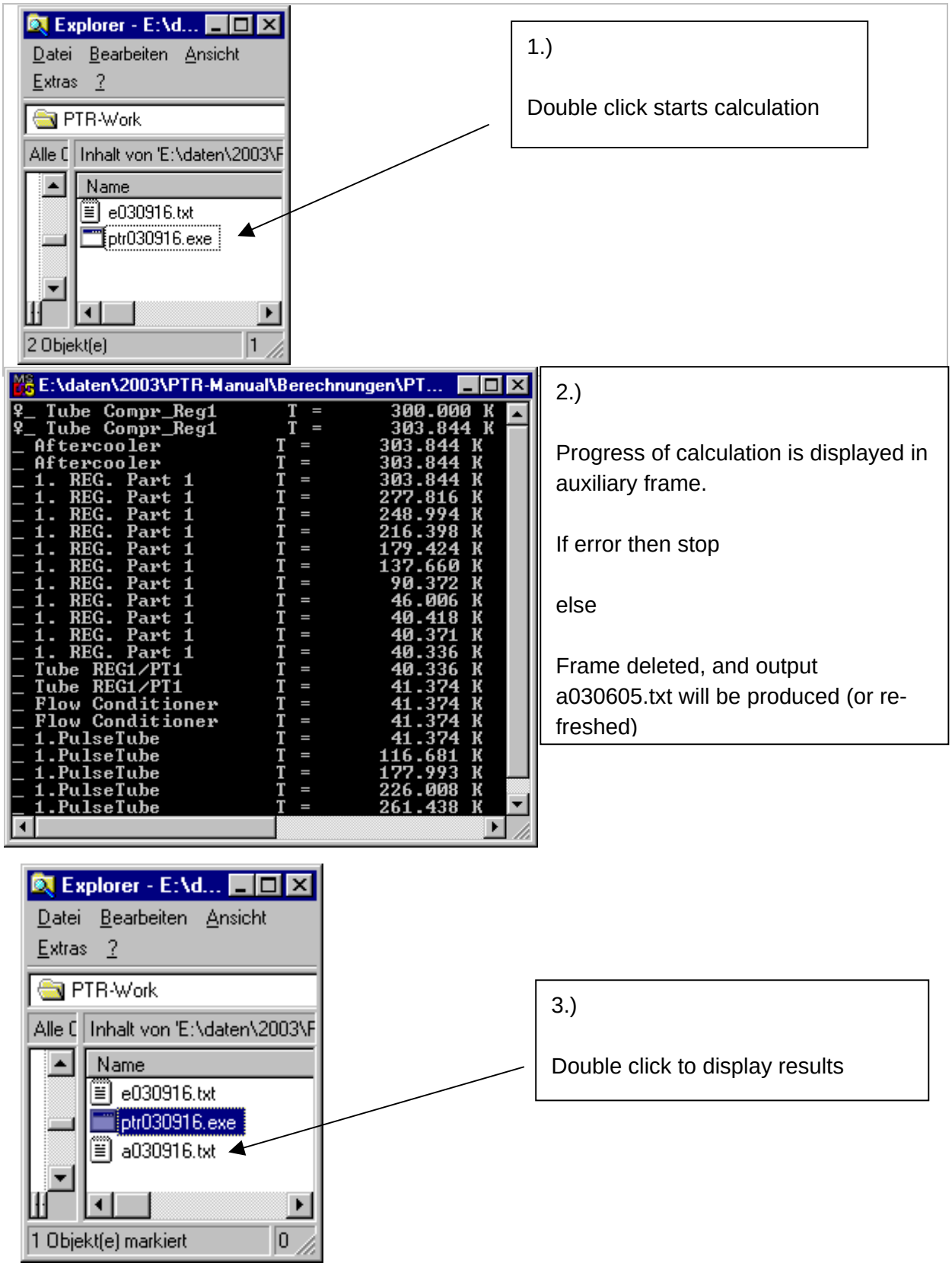

Fig. 3-3 Explanation for running the calculation

3.1.2 Inspection of the results

Now you may continue by considering the output file a.txt (Appendix A. The list is organized in 3 main groups:

(A) A copy of the input data

(B) Table of results for the individual components of the PTR

(C) Additional information

Some results are highlighted. The blue fields indicate that this configuration is expected to yield 40 W at 42 K together with 0.54 W at 4.2 K. Moreover the red marks indicate the work flow Wx (pV-power) at different positions. It is shown that 887 W are being supplied by the compressor, 85 W and 3.6 W must be rejected at the hot end of the first and second stage pulse tubes, respectively.

Much additional information is given in the arrays of the group (B) with the columns

(1)	Time averaged temperature	T
(2)	Amplitude of pressure	p
(3)	Phase angle of pressure	phi(p)
(4)	Amplitude of volume flow	U
(5)	Phase angle of volume flow	phi(U)
(6)	Work flow	Wx
(7)	Longitudinal heat flow	Qx
(8)	Total energy flow	Ex
(9)	Any variable from the list 'param.txt	Val(i)
(10)	Any variable from the list 'param.txt'	Val(j)

Graphical outputs can be easily obtained when the list is imported into a standard graphics programme. For getting smooth curves it will become necessary to increase the number of lines in the arrays of some components. This is done with the parameter 'mstep' of the input file. The group (C) gives some information on mass flows requirements. Much more details are hidden in this list. Many of them will be needed for getting a good cooler design. But much skill and experience will be necessary for the design of a 4K-PTR. Hence, one should first become familiar with a simpler single stage PTR.

4 Single stage PTR

No modification of the source code is required for treating the single-stage PTR. All can be done just by change of the input list. This will be demonstrated by the following example where the performance of the same PTR, but with disconnected second stage will be studied. For this procedure we open the input file e.txt and we copy the previous data block to the top of the existing file. The code works so that only the uppermost 32 lines will be read. All lower lines may be considered as comments. Also the first line is treated as comment. Here we can write the comment **'Example 2**: Single-stage 50K-PTR'. Now those uppermost input lines can be modified. (If the two-stage configuration is to be used ones more, it can just be copied back to the top of the file).

The second stage components can be eliminated by setting their length to zero (parameter Length).

ATTENTION 1: As seen in Fig. 3-1, the gas flow is bifurcating at section #5. When the length of that section would be set to zero, the parameters which describe the fractions of gas flow going into the second stage would get lost. Hence the length of section #5 should never be set to zero, but it may be set to a very small value, typically 1.0e-6 m.

ATTENTION 2: It is not allowed to delete the complete lines, because the code will always read the same number of variables required for the complete system with 20 sections. Input parameters in lines with zero length are treated as dummies. The may be set to zero.

All variables may be entered in free format separated by at least one blank. Additional blanks may be typed to improve the readability. The modified input list is shown in Fig. 4-1. For further simplification, only the main components, namely the parts regenerator (section #3), cold end heat exchanger (section #6), pulse tube (section #7) and hot end heat exchanger (section #8) are being considered. Two more parameters are to be adjusted: a) The parameter 'Volumflow st1/st2 ' describing the fraction of gas flow going into the first stage pulse tube. It must be set to 100 % for a single-stage PTR, and b) the parameter 'rel. dc-flow in PT2' should be set to zero.

Running this configuration will yield a first stage temperature of about 50 K, and a very high temperature will result at the hot end of the pulse tube. The cold end temperature is decreased by increasing the parameter 'DeltaEx' of the regenerator. This means that the losses in the regenerator will increase, and the hot end temperature at the tube will decrease when more power given by the parameter 'DeltaEx' of the tube is increased. The meaning of those parameter will be explained in chapters 5 and Appendix D. After a few runs of trial and error with modifications of those two parameters (highlighted in Fig. 4-1), one will find a configuration which can lift a power of 106 W from 50 K to 300 K.

Those examples should give a rough feeling for using this code. Real design work will require much more of the information hidden in the files of input and output data. Some knowledge on the theoretical background of the model will be helpful.

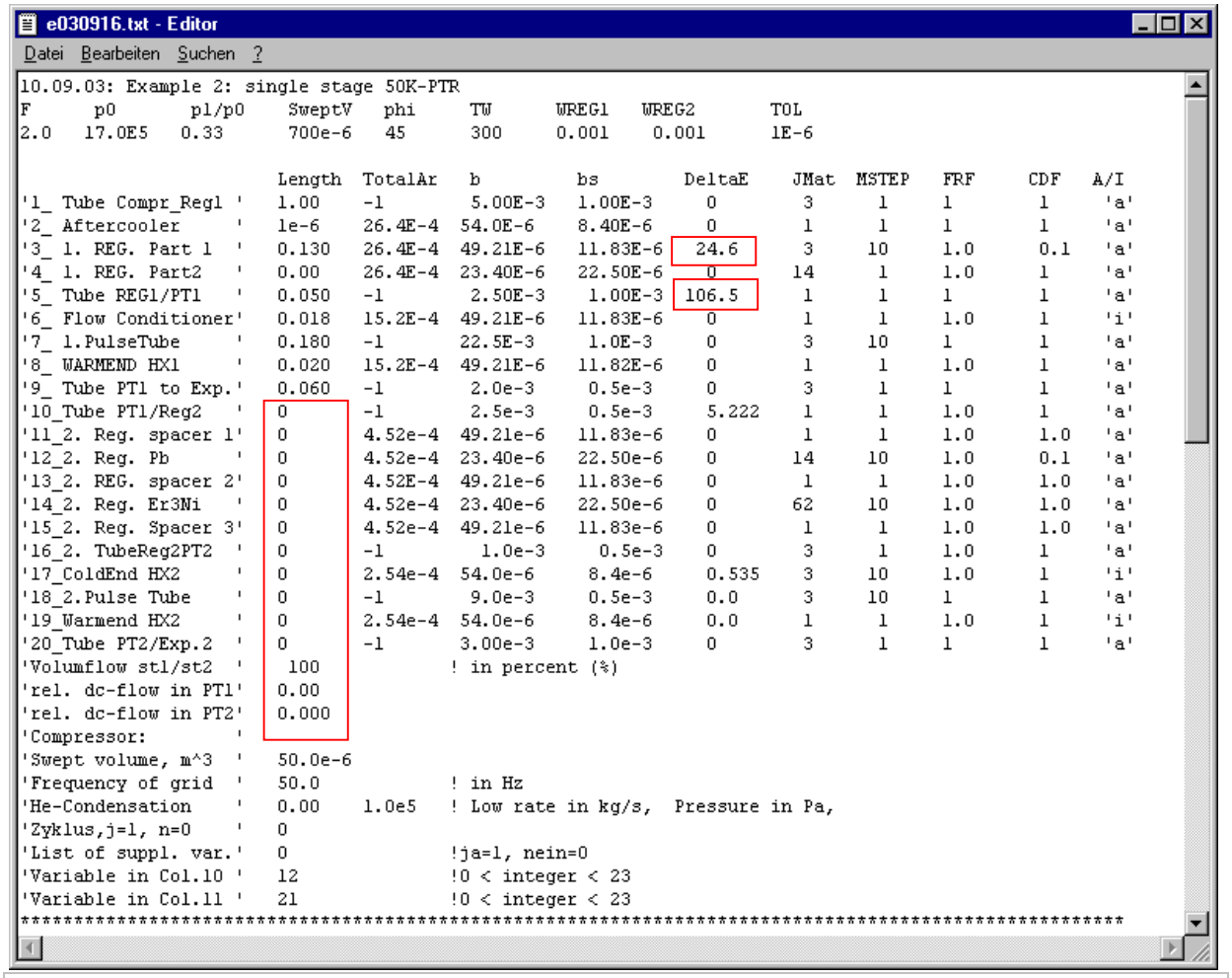

e030916.txt - Editor

Datei Bearbeiten Suchen ?

```
10.09.03: Example 2: single stage 50K-PTR
F       p0        p1/p0     SweptV    phi       TW       WREG1    WREG2        TOL
2.0    17.0E5    0.33       700e-6    45        300      0.001     0.001       1E-6

                          Length   TotalAr    b          bs         DeltaE     JMat   MSTEP    FRF      CDF    A/I
'1_ Tube Compr_Reg1 '     1.00     -1         5.00E-3    1.00E-3      0         3       1       1        1      'a'
'2_ Aftercooler     '     1e-6     26.4E-4    54.0E-6    8.40E-6      0         1       1       1        1      'a'
'3_ 1. REG. Part 1  '     0.130    26.4E-4    49.21E-6   11.83E-6    24.6       3      10       1.0      0.1    'a'
'4_ 1. REG. Part2   '     0.00     26.4E-4    23.40E-6   22.50E-6     0        14       1       1.0      1      'a'
'5_ Tube REG1/PT1   '     0.050    -1          2.50E-3    1.00E-3   106.5       1       1       1        1      'a'
'6_ Flow Conditioner'     0.018    15.2E-4    49.21E-6   11.83E-6     0         1       1       1.0      1      'i'
'7_ 1.PulseTube     '     0.180    -1         22.5E-3     1.0E-3      0         3      10       1        1      'a'
'8_ WARMEND HX1     '     0.020    15.2E-4    49.21E-6   11.82E-6     0         1       1       1.0      1      'a'
'9_ Tube PT1 to Exp.'     0.060    -1          2.0e-3     0.5e-3      0         3       1       1        1      'a'
'10_Tube PT1/Reg2   '     0        -1          2.5e-3     0.5e-3      5.222     1       1       1.0      1      'a'
'11_2. Reg. spacer 1'     0        4.52e-4    49.21e-6   11.83e-6     0         1       1       1.0      1.0    'a'
'12_2. Reg. Pb      '     0        4.52e-4    23.40e-6   22.50e-6     0        14      10       1.0      0.1    'a'
'13_2. REG. spacer 2'     0        4.52E-4    49.21e-6   11.83e-6     0         1       1       1.0      1.0    'a'
'14_2. Reg. Er3Ni   '     0        4.52e-4    23.40e-6   22.50e-6     0        62      10       1.0      1.0    'a'
'15_2. Reg. Spacer 3'     0        4.52e-4    49.21e-6   11.83e-6     0         1       1       1.0      1.0    'a'
'16_2. TubeReg2PT2  '     0        -1           1.0e-3     0.5e-3      0         3       1       1.0      1      'a'
'17_ColdEnd HX2     '     0        2.54e-4    54.0e-6     8.4e-6      0.535     3      10       1.0      1      'i'
'18_2.Pulse Tube    '     0        -1          9.0e-3     0.5e-3      0.0       3      10       1        1      'a'
'19_Warmend HX2     '     0        2.54e-4    54.0e-6     8.4e-6      0.0       1       1       1.0      1      'i'
'20_Tube PT2/Exp.2  '     0        -1         3.00e-3     1.0e-3      0         3       1       1        1      'a'
'Volumflow stl/st2  '      100             ! in percent (%)
'rel. dc-flow in PT1'     0.00
'rel. dc-flow in PT2'     0.000
'Compressor:        '
'Swept volume, m^3  '     50.0e-6
'Frequency of grid  '     50.0             ! in Hz
'He-Condensation    '     0.00     1.0e5   ! Low rate in kg/s,  Pressure in Pa,
'Zyklus,j=1, n=0    '     0
'List of suppl. var.'     0                !ja=1, nein=0
'Variable in Col.10 '     12               !0 < integer < 23
'Variable in Col.11 '     21               !0 < integer < 23
*****************************************************************************************************************
```

Fig. 4-1 Input file of a single-stage PTR with 116 W at 50 K refrigeration power

5 Theoretical background

5.1 The basic model

Those calculations are based on the thermoacoustic theory [Rott75], [Rott80], [Swift97] describing the conversion of mechanical and thermal energy of an oscillatory gas flow in ducts with solid walls. A very useful work on this problem has also been done by Xiao [Xiao95]. Our calculations are strongly based on that work, and we also use the same terminology. So it is recommended to have that paper [Xiao95] in hand when reading the following chapter. Then it will not be necessary to give detailed explanations to all equations and terms written here.

The basic element is a circular channel with radius *b* and wall thickness b_s as shown in Fig. 5-1.

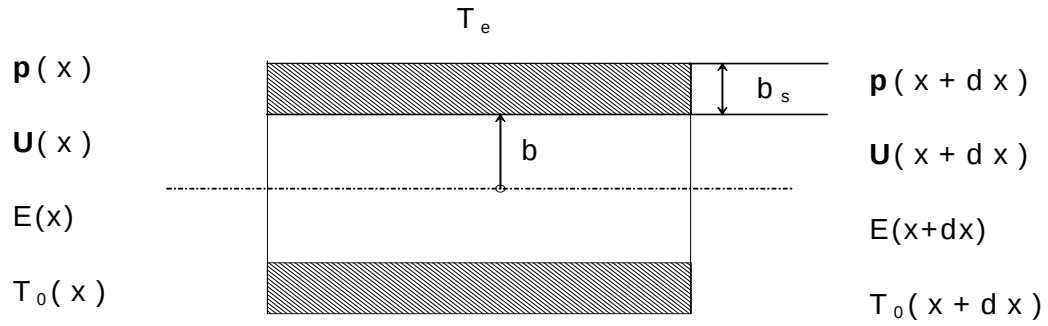

Fig. 5-1 Geometry of the sound channel.

The gas flow at the position x is described by the mean temperature T_0 , the pressure

$$\tilde{p} = p_0 + \hat{p}e^{j\omega t} \tag{5.1}$$

and the volume flow

$$\tilde{U} = \hat{U}e^{j(\omega t+\varphi)} \tag{5.2}$$

The fact that the volume flow U has no higher harmonics implies that the pressure amplitude must be small

$$\hat{p} / p_0 << 1 \tag{5.3}$$

This is taken into account when the following expressions are derived from Navier-Stokes equations.

For laminar flow in circular channels, the shear force and the transversal heat flow can be described by analytic expressions. Hereby the two-dimensional problem is reduced to a linear one with

$$\frac{d\tilde{p}}{dx} = -Z_F\tilde{U} \tag{5.4}$$

and

$$\frac{d\tilde{U}}{dx} = -\frac{1}{Z_C}\tilde{p} + \beta_0 \frac{dT_0}{dx} \tag{5.5}$$

So far we have two complex equations (4 real equations) for 5 variables, the complex quantities $\tilde{p}$, $\tilde{U}$, and the real variable $T_{0.}$ Further correlations will be required. They result from time-averaged effects of acoustic energy flows. When just the first harmonic is considered, the acoustic work and heat flows become

$$W_x = \frac{1}{2} Re[\tilde{U}\tilde{p}^*] \quad ^{*)} \tag{5.6}$$

and

$$Q_x = -\frac{1}{2} T_0 \beta_0 \, Re[\tilde{U}\tilde{p}^* f_{qx}] - A_f K_e \frac{dT_0}{dx} \tag{5.7}$$

respectively, and the longitudinal total energy flow is

$$E_x = W_x + Q_x \tag{5.8}$$

The transverse energy flow is equal to the transverse heat flow (rigid wall). Hence E_x will be constant in all thermally isolated ('adiabatic') sections, and it will only change when heat is absorbed from the environment. This will cause

$$\left(\frac{dE_x}{dx}\right)_1 = -h_w U_w \left(T_0 - T_c\right) \tag{5.9}$$

Additionally, the energy of the gas in the fixed cell with length dx will change when there is a time-averaged non-zero mass flow, $\dot{m}_{DC}$.

This term is

$$\left(\frac{dE_x}{dx}\right)_2 = -\dot{m}_{DC} c_{p0} \frac{dT_0}{dx} \tag{5.10}$$

So we get

$$\frac{dT_0}{dx} = \frac{\frac{1}{2} Re[\tilde{U}\tilde{p}^* (1 - T_0 \beta_0 f_{qx})]}{A_f K_e} \tag{5.11}$$

and

---

*) For harmonic functions of p and U=dV/dt, the following expressions are identical

$$W_x = f \oint p dV = f \int_0^{1/f} (p_0 + \tilde{p})\tilde{U} dt = \frac{1}{2} Re[\tilde{U}\tilde{p}^*] = \frac{1}{2} \hat{p}\hat{U} \cos(\varphi)$$

where the symbols 'tilde' , 'hat' and 'asterisk' mark time dependent part, amplitude, and conjugate of the variables, respectively

$$\frac{dE_x}{dx} = h_w U_w \left(T_e - T_0\right) - \left(\dot{m}_{DC} C_{p0}\right) \frac{dT_0}{dx} \tag{5.12}$$

So the system is described by the 6 variables *Re(p), Im(p), Re(U), Im(U), T_0, and E_x. They are evaluated from the differential equations* (5.4)*,* (5.5)*,* (5.11)*, and* (5.12)), The constants Z_F, Z_C, f_{WT},f_{qx}, and K_e are functions of the channel geometry and of fluid and solid material parameters. Here we use the analytic expressions derived for simple circular ducts [Xiao95]. The basic assumptions of this model are:

1. The problem is two dimensional (constant cross sectional areas)
2. The sound field is at periodically working condition, and the mean fluid velocity is zero
3. The acoustic amplitudes are low enough to avoid turbulence [Merk75] so that

$$Re_\omega = \rho_0 u \delta_\mu / \mu_0 << 500 \tag{5.13}$$

4. The displacement of gas particles is much smaller than the acoustic wave length *($u/(2\pi a_0)<<1$)*
5. The transverse heat flow from the solid wall to the environment is proportional to the temperature difference

Many components of the PTR will be operated within an evacuated containment thus that there will be no overall transversal heat flow. This means that the coefficient of heat transfer, h_w, is zero at periphery with perimeter U_w. The other extreme for ideal heat transfer to the surrounding with temperature T_e. This means that $dT_0/dx=0$ in such components. Only these two extremes will be considered for the evaluation of cooler. The different section 'adiabatic' decribed by $(dE_x/dx)_1=0$ or they are 'isotherm' described by $dT_0/dx=0$. The parameter 'A/I' in the input list is used to adjust any of the 20 sections either to 'a' (adiabatic) or to 'i' (isotherm).

5.2 Adaptation to real regenerator structures

5.2.1 Friction and heat transfer

So far, the model is valid only for long circular ducts such as the pulse tubes and the connecting tubes, but end effects are neglected, and it must be checked if the conditions for non-turbulent flow are fulfilled. The theory can also be applied to regenerators made from bundles of parallel capillaries. But most real regenerators are made from packages of wire mesh or microspheres. In that case we describe such structures by equivalent packages of short circular channels which have such dimensions that a) the porosity, b) the wetted surface, and c) the flow resistance become the same for the real and the equivalent structures

Let us assume that the internal structure is given by parameters such as porosity ε and particle size with diameter D_s of spheres or the with diameter D_w of wires, and also the total volume of the active regenerator structure be given by the inner diameter of the shell, D_R, and the length L. The porosity

$$\varepsilon = 1 - \frac{\rho_{poros}}{\rho_{solid}} \tag{5.14}$$

is easily obtained from the mass and the volume of the porous stack and from the known density of the bulk solid. The volume of solid material is

$$V_{solid} = V_{Reg}(1-\varepsilon) = L_w \frac{\pi}{4} D_w^2 \tag{5.15}$$

for the mesh and

$$V_{solid} - N_{spheres} \frac{\pi}{6} D_s^3 \tag{5.16}$$

for the spheres package. Here L_W is the total length of wire and N_{speres} is the total number of spheres for filling the regenerator volume. Analogously the wetted surface is

$$A_{wet} = \pi D_w L_w \tag{5.17}$$

for wires, and

$$A_{wet} = N_{spheres} \pi D_s^2 \tag{5.18}$$

for spheres. The ratio of both becomes

$$\frac{V_{solid}}{A_{wet}} = \begin{cases} D_w / 4 & for\ mesh \\ & and \\ D_s / 6 & for\ spheres \end{cases} \tag{5.19}$$

For the channels with the geometry shown in Fig. 5-1 we get

$$\varepsilon = \frac{b^2}{(b + b_s)^2} \tag{5.20}$$

and

$$\frac{V_{solid}}{A_{wet}} = \frac{(b + b_s)^2 - b^2}{2b} \tag{5.21}$$

When we assume that the porosity ε and the ratios V_{solid}/A_{wet} of real structures and of the equivalent parallel tube bundle are the same, rearrangement of (5.19), (5.20), and (5.21) yields

$$b_s = b\left(\frac{1}{\sqrt{\varepsilon}} - 1\right) \tag{5.22}$$

and

$$b = \frac{\varepsilon}{1-\varepsilon} \begin{cases} D_w / 2 & for\ mesh \\ & and \\ D_s / 3 & for\ spheres \end{cases} \tag{5.23}$$

The so calculated channel diameter *2b* is equal to the hydraulic diameter defined as 4 times flow area divided by wetted perimeter. It is in good agreement with data derived from other models [Man55].

In the basic model, pressure drop and heat transfer from the fluid to the solid are calculated for laminar flow in very long ducts. Inlet and outlet effects are being neglected. Hence pressure drop and heat transfer will be underestimated. To be more realistic, those channels have to be subdivided in many very short sections so that the end effects will dominate. Such configurations become similar to porous beds. Respective correlations for stacked mesh and for sphere-bed-matrices are given in literature [Kays84], [VDI77]**.** The evaluation of those data is given in Appendix B. The friction factor and the heat transfer coefficient (expressed by the Nusselt number) become power functions of the Reynolds number which proves to be in the range 30<Re<300 for regenerators operated in the range 4 K < T < 300 K (Fig. 3 of A). We have not succeeded to implement those correlations precisely into the theoretical model. But we believe that a reasonable correction is obtained by modifying the viscosity and the thermal conductivity of the fluid so that those terms yield the expected enhancement of friction and heat transfer. Hence, we simply replace the viscosity η_0 and the thermal conductivity k_0 by the apparent values

$$\eta_{apparent} = \eta_0 \left(2.62 + 0.033\, Re\right) \cdot FRF \tag{5.25}$$

and

$$k_{apparent} = k_0\ 0.0845\, Re^{0.65} \cdot FRF \tag{5.26}$$

With

$$Re = \frac{\rho_0\, \hat{U}\, 2\, b}{A_F\, \eta_0} \tag{5.27}$$

Those pressure drop and heat transfer correlations have been obtained for steady flow measurements, but it has been shown recently [Nam02b] , that the pressure drop does not change up to frequencies of 10 Hz. There is an enhancement at higher frequencies, but precise correlations are not known. We have therefore introduced an empirical factor 'FRF' (flow resistance factor), which will be read from the file of input data for each individual component. It is known that the heat transfer will be improved when the pressure drop increases. So it might be legal to multiply both, the viscosity (5.25) and the conductivity (5.26) with the same factor. It may also be used to take account of the higher flow resistance of sharp edged powders [VDI77].

ATTENTION: The correlation for apparent viscosity Eq.(5.25) and apparent thermal conductivity Eq.(5.26) are only used for porous materials with hydraulic diameters less than 0.1 mm. Laminar flow correlations without corrections of inlet effects are used for cylindrical tubes. But empiric adjustment with the flow resistance factor, FRF, can also be done in this case.
A similar effect would be obtained by describing the enhanced friction and heat transfer by the introduction of a factor of tortuousness to describe an increased length of the path of a fluid element when it passes the porous matrix. This approach is done in other numeric codes [Ged95].

REMARK

It was found that in some cases the Prandtl number defined as

$$\mathrm{Pr} = \frac{\eta c_p}{k} \tag{5.28}$$

becomes unreasonable values when it is calculated with $k_{apparent}$ and $\eta_{apparent}$. To overcome this problem, we have therefore modified the modified the thermal conductivity so that it is calculated from $\eta_{apparent}$ and the normal Prandtl number Pr_0 which is in the range of 0.7 for He gas. This modification with

$$k_{apparent} = \frac{\eta_{apparent} c_{p0}}{Pr_0} \tag{5.29}$$

is being used in the codes later than ptr030506. The so calculated results do not differ much from previous ones. But we have not yet checked this empiric correlation for correctness.

5.2.2 Longitudinal heat conduction

In the basic model, the longitudinal heat flow is calculated as if the regenerator would be composed of a solid rod with the cross section A_s resulting from the total porosity and the total cross section. But it is known that the effective thermal conductivity of stacked screens and of microsphere matrices is much smaller [Lew98]. This conductivity degradation factor CDF is not well known in most cases. For taking account of this fact, the thermal conductivity of the solid material is decreased only in the expression (5.30) where the term K_e describes the effective longitudinal conductivity

$$K_e = K_0 \frac{1}{\delta_K^2} \left| \frac{\tilde{U}}{A_f \omega} \right|^2 g_{qx} + K_0 + \frac{A_s}{A_f} K_{so} \cdot \mathrm{CDF} \tag{5.31}$$

Here the term K_{s0}, the thermal conductivity of the solid, has been replaced by K_{s0} *CDF. But in other equations describing the transversal heat flow, i.e. the thermal diffusion into the solid, characterised by the thermal penetration depth

$$\delta_s = \left(\frac{2K_{s0}}{\rho_{s0} C_{s0} \omega} \right)^{\frac{1}{2}} \tag{5.32}$$

the conductivity is not changed.

6 The numeric procedure

6.1 The concept

All components (tubes, regenerators and heat exchangers) are now described by the same type of elements as shown in Fig. 5-1**.** They are characterised by length (Length), total cross sectional area (TotalAr), hydraulic diameter (2b), wall thickness (b_s), and the material of the

wall (jMat). Regenerators and heat exchangers are composed of many of them in parallel. The thermoacoustic heat transportation in such channels is described by the 6 variables.

$$y(x) = \begin{pmatrix} Re(\tilde{p}) \\ Im(\tilde{p}) \\ Re(\tilde{U}) \\ Im(\tilde{U}) \\ E_x \\ T_0 \end{pmatrix} \tag{6.1}$$

They are coupled by the ordinary differential equations

$$F(y, y', x) = \begin{pmatrix} Re(Eq\ 2.4) \\ Im(Eq\ 2.4) \\ Re(Eq\ 2.5) \\ Im(Eq\ 2.5) \\ (Eq\ 2.11) \\ (Eq\ 2.12) \end{pmatrix} = 0 \tag{6.2}$$

The following terminology will be used:

a) y_i describes the complete array of y in the component with the number i.

b) $y_i[k]$ is the k-th variable of y in the component i.

c) $y_i(x)$ is the total array of x in the component I at the position x.

The problem is solved with the IMSL subroutine DIVPAG. Some of the coefficients in the differential equation (6.2) are complex and there must also be handled Bessel functions with complex argument. Respective subroutines are also taken from IMSL. The thermodynamic properties of the fluid are calculated from the real gas code HEPROP [Han75] , an early version GASPAK , and properties of wall materials (specific heat and thermal conductivity) are calculated by using the code CRYOPROP [Eck97]. (Properties for temperatures above 300 K are approximated by the value at 300 K, the upper limit of this code). New regenerator materials such as rare earth compounds, GOS and others are added separately. Their specific heat is evaluated by interpolation of tables cp(T) obtained from various sources. The evaluation is done with the IMSL subroutine DCSIEZ. All materials are selected by the parameter '*jMat*' in the input data file e.txt. Presently there is access to the 67 materials listed in appendix C.

The calculation is done as follows: For given initial values y_0, the differential equation is solved for the first section to get y(x) at any position of 0< x< Length. The final value is $y_1=y_1(Length_1)$. All component of y_1, except $y_1[5]=E_x$, will be used as initial value for the next component. The parameter E_x describes the total energy flow in the component, the sum of heat and work flow). E_x is a function of intrinsic losses (production of entropy) and of externally supplied heat. The intrinsic loss is not known a priory, but it is known that it depends on

the temperature. Vice versa, the initial value $E_{x,0} = y_0[5]$ can be modified so that any desired end temperature is obtained. This process is continued for each component until temperatures given at certain edge points are reached. When treating the very complex system as considered here, many additional parameters must be modified stepwise for getting a reasonable solution for the whole system. Our experience is that automatic loops will not be very helpful in many cases. We prefer do make most of those iterations 'manually' by trial and error, and we recommend the procedure as displayed in Fig. 6-1. We should begin with first stage components marked by the yellow fields.

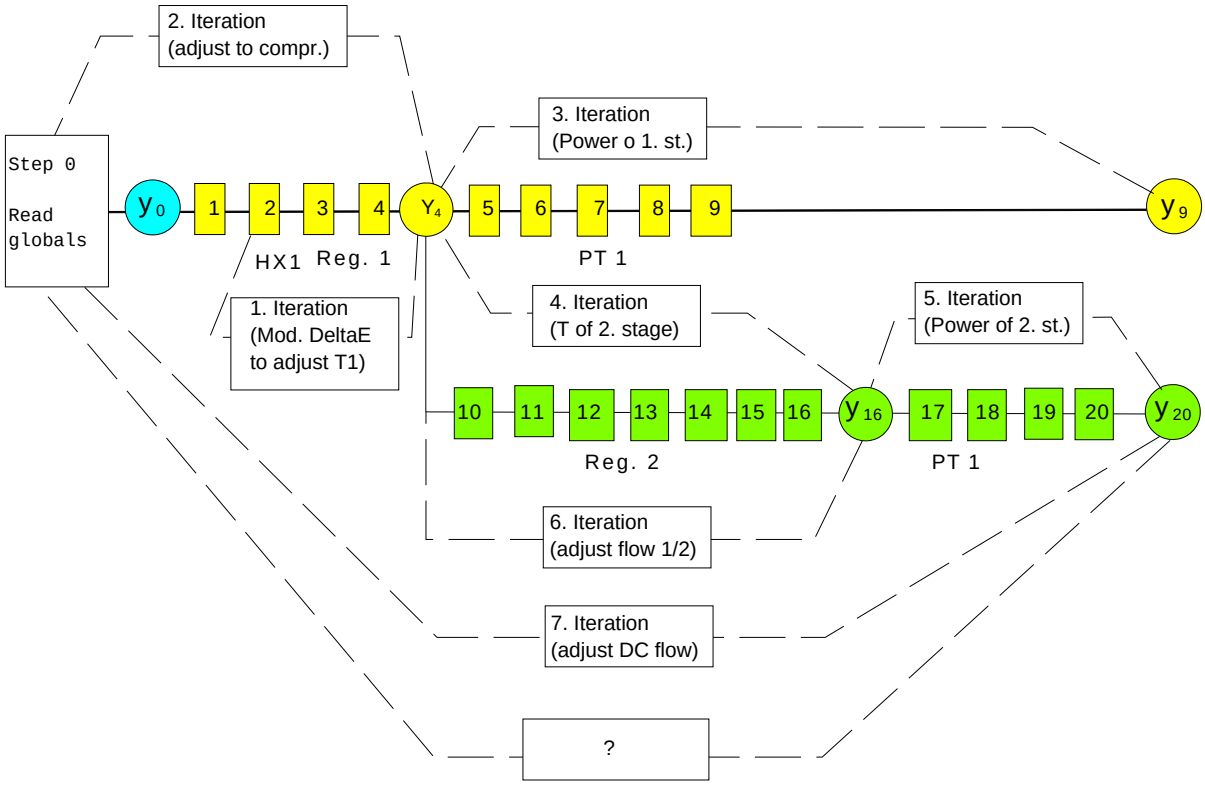

Fig. 6-1 Scheme of iteration loops for solving a two-stage PTR problem

6.1.1 Single stage PTR

Step 1: All parameters of the input list are read, and the initial conditions

$$y_{=} = \begin{pmatrix} \hat{p} \\ 0 \\ \hat{U}\cos(\varphi) \\ \hat{U}\sin(\varphi) \\ T_w \\ E_{x,0} = \frac{1}{2}\hat{p}\hat{U}\cos(\varphi) \end{pmatrix} \tag{6.3}$$

are set. Also the DC flow parameters 'mdc1' and 'mdc2' should be set to zero. It is assumed arbitrarily that the initial pressure phasor is real, and there are good arguments [Hof99] that it should lag behind the volume flow U by of phase angle of about 45 °. All components of the system are described by the same set of differential equations. But the coefficients differ. They wille be calculated from the individual data given in the input file e.txt. The results at the end of one segment is continuously transferred to the inlet of the next segment. Only in heat exchangers, the energy flow Ex will be changed by external intervention. How it changes will depend on the performance of such components, namely the effective heat transfer coefficient h_e as defined by Eq.(5.9). No specific correlations for this coefficient are implemented in our code. Instead of that, h_e is set to zero, and E_x is modified by DeltaEx which describes the total transversal heat flow of the heat exchanger segment. The value of DeltaEx is not known a priori. It must be evaluated iteratively so that the desired performance of the cooler (i.e. the desired cold end temperature) is obtained. Implicitly the value of Ex describes the slope of the temperature curve $T_0(x)$ at the inlet of a segment. The target of T_0 at the outlet will be hit when the next shot is done with another initial slope. When the target is failed too much so that the temperature runs out of the valid range given by properties codes of the fluid or the solid, the calculation will be stooped by an error message, and the auxiliary window will gibe information in which segment the error has occurred. This will help to make the next shot with a more appropriate value of DeltaEx. The total energy flow is a basic parameter for working with the code. A more detailed comment is given in Chapter 6.1.1.1.

When working with a totally new data set, one should begin with the design of the first stage regenerator such that the desired temperature can be achieved for a given work flow supplied by the compressor. For avoiding errors occurring at component with numbers greater than 4, it is a good choice to set the length to zero (or to very small values) for all those components. Now continue with:

Iteration 1. DeltaEx of the first stage regenerator can be modified stepwise until the desired first stage temperature is achieved.

Iteration 2. The initial volume flow U is obtained from the swept volume of a fictive piston compressor applied to the first stage regenerator. This configuration will correspond to a so-called Stirling type PTR with the swept volume V_{swept}. But the flow can also be actuated by valves connected to high and low pressure reservoirs. Any type of valved compressor may be used to pump the gas from low to high pressure reservoirs. The mass flow supplied by this compressor is approximated by

$$\dot{M}_{Compr.} = f_C \frac{p_0}{RT_w}\left(1 - \frac{\hat{p}}{p_0}\right) V_{swept,C.} \tag{6.4}$$

Where $V_{swept,C}$ is the swept volume of this compressor running with the frequency f_C. This volume is being filled from the low pressure reservoir. On the other hand, the mass flow consumed by the cold head is

$$\dot{M}_{PTR} = f \int_0^{\tau/2} \rho_0 U dt \approx f \frac{p_0}{RT_w} V_{swept} \qquad (6.5)$$

Both quantities are compared at the end of the output file. If they do not agree sufficiently, the input parameter 'SweptVol' or the pressure ration 'p1/p0' must be changed.

Iteration 3: When PTR is of single stage type, the parameter describing the ratio of flows in first to second stage must be set to 1.0 (100 % in PT1). No calculations are done for the components 10 to 20 in this case, but the input file is being read. Therefore, the respective data field must be filled, but the values are treated as dummies. **Caution**: The calculation will stop without error message, when the input file has not the correct number of data!

Next, the data field for the components 5 to 9 must be filled with the respective parameters of geometry and material.

Iteration 3. The energy flow in the pulse tube, the parameter 'DeltaEx' of the component 7 is modified stepwise until the desired hot end temperature $y_9(6)=T_{hot}$ is achieved. The so obtained value of DeltaEx is the refrigeration power. It is important that this calculation is done for zero DC flow in both pulse tubes. This is done by setting the parameters 'rel. dc-flow in PT1' and 'rel. dc-flow in PT2' to zero. The relative DC flow is defined as the ration of DC mass flow in a pulse tube to the amplitude of AC mass flow supplied by the compressor (position 0).

The so obtained performance of a single stage PTR is certainly not yet the optimum. It may be improved by modification of the geometries of the components and/or by modification of the operational parameters such as frequency, pressure ratio and swept volume. Hence the previous steps have to be done repeatedly. Even an experienced user will need 10 to 100 runs for obtaining a reasonable optimum configuration. Some advices for facilitating this work will be given in chapter 7.

6.1.1.1 Some comments on handling of the energy flow parameter 'DeltaEx'

It has been mentioned that the total energy flow Ex is an independent variable in the system of differential equations. The temperature demanded at the outlet of any component is obtained by setting the adequate initial value of Ex at the inlet. The method used here might be a little bit inconvenient. Hence it should be explained in some more details. Fig. 6-2 shows the scheme of a simplified PTR. The axial energy flows, the work flow W_x, the heat flow Q_x and the enthalpy flow E_x are plotted in the lower graphs. It is assumed that transversal heat flow is only possible in heat exchangers, namely the aftercooler and the cold end heat exchanger CHX. All other components are thermally insulated (no radial energy flow). Hence the total, axial energy flow must be constant in such 'adiabatic' components.

The compressor pushes the work flow $W_{x,in}$ into the first component, a connecting tube representing a dead volume. Most people might expect that the workflow at the outlet of this section will be smaller. But the total energy E_x (the enthalpy) must be constant. Hence the

decrease in axial work flow must be compensated by an opposed heat flow, a heat flow from the aftercooler to the compressor. This is not possible when there is no heat sink in the compressor. Hence the temperature of the compressor will increase so far that the heat flow becomes zero, and the work flow will stay constant in that section. But one should note that the temperature in such 'adiabatic' components will not be constant.

Next, this workflow is fed into the aftercooler. In the ideal case, one may neglect the dead volume and the friction loss of this device. Then the work flow will stay constant. But the total energy flow will decrease due the radial heat rejection to cooling water or air. The axial heat flow results from Eq.(5.8). In the regenerator' (an adiabatic' component) E_x is constant. The mass flow may also be assumed constant in the ideal case, but the volume flow decreases with decreasing temperature, and the work flow will do the same. This must be compensated by a negative heat flow Q_x (heat is rejected towards the aftercooler). The cold end heat exchanger is complementary to the aftercooler, the work flow is constant and the enthalpy flow is increased by the applied heater. Finally we come to the pulse tube. E_x is close to zero but negative. This is because of of small negative heat flow due to the temperature gradient, and the work flow is nearby constant, it drops slightly complementarily to the small heat flow. This work flow given by

$$W_{x,Exp} = \frac{1}{2}\hat{p}\hat{U}_{PT,h}\cos(\varphi) \qquad (6.6)$$

will be extracted by the expander piston, where $U_{PT,h}$ is the volume flow at the hot end of the tube. The insert a) displays the energy flows in this type of cooler.

In the present model, the heat exchangers are specified only by the porosity and the hydraulic diameter (the same as the regenerators). But no data on the radial heat flow characteristics are implemented. Hence we cannot describe the profile of the total energy flow E_x in those components. We have now two options to overcome this problem. Both options can be adjusted with the parameter 'A/I' of the input list.

a) 'Isothermal' option. ('A/I'='i')

In this case it is assumed that the time averaged temperature T0(x) is constant, and the basic equations will be solved with $dT_0/dx=0$

b) 'Adiabatic' option ('A/I'='a')

In this case the heat exchangers are assumed to have no transversal heat flow to the surrounding. Instead of this, there must be longitudinal heat flow which is fictively removed at the ends. This heat flow is controlled by the parameter E_x. But we also know that the temperature profile in adiabatic components is governed by E_x. So we can adjust the energy flow within such heat exchangers so that the temperature T_0 becomes nearby constant. This value will differ from the total heat flow to be applied or removed from the heat exchanger. This must be compensated by a second fraction of E_x applied at one (or both) end of that component. This option will yield some more information than the previous one. But the handling of such calculations will be a bit more complicated. Some more explanations may be helpful.

In real heat exchangers the enthalpy flow E_x will change continuously due to the transversal heat flow. But when constant enthalpy flow is assumed in such sections, the heat flow absorbed or rejected is taken into account by stepwise change of enthalpy flow at the ends ($\Delta E_{x,a}$ and $\Delta E_{x,b}$). The sum of both steps equals the transversal heat flow. The temperature profile in such adiabatic sections is a function of E_x. Hence the enthalpy flow within the heat exchanger has to be adjusted so that the resultant temperature profile becomes nearby constant (Fig. Fig. 6-2 b). In this case, the constant E_x value will be roughly the average of the variable values of configuration a).

When the temperature of the heat exchanger is not an important parameter, as it is for many parametric studies, the procedure may be simplifies as shown by the insert c). Here we assume zero enthalpy flow in the heat exchanger. But for achieving the desired target temperature at the cold end of the regenerator, E_x must be increased by $\Delta E_{x,1}$ at the hot end of the regenerator. This enthalpy value, $E_{x,Reg,hot}$, the red point in all graphs. $\Delta E_{x,1}$ describes the loss of the regenerator. And the equivalent step of enthalpy flow at the end of the cold end HX describes the net cooling power lifted from temperature at the cold end of the pulse tube to its hot end temperature.

The present computer code has been adjusted to this configuration c) where the enthalpy flow in the aftercooler is automatically set to zero. Alternatively, $\Delta E_{x,1}$ can be supplied to the aftercooler as show in the insert c). In this case the flow of total energy will be closer to the average value resulting from the more realistic configuration a), and there will be less calculated temperature increase in the heat exchangers. This configuration is given the preference for most calculations. The initial energy flow $\Delta E_{x,0}$, the acoustic work flow supplied by the compressor must not be entered in the list of input data. It is calculated by the code.

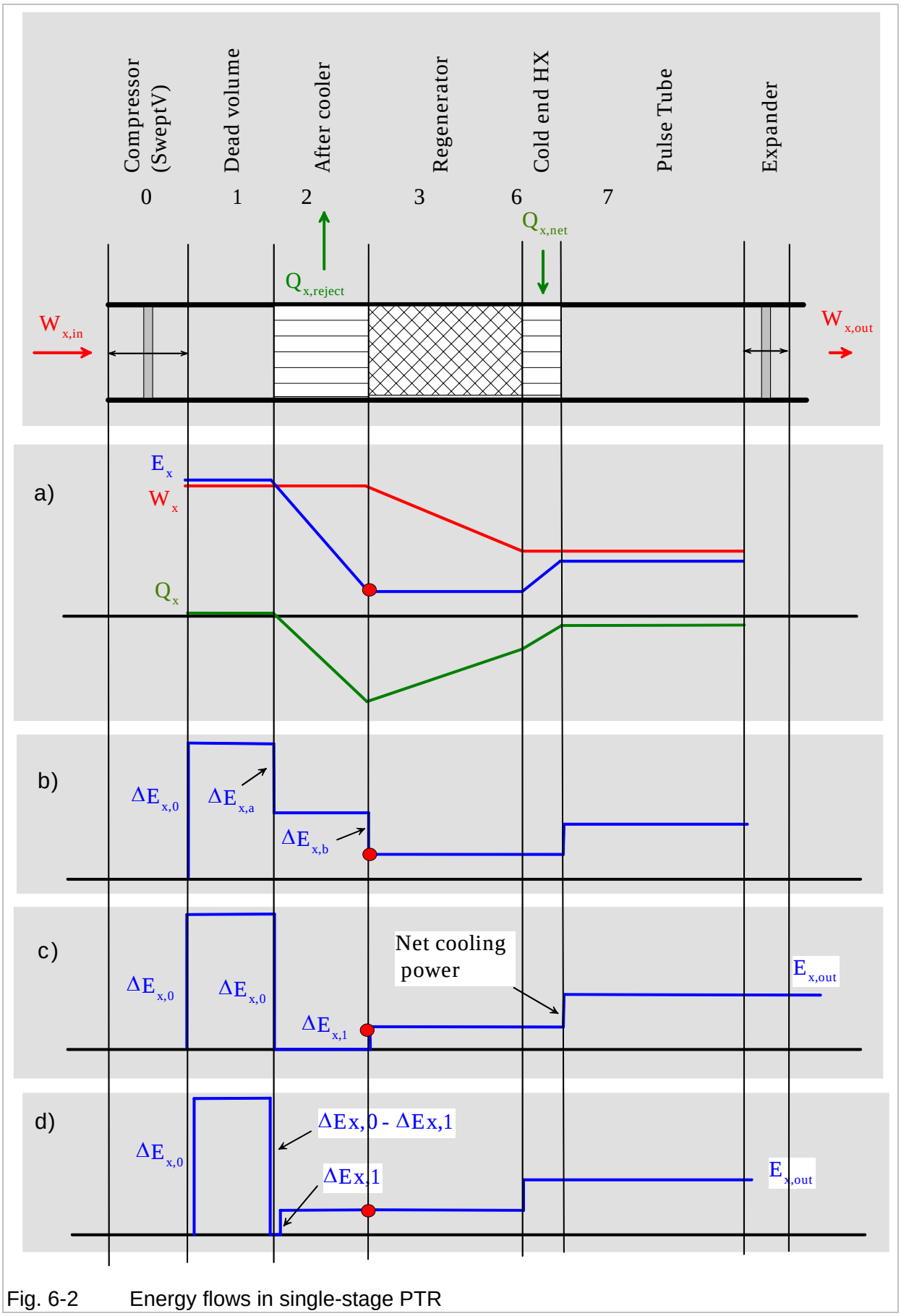

Fig. 6-2 Energy flows in single-stage PTR

6.1.2 Two-stage PTR

Let's now come back to Fig. 6-1. The calculation of the second stage is initiated automatically when the gas flow in this branch becomes greater than zero. This is done by setting the value of the parameter 'Volumeflow st1/st2 ' to less than 100. A good initial value is 70. This means that 70 % of the volume flow given by y_4 goes to the first stage pulse tube and 30 % to the second stage regenerator (first step of iteration 6). Then

Iteration 4 will adjust the second stage cold end temperature, and

Iteration 5 will evaluate the second stage refrigeration power. For obtaining a good performance of the second stage, it is not only important to select the suited material and size of the components. The DC flow will also become very important mainly for refrigeration in the 4 K range [Hof02]. The proper value is found by

Iteration 7. Adjustment of DC flow. A positive DC flow, i.e., a DC flow from the regenerator to the tube will transport additional energy from the hot to the cold end of the regenerator, but it will also lift energy from the cold to the hot end of the pulse tube. The optimum proves to be close to zero for a single stage PTR, and a small positive DC flow will improve the performance of the second stage.. Those quantities are adjusted with the parameter 'rel. dc-flow in PT1' and 'rel. dc-flow in PT2'. It describes the ratio of DC mas flow in the pulse tubes to the amplitude of the alternating (AC) mass flow at the hot end of the first stage regenerator. The sum of both DC flows is in the first regenerator. Hence the first stage calculation (iteration 1, 2 and 3) must be re-adjusted when any of the DC flows is changed. A good initial value for the relative DC flow in PT 2 is 0.001 to 0.002. For finding the optimum, we recommend to observe the parameter Qx at the cold end of the second stage pulse tube. It is printed in the output file. For zero DC flow, Qx describes the heat flow caused by irreversible losses in the tube. The DC flow may be increased until Qx becomes close to zero, but it must never become positive. This would cause a runaway to very low (or negative) temperature in the pulse tube.

6.2 Numeric accuracy

The FORTRAN source code must be compiled with double precision. The execution file ptr.exe has been obtained by use of the compiler Lahey/Fujitsu Fortran 95 with IMSL40. The compiler command is "LF95 -dbl ptr.f heprop.obj cryopropv301.obj" . So the precision of the intrinsic data is much higher than displayed in the output. The parameter for setting the maximum number of iterations (param(4) in the call of DIFPAG) is 30000. The final accuracy can be adjusted with the parameter 'TOL' in the input file. The calculation of the complete two-stage PTR is normally done within less than 3 seconds. If it takes longer, the TOL parameter may be decreased.

7 Advices for handling the data

7.1 Inspection of the alpha-numeric list

As mentioned before, many iterative steps are required for getting a reasonable lay-out of the PTR cold head. A comprehensive inspection of the output data is required after each step. Some times it more advantageous to inspect the listed output, in other cases plots will giver the better information. Hence, input and outputs should be organized so that all data can be visualised just by a few mouse clicks. We find that it is a good practice to have the input and the output as text files (eyymmdd.txt and ayymmdd.txt). So they can be opened very fast just by a mouse click in the windows explorer. For normal application only the files PTR.exe and e.txt are required. Double click to PTR.exe will run the code and produce the output a.txt in the same folder. Reference files of e.txt and a.txt should be maintained in a separate folder. Inspection of the numeric output is done just by a further mouse click. The input file e.txt may be kept open, but a save command is required before a next run. The first block of the output is more ore less a copy of the input data. The next blocks contain arrays of some of the most relevant data of all components, i. e.

x	axial position within the component
T	The time averaged temperature
p	amplitude of pressure oscillation
phi(p)	phase angle of pressure
U	amplitude of volume flow
phi(U)	phase angle of volume flow
Wx	work flow
Qx	heat flow
Ex	total energy flow

In addition, any of the variables listed in the file 'parameters.doc' (s. Table 8.2-1) may be listed in the next two columns. This option is activated with the parameter 'List of suppl. var.' of the input file together with the specifications inserted in the field 'Variable in col. 10' and 'Variable in col. 10'. This can be helpful for optimising the cooler.

The length of each data array can be set with the parameter 'MSTEP'. (mstep > 0).

Additional information is given in the last block. It contains

a) Pressure drop in the regenerators (real and imaginary part of pressure oscillation)

b) Rate of Helium condensation. This option is activated by the parameter 'He-Condensation' with input of flow rate (g/s) and pressure (Pa) of a gas flow

which is pre-cooled by ideal thermal conduct to regenerators and cold stages (see Chapter 8.1).

c) Check of mass flow supplied by the compressor of a GM type cooler and the demand of the cold head.

The length of the output file can be controlled with the parameter 'mstep'. The number of lines for the respective segment is mstep+1. The output for a given segment will be suppressed fully when the length (parameter 'length') is set to zero. In some cases the zero will cause numeric problems. In this case the length should be set to a very short value such as 1.e-6 m.

ATTENTION: When the calculation has stop abnormally, the intrinsic buffer of the solver will not be emptied, and the last group of some 30 lines will not be copied to the output. If you feel that important information might be hidden in this block, it will be helpful to increase the parameter 'mstep' of the component indicated in the last lines of the auxiliary window.

7.2 Graphical presentation

7.2.1 Single-stage PTR

The ordered list of the output can be imported in any graphics programme. Here we are using the programme PlotIT, and we have prepared some frames to be used in the beginning. They may be modified as to the demand of users. Other graphic codes might work similarly. For getting smooth curves, the length of the output for the segment to be considered should not be too small. For plotting some of the main data of a single stage PTR, we expand 'mstep' to 20 for the regenerator and the pulse tube **(example 3**). The output calculated for this configuration will be considered as a reference and is stored in as a2st50K_ref.txt in the folder /PTR-INITIAL/Plots/single stage/. Then we have to prepare reference plots for some quantities such as temperature, phase shift, and energy flows in both components, and we will add modified curves from the output a.txt in the actual work folder to the graphs (dotted curves).

When the next run has been done with modified input parameters, it will be easy to refresh the graphs with the new data while maintaining the reference curves. This is done just by deleting the file a.txt from the PlotIT surface and re-opening the new file a.txt. The graphic screens of the individual plots must be refreshed. Here we repeat this process:

1. Activate PlotiT

2. Open /Plots/single-stage

3. Click to reference graphs to be diplayed (T(Reg1), T(PT1), Energy(Reg), Energy(PT1),…)

4. Arrange the graphs

5. Activate Explorer

6. Modify {Ptr-work/e.txt **(Example 4**: increase the regenerator loss from 24.6 to 28.0 (New data list is Example 4).

7. Run calculation (click ptr.exe)

8. Bring PlotiT to foreground

9. Open PTR-work/a030916.txt from PlotiT

10. Plot new data into the reference graphs

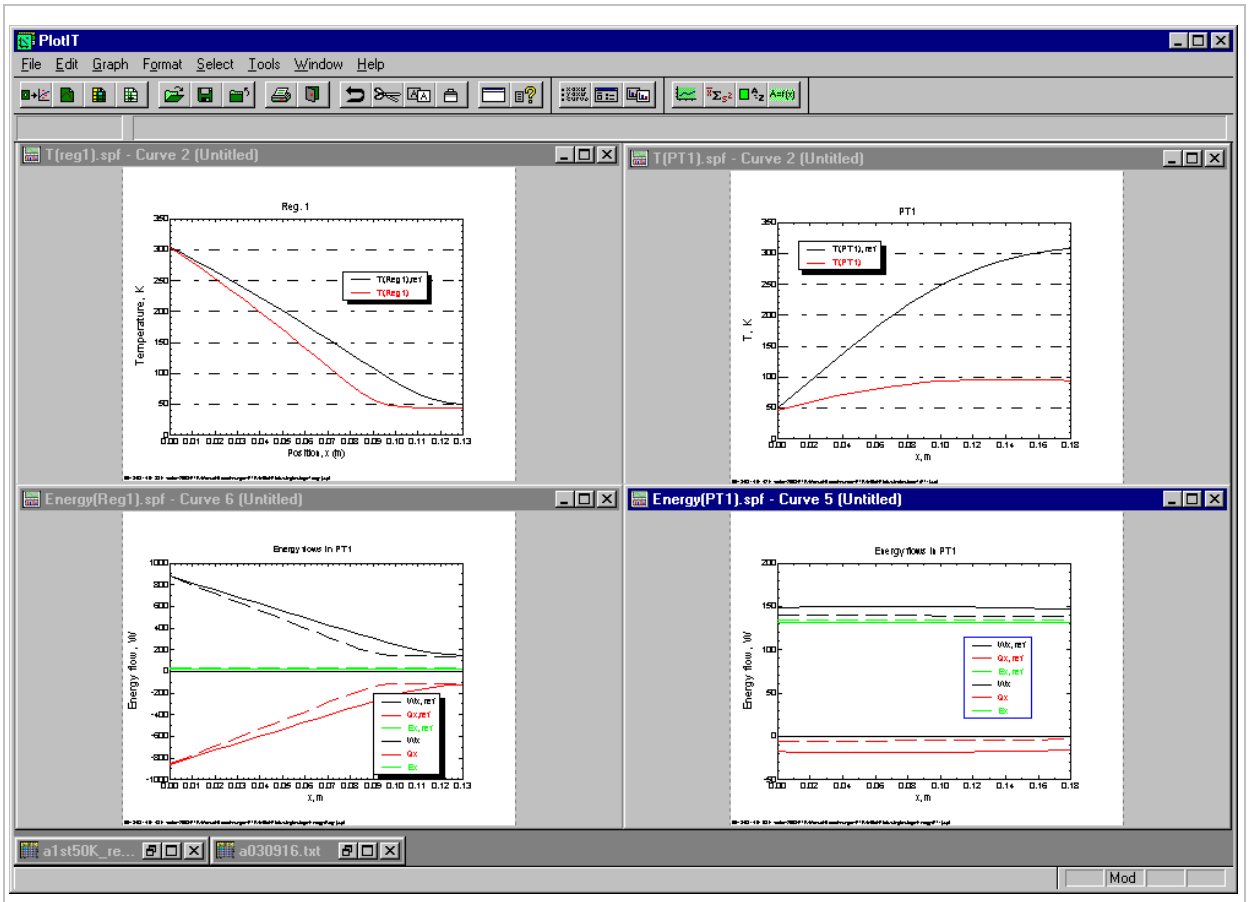

Fig. 7-1 Graphical presentation of the reference data file. Upper field: Temperatures in regenerator and in pulse tube; lower field: Energy flows

So you should have obtained the graphs of temperatures and energy flows in the regenerator and in the pulse tube as shown in Fig. 7-1. Now you may run the ptr-code with another input.

The graphs can be easily refreshed by deleting the old output file a030602 and loading the new one from the folder Ptr-work into the plot programme. The reference curves will not be changed. It is shown there that the refrigeration temperature has dropped from about 50 K to 45 K when the regenerator loss was increased. But the hot end temperature of the pulse tube has become lower than ambient. Hence the parameter DeltaE of the pulse tube unit (the refrigeration power) must be decreased in order to obtain the former temperature of 300 K

7.3 Phasor presentation

The complex variables, the pressure swing of pressure, p, and the swing of volume flow, U, are listed in the form of amplitude and phase angles. So those quantities may also be plotted as vectors (phasors in the complex plain). This will often give a more convenient presentation of the cooler. This is exemplified in Fig. 7-2 for the two-stage PTR according to Example 1. The values of the respective output have been used to plot the phasors of pressure and volume flow at some characteristic positions, namely the hot and cold ends of the first regenerator, hot and cold ends of the first stage pulse tube, and the equivalent positions of the second stage. Such phasor graphs will not be produced automatically with the present software. Here we have manually copied the data of amplitudes and angles from the numeric output into fields of Micrografx Designer software.

It is remarkable that the volume flow lags behind the pressure at the hot ends of both pulse tubes. This means that phase shifters with 'inductive' characteristics will be required for obtaining the calculated performance. The calculation does not say how those devices should be made. They can be actively driven piston expanders or they can result from the superposition of gas flows with different phasor characteristics as it is for the 'double inlet' configuration. Also inertance type phase shifters may be considered for PTRs running at higher frequency. This will be discussed separately in Chapter 9.

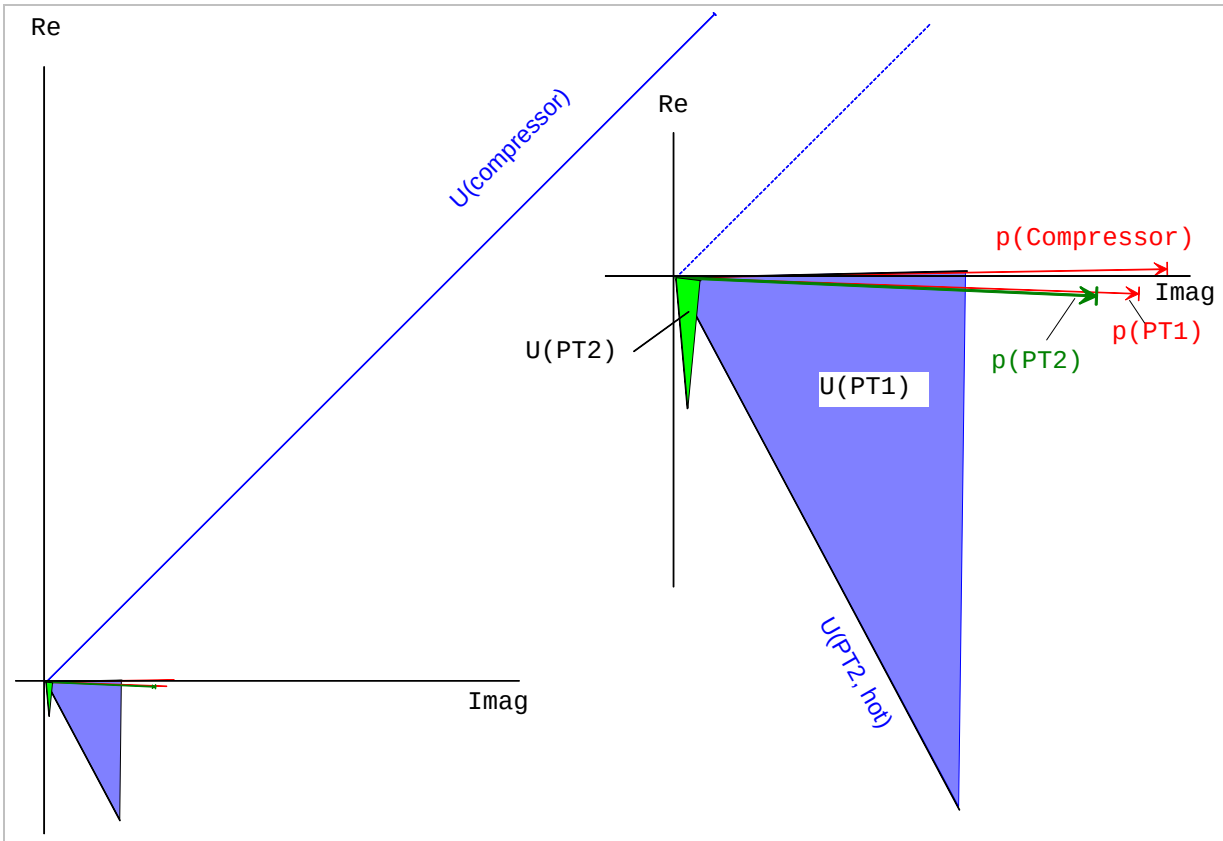

Fig. 7-2 Phasor diagram of the two-stage PTR (with enlarged part on the right)

7.4 One cycle presentation

If phasor presentation is not convenient, there is also the option to display data as function of time. That option is activated when the parameter *'One Cycle '* is switched from 0 to 1. This will produce lists of some variables as function of time. Here we have selected such variables which can be easily controlled by measurements, namely pressure, p, and volume flows, U, at the hot ends of the first stage regenerator (REG), the first stage pulse tube (PT1), and the second stage pulse tube (PT2). Those quantities will be written into the files REG.txt, PT1.txt and PT2.txt, and they may be plotted versus time or versus the angle. (All data are also given in the Excel file 'zyklus.xls'). In those files we have additionally listed the actual 'pV-power', namely the quantity

$$pU = \hat{p}\cos(\omega t)\hat{U}\cos(\omega t + \varphi) \tag{7.1}$$

The folder 'Ptr-work' will now contain the files as listed in Fig. 7-3. The new files have been produced with **example 5**, a modification of example 1. They will not be deleted automatically when the parameter 'One Cycle' has been de-activated for a future run. So they may be deleted manually. An example for using this option will be given in Chapter 10.

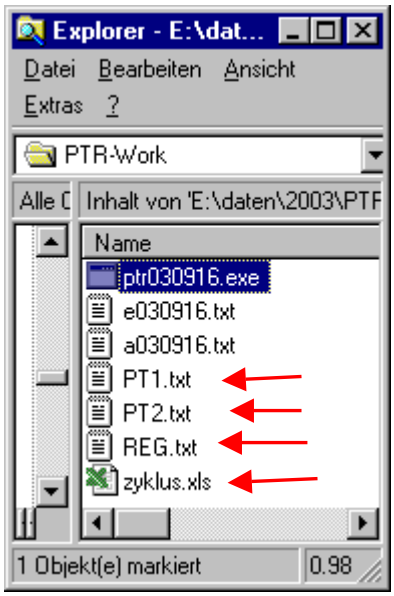

Fig. 7-3 Files in the folder 'Ptr-work' when the parameter 'One Cycle ' has been activated.

8 Special parameters of the input list

The lower lines of the input list will give access to some additional features of the code.

8.1 Liquefaction of Helium

The two-stage PTR code has also implemented a subroutine for calculating the rate of He gas to be condensed from room temperature. It is assumed that this gas flow has ideal thermal contact to both regenerators and cold end heat exchangers as shown in Fig. 8-1**.** The calculation is actuated when the flow rate in the parameter field 'He-Condensation ' is set to a value greater zero. This gas flow $\dot{m}_{He}$ with the specific heat $C_{p,He}$ will change the enthalpy flow in the regenerators so that Eq. 2.12 becomes modified to

$$\frac{dE_x}{dx} = h_w U_w (T_e - T_0) - (\dot{m}_{DC} C_{p0} + \dot{m}_{He} C_{p,He}) \frac{dT_0}{dx} \qquad (8.1)$$

And it is assumed that the final condensation occurs at the cold end heat exchanger of the second stage. Hence there will be the heat load

$$\dot{Q}_2 = \dot{m}_{He} L_{He} \qquad (8.2)$$

Such configurations have been evaluated earlier [Hof03]. The ptr code used for this paper had also the option for condensation of other gases than helium. The properties code GASPAK was implemented there. This has not been done in the present version.

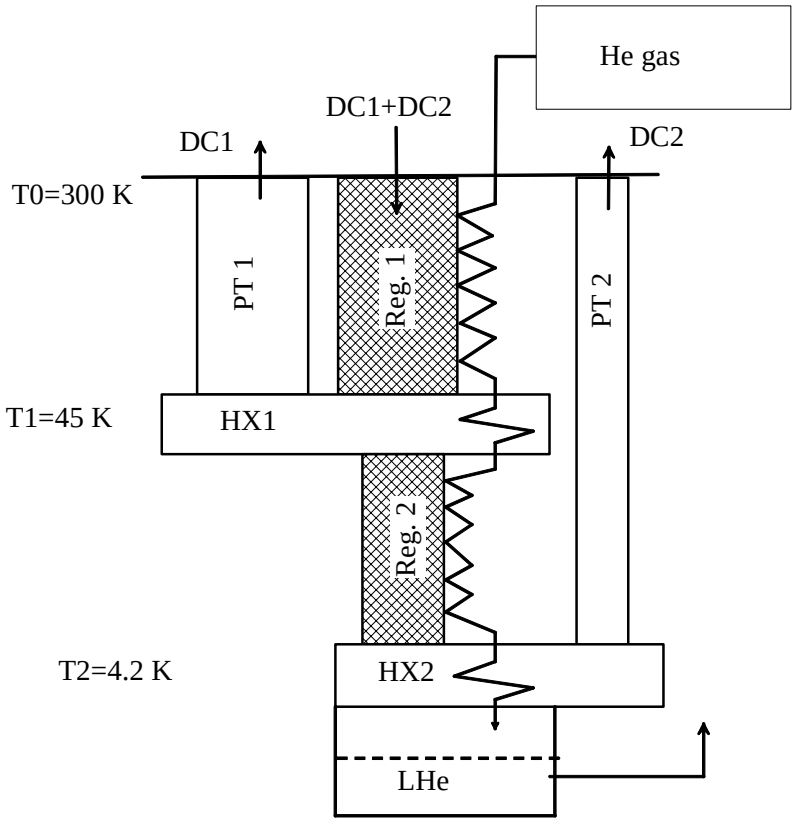

Fig. 8-1 Scheme of a PTR used to liquefy helium gas

8.2 Access to supplementary variables

One may hay remarked, that the last two columns of the output are empty. They have been prepared to be filled with any of other variables which have been calculated by the solver program, but are hidden normally. Those variables are listed in Table 8.2-1. They are made accessible when the parameter 'List of suppl. var.' of the input file is set to 1, and when the numbers of two of the variables of interest are set in the following lines.

The parameter 'List of suppl. var.' =1 will also activate an additional subroutines for calculating the swing of temperature in the matrix of the regenerators. The variable V(19) is calculated from the simplified correlation

$$\Delta T_s = \int_0^{\tau/2} \frac{\dot{m}\, c_{p,0} \dfrac{dT}{dx}}{\left(\rho_s\, c_{p,s} A_s + \rho_0\, c_{p,0}\, A_f\right)}\, dt \qquad (8.3)$$

Where the indices 'o' and 's' describe the states of the fluid and of the solid, respectively. A_f and A_s are the cross section areas of fluid and solid. A more precise correlation is given by Eq(13) in ref. [Xiao95] . This term is evaluated for the position b+b_s/2 of Fig. 5-1, so it should describe roughly the mean of the temperature amplitudes at the innermost position of solid particle (wires or spheres).

As example for using this supplementary information, we consider an input file with a second stage regenerator composed of three materials, Pb, and HoCu2 (**Example 6**), and we have activated the output for the display of the volumetric specific heat of those materials and the temperature swing of the matrices according to variable V(20). The calculated values of T_0, $T_0+\Delta T_s$, and the specific heat of the solids are plotted in Fig. 8-2. The length of the Pb section has been chosen so that there will be a smooth transition of its specific heat to that of the HoCu2 section.

When running the calculation with the input of Example 6, you will find that the message 'calculation of temperature swing' is displayed in the auxiliary window, and the hole calculation will need more time. This may be tiresome if you need many shots for finding a consistent set of input data. Hence we recommend to do all calculations with inactivated parameter 'List of suppl. var.' as long as you have not yet found a reasonable solution.

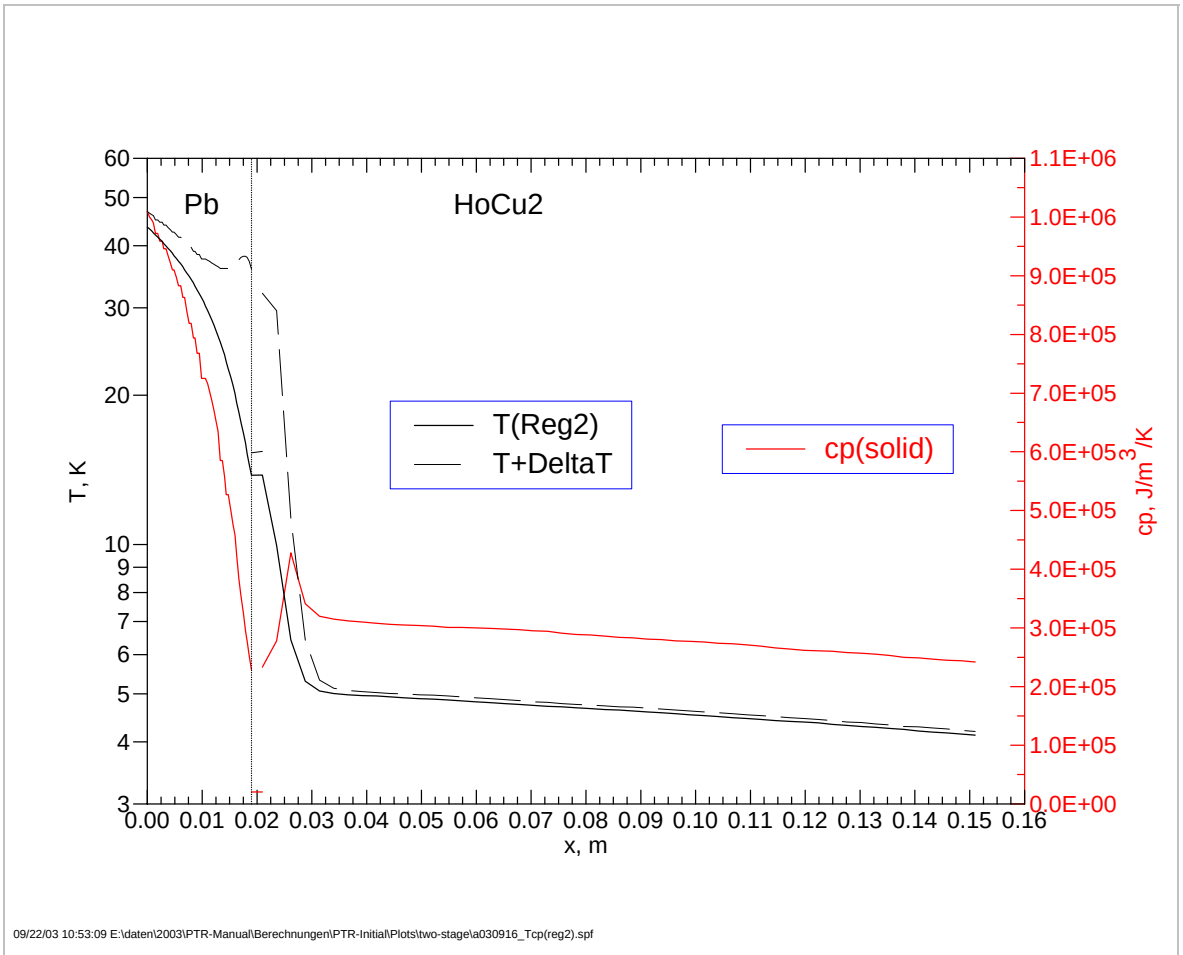

Fig. 8-2 Example for display of supplementary variables V(15) and V(20) together with the temperature profile of a second stage regenerator composed of Pb and HoCu2

Table 8.2-1:List of variables V(i):

	V(i)	Name	I
1	x	Position	M
2	T_0	Mean temperature	K
3	$Re(p)$	Real part of pressure swing	Pa
4	$Imag(p)$	Imaginary part of pressure swing	Pa
5	$Re(U)$	Real part of volume flow	m^3/s
6	$Imag(U)$	Imaginary part of volume flow	m^3/s
7	W_x	Work flow	W
8	Q_x	Heat flow	W
9	E_x	Total energy flow	W
10			
11	δ_μ	Viscous penetration depth	M
12	δ_k	Thermal penetration depth in fluid	M
13	δ_s	Thermal penetration depth in solid	M
14	$c_{p,0}$	Specific heat of fluid	J/kg
15	c_s	Volumetric specific heat of solid	$J/m^3/K$
16	k_0	Thermal conductivity of fluid	W/m/K
17	$k_{s,0}$	Thermal conductivity of solid	W/m/K
18	k_e	Effective thermal conductivity	W/m/K

19	AT_{solid}	Amplitude of temperature swing in mid of matrix material (approximated)	K
20	AT_s	Amplitude of temperature swing in mid of matrix material (Eq 13 of Ref. 1)	K
21	Re	Reynolds number	
22	Re_ω	'acoustic' Reynolds number (s. Cryogencs35(1995)p16)	

8.3 The GM-type PTR

So far it has been assumed that the cooler is driven by a piston compressor with the swept volume 'SweptV' and with a dead volume given by the section '1_ TubeComprToReg1 '. For operating such coolers at low frequencies around 2 Hz as it is required for achieving temperatures in the rang of 4 K, piston compressors with very large swept volume would be required. They would be bulky and expensive, and they are not commercially available. So it became a good practice to use the more compact compressors of the same type as they are used in conventional refrigeration technique. Their only purpose is to pump a sufficient flow of He gas from low to high pressure reservoirs. The flow from those reservoirs to the cold head is controlled by separate devices such as rotary or solenoid valves. In the present model it is assumed that sinusoidal gas flows are produced by those valves.

In this case, the mean pressure and also the pressure ratio will depend on the capacity of the compressor. The mass flow supplied by the compressor with swept volume given by the parameter 'Swept volume, m^3 ' and the working frequency given by 'FrequenyOfGrid, Hz ' and the mass flow required by the cold head are treated separately in our model. The comparison is given in the lower lines of the output file. Both term differ by about 1 % in the previous example. The input parameters of the cold head must be modified when the difference becomes too great.

Another serious fact is that such 'low frequency' PTRs will be operated with high pressure ratios (the ration of pressure amplitude to mean pressure) in the range of 2. This will cause higher harmonics in the volume flow. Additional higher harmonics will be caused when the gas flows are controlled by solenoid valves (open/close valves). It cannot be expected that the predictions obtained from the model which is based on a small amplitude approximation will be very precise. But the experience shows that prediction is not too bad. Typically the cooling power of a 4K-PTR proves to be overestimated by about 30 %. More details on such experiments will be given in Chapter 10.

8.4 Stirling type PTR (50/60 Hz) coolers

One basic assumption of the model is that all dimensions (L) of the cooler are much smaller than the acoustic wave length (λ). Assuming $L<10\lambda$ and a lowest sound velocity of 300 m/s

this criterion yields L>3000/f, where f is the frequency. Hence the model should be applicable up to frequencies in the range of 1000 Hz. Under this aspect it can also be used for the design of 50 Hz coolers, a field where good linear motor piston compressors are available [CFIC]. A PTR equipped with such a 2.6 kW linear compressor has been reported to yield 150 W at 77 K. Further details on its design are not known. But in the next example (**Example 7**), we will study how the single-stage PTR of example 2 is to be modified for obtaining a comparable performance. This is done with the assumptions:

- Operating frequency: 60 Hz
- Regenerator and heat exchangers made of 200 mesh stainless steel (same as before)
- Mean pressure: 17 bar
- Pressure ratio, p1/p0 (i.e Amplitude(p)/p_0): 0.2
- pV-work flow supplied by the compressor, Wx: 2000 W
- Inline configuration (zero length of the U-shape connection, segment #5)

For this study, we copy the data block of example 2 to the top of the input file and give it the name example 7. Here we change first the parameter of *f* and *p1/p0*, and *SweptV* must be reduced until the initial work flow Wx becomes about 2000 W. A new initial value may be obtained from

$$SweptV_2 = SweptV_1 \frac{f_1}{f_2} \frac{Wx_2}{Wx_1} \frac{(p1/\,p0)_1}{(p1/\,p0)_2} \tag{8.4}$$

The final value of 82 cm^3 will be found by a few trials. For simplicity, we first neglect the dead volumes of the sections 1, 2, 5, and 8 length=1e-6). Now will be seen that the temperature in the regenerator does not decrease enough. The 77 K level will be obtained when DeltaE of section #3 is increased to 30 W. But with this run, the auxiliary window remains open, and it is indicated that the calculation has stopped in segment #7 (1. PulseTube). Obviously the refrigeration load DeltaEx of segment #6 must be reduced. The hot end temperature of about 300 K will be achieved when this term, the effective refrigeration power, is reduced to 37 W. This is much less than expected. So we have to find the reason of this discrepancy.

A view to the output list shows that pressure amplitude has dropped in the regenerator from 3.4 to 1.9 bar, and there is also much phase shift mainly of the volume flow. Both term will be reduced when the length of the regenerator is reduced. We assume halve the previous length 65 mm). But we also see that by this measure, the cold end temperature become too high. Hence the regenerator loss, DeltaEx of #2 must be increased to 62.8 W for meeting the 77 K target, and the refrigeration load will become 185 W. The pulse tube still has the same geometry as it was for the previous 2 Hz cooler, but one should expect that this is not yet the optimum. The temperature profile seen in the output file shows that the highest temperature is at the position x=0.12 m. So we may cut the tube to that length, and we may increase the

refrigeration power by a few more watts for decreasing the hot end temperature to 300 K. There is another point of interest , namely the cold end heat exchanger (section #4). It has been assumed to be made of 200 mesh Cu screens, and it is seen that this configuration will cause rather high losses (the work flow is decreased from 277 W to 258 W).

Such an improvement is done in the next **example 8**. Here we have also added other components such as connection tubes and heat exchangers. It is not intended to optimise the whole configuration. We will only show how this could be done. So we assume the compression space (section #1) to have about the same volume as the swept volume of the compressor, an we assume aftercooler (section #2), cold and hot end heat exchangers (sections #4 and #6) tube made of 20 mm long stacks of Cu mesh (100 mesh screen with 0.1 mm diameter of wires). The laminar channel parameters become b=0.103 mm and bs=0.0225 mm. The longitudinal temperature gradient is being neglected in all heat exchangers ('A/l'='i'). This configuration yields a 77 K refrigeration power of about 250 W. Obviously, the losses caused by the additional components is overcompensated by the improvement of the cold end heat exchanger. But this does not mean that the heat exchangers of this example will work properly, so that the real heat flow will be transferred to the secondary coolant at their peripheries (see also Chapter 12). The present code takes only account of the dead volume and the friction loss. Further calculations must be done separately.

The code also does not say how the work flow is to be rejected from the pulse tube. It only gives the vectors of pressure and volume flow, with other words, it gives the acoustic impedance

$$Z_{PT,h} = \frac{\tilde{p}_{PT,h}}{\tilde{U}_{PT,h}} \tag{8.5}$$

at the hot end of the tube. The expander connected for extraction the work flow from the pulse tube can be realised by different ways. This will be discussed in Chapter 9.

9 Expanders

9.1 Inertance tube expander

The basic thermoacoustic equations given in chapter 5 have been derived from continuity, momentum, and energy equation, where the Euler equation (momentum) is taken as

$$\frac{\partial p}{\partial x} = -\rho_0 \frac{\partial u}{\partial t} - \mu_0 \nabla_n^2 u \qquad (9.1)$$

with the flow velocity *u,* the fluid density $\rho_{0,}$ and the viscosity μ_0. This means that the first order inertial term (first term on the right hand side) is included. Hence, inertance tube phase shifters can also be treated with our model. The scheme of such a cooler is shown in Fig. 9-1. The tube of the phase shifter must on the one hand have a sufficiently small diameter so that the inertial effect of the accelerated fluid plays a role for the pressure drop. On the other hand, the expansion work, the work flow coming from the pulse tube must be dissipated by friction, and the heat produced by this process must be rejected to the ambient. It amounts to about 330 W in the present example, and it will certainly be a problem to reject this heat flow from the periphery of a thin tube. If there is not sufficient heat transfer, the gas within the tube will be cycled more in an adiabatic than in an isothermal process. But then the heat caused by friction must be removed by a gas flow, and it must be rejected by heat exchangers at the ends. This is being assumed here (inertance tube and buffer volume are placed in vacuum). The temperature profile in such tubes depends on the total longitudinal energy flow. A temperature profile with $T_0(x)$ close to 300 K can be obtained in the inertance tube when the total energy flow E_x is adjusted appropriately. This will be done with the heat exchangers HX_W and HX_B at both ends of the tube. Both together must remove the total of the dissipated work flow., but each of them may reject different fractions required to obtain the desired temperature profile in the tube.

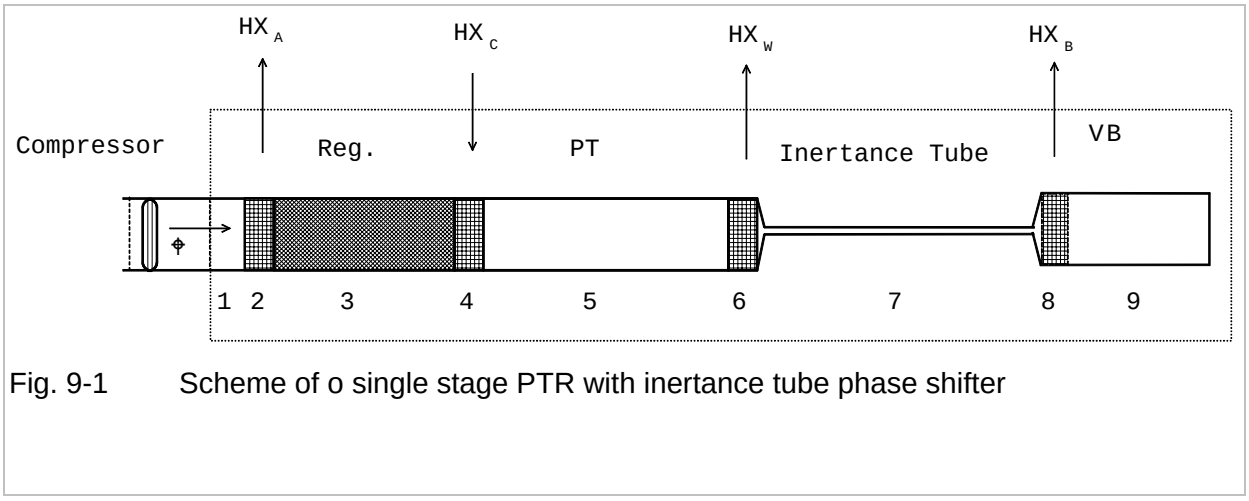

Fig. 9-1 Scheme of o single stage PTR with inertance tube phase shifter

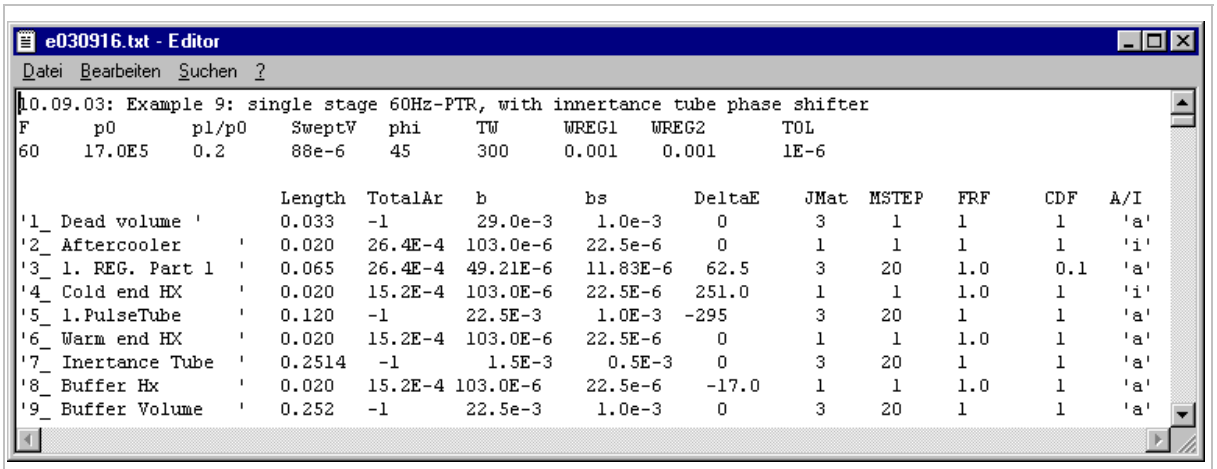

Fig. 9-2 Input data file of a single-stage PTR with inertance tube phase shifter (The lower lines are not shown, but they must be filled with dummies).

The data set of such a system is given in Fig. 9-2. The system is the same as in the previous example, only the segments #7, #8, and #9 have been added, and the not needed segments (2nd part of the first stage regenerator, U-shape connecting tube of the previous arrangement (example 8) have been omitted, and the subsequent segments have been shifted to their places. The names in the first column have also been changed. (Those names will be copied into the new output list).

The lay-out of the inertance phase shifter is done on the following base:

1. All work flow must be dissipated in the tube. This means that diameter and length must be chosen so that $W_x = 0.5\,\hat{p}\hat{U}\cos(\varphi)$ becomes zero at the entrance of the buffer volume where volume flow and pressure are connected by

$$\tilde{U} = \frac{V_B}{p_0}\frac{dp}{dt} = \frac{V_B}{p_0}\,j\omega\tilde{p} \qquad (9.2)$$

   This means that the phases of pressure and flow rate must adjust so that the pressure will lag by 90° behind the volume flow, i.e. $\cos(\varphi) = 0$. But at the opposed end, the connection to the pulse tube, the flow rate should lag by about 45° behind the pressure. Hence, the inertance tube must do a phase shift of more than 90°.

2. Buffer volume (radius and length of a cylinder) must be chosen so that the volume flow at the closed end (right hand end) become zero. The gas column will act like a spring.

3. The enthalpy flows (E_x) must be adjusted so that temperature close to 300 K are achieved in all segments #6 to #9.

Some results of this calculation are plotted in the next graphs. The phase shift caused by the inertance tube is seen in Fig. 9-3. In the section #7, the tube with 3 mm inner diameter the phase angle of the volume flow does not change, but the pressure phase is shifted by about 170 °. The length of this tube is being cut at the position where the pressure lags by 90° behind the volume flow. In this calculation it has been assumed that the gas in the buffer volume is compressed adiabatically. The gas column will be compressed like a spring. This means that the volume flow will drop steadily, and it must become zero at the closed end. This difference in phase angles is being maintained in the buffer volume. (The steep increase at its closed end might be a numeric artefact). In Fig. 9-4 we have plotted the different energy flows, and it is seen that the work flow decreases to zero in the inertance tube. But because of conservation of total energy, there must be an opposed heat flow in this tube. The negative sign means that there is a heat flow from right to left. So it can be rejected by the section 6, the hot end heat exchanger. All energy terms become very small in the buffer volume (section 9). But due to intrinsic losses, the enthalpy flow will not become zero. A small negative value must be assumed, and in the present calculation it has been adjusted so that the temperature in the buffer volume should be close to 300 K. This cannot be achieved with the present configuration. We could only find a solution with temperatures close to 300 K at both ends. But there is a high temperature peak within this tube. This is shown in Fig. 9-6. The high of this temperature peak depends on the amplitude of pressure in this volume.Fig. 9-5 In we have plotted the pressure amplitude along the whole system. It is surprising, that this quantity does not drop continuously. It has a minimum within the inertance tube, and the pressure amplitude in the buffer becomes rather high. This effect will be reduced by assuming a smaller diameter and length of the inertance tube. But in that case the velocity will become very high.

The mentioned temperature peak in the buffer volume can be suppressed by switching the parameter 'A/I' from 'a' to 'i'. The resultant length of the buffer cylinder will become nearby the same. We believe, however, that the adiabatic treatment is more realistic, because of the small length of thermal penetration which is much smaller than the radius of this cylinder.

Those results should be considered more or less as an academic exercise. The resultant inertance tube is very small, and the flow velocity within this 3 mm i. d. tube becomes very high, it would even exceed the sonic velocity. This is in strong conflict with the fact, that the pressure drop has been calculated on the assumption of laminar flow. Other correlations for dissipation in the high turbulent oscillating flow will be required for obtaining more realistic results.

Corrections for turbulent flow

A simple measure is to use the empiric flow resistance factor FRF. The present model is based on the assumption of laminar flow in all sections. Some modifications have been added for describing the flow in porous beds (chapter 5.2.1). Respective subroutines are activated only when the hydraulic diameter is less than 0.1 mm. So it will not be activated for the inertance tube, and the pressure drop

$$\frac{\Delta p}{\Delta l} = \zeta \frac{\rho_0 u^2}{2} \qquad (9.3)$$

will be described by Hagen-Poiseuille law with the friction factor

$$\zeta_L = \frac{64}{\mathrm{Re}} \tag{9.4}$$

where the Reynolds number is given by

$$\mathrm{Re} = \frac{\rho_0 u d}{\eta} = \frac{4\rho_0 U}{\pi \eta d} \tag{9.5}$$

This describes the pressure drop for laminar flow (Re<3000) in smooth tubes. For higher flow velocities with 3000<Re<100000, the pressure drop in smooth tubes may be described by the Blasius correlation

$$\zeta_T = \frac{0.3164}{\sqrt[4]{\mathrm{Re}}} \tag{9.6}$$

The ratio of both is equivalent to the FRF factor. Is plotted in.Fig. 9-7. Accordingly, the value of FRF can range up to 100. But when FRF is increased, the diameter of the inertance tube must also be increased and the Reynolds number will decrease. So one might expect that a consistent set of tube dimensions and the appropriate value of FRF can be found by some iterations. But this does not work. For too great values of the empiric flow resistance factor FRF we will get the situation that the work flow becomes zero due to the fact that the amplitude of pressure and not its *cos(ϕ)* becomes zero. In this case, the tube will work like an orifice. This is seen to happen for FRF>30 in the present case. But quite reasonable results will be achieved for smaller values of FRF.

One result of such calculation is obtained from the **example 10** in the file e030916. Here we have assumed FRF=10, and the resultant inertance tube with 7 mm inner diameter becomes a length of 0.906 m. The amplitude of the pressure is seen to drop from 2.4 bar at the pulse tube to about 0.5 bar at the end of the buffer volume. .This pressure swing in the buffer volume is caused by a gas flow with an amplitude of 10 l/s at its open end. Hence, this volume becomes about 1.5 ltr.

Those examples show, that there is still a wide range of uncertainty. More precise predictions will require better data on pressure drop of oscillating flow. Much efforts for improving such predictions are still being done [Schunk03], [Luo03b], [Rad03]. Nevertheless, the FZKPTR code may be considered as a valuable tool for parametric studies on such systems.

Those few examples should give some feeling on how much of information can be gained from such calculations. So it can contribute much to deeper understanding of the processes running in such systems. Other configurations of the phase shifter are also possible. A lot of skill and experience is required for finding the optimum. The non-experienced user may easily get lost.

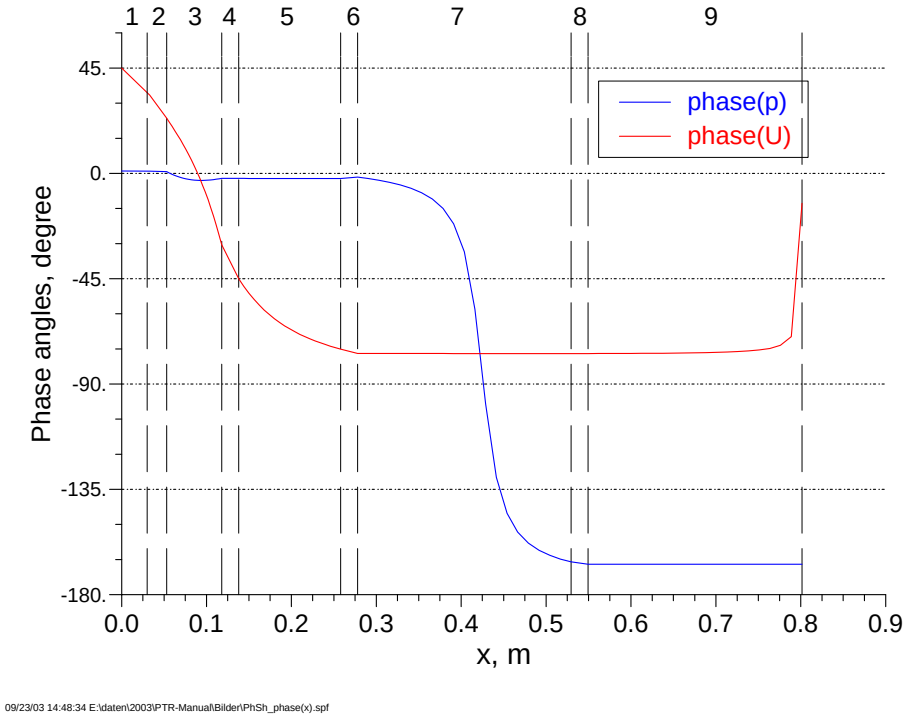

Fig. 9-3 Phase angles of pressure and volume flow in the components of a single-stage PTR with inertance tube phase shifter

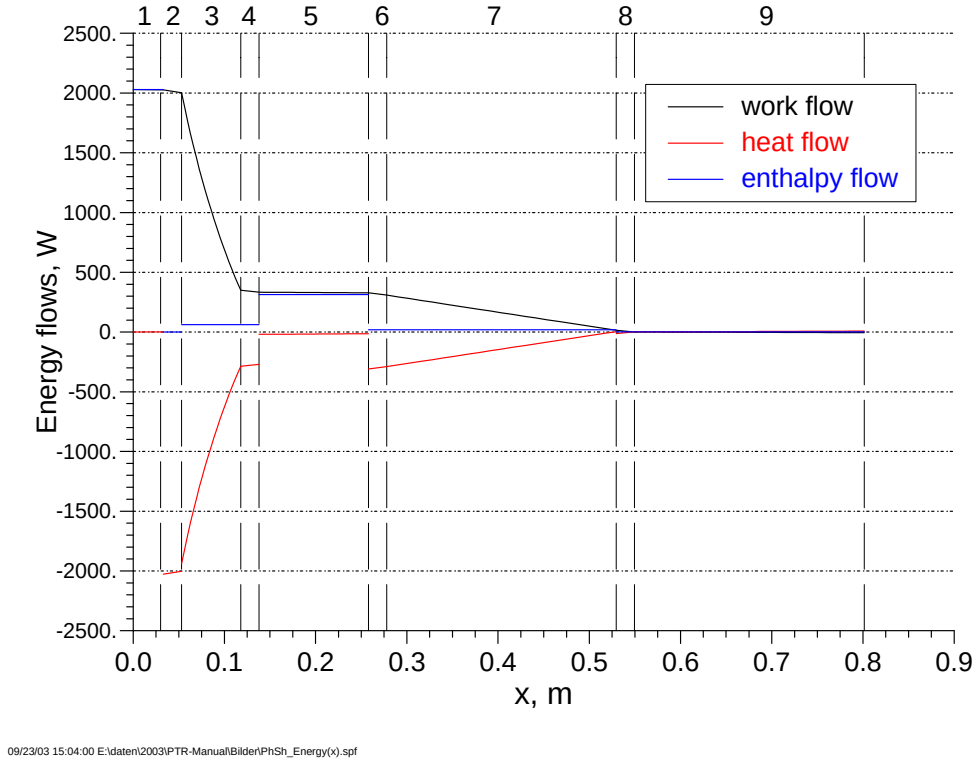

Fig. 9-4 Energy flows (work, heat, and enthalpy) in the components of a single-stage PTR with inertance tube phase shifter

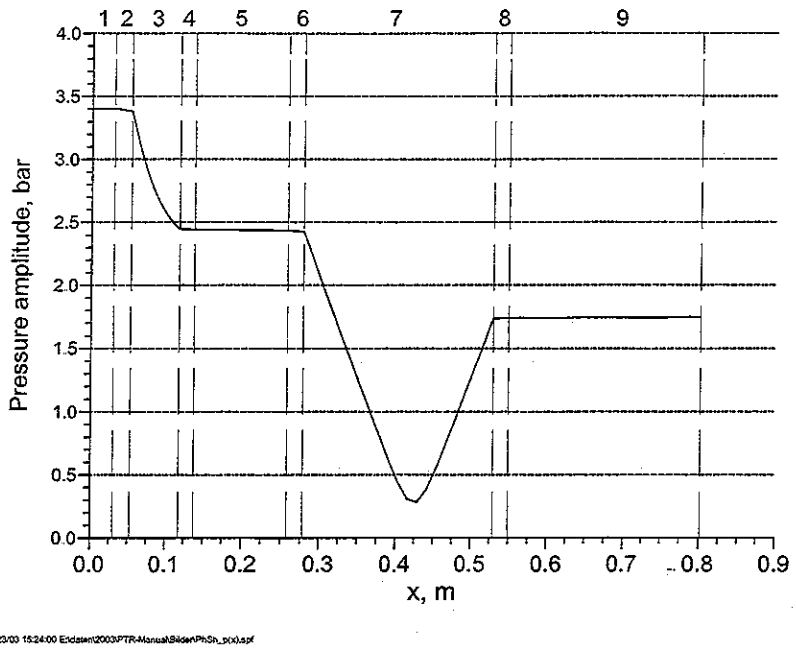

Fig. 9-5 Pressure amplitude in the components of a single-stage PTR with inertance tube phase shifter

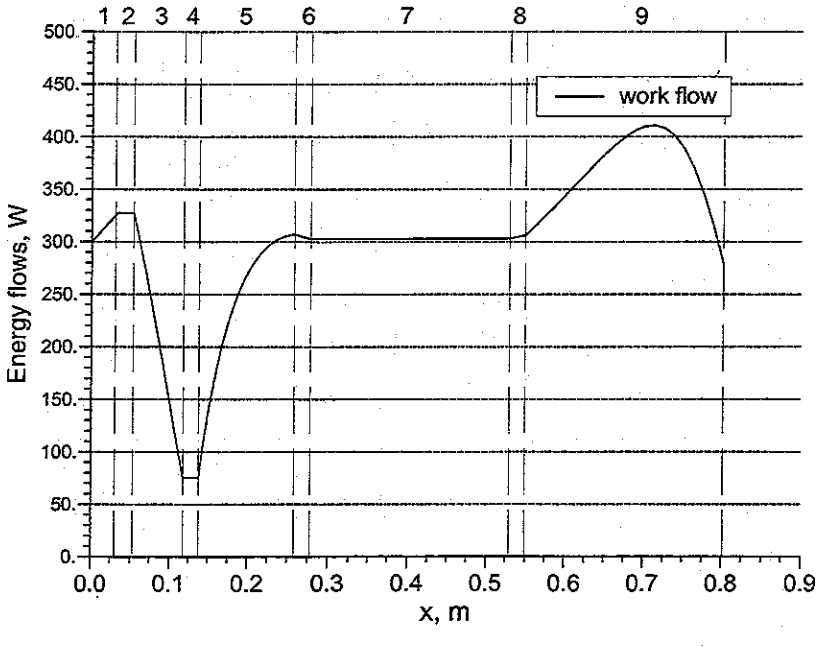

Fig. 9-6 Temperature in the components of a single-stage PTR with inertance tube phase shifter

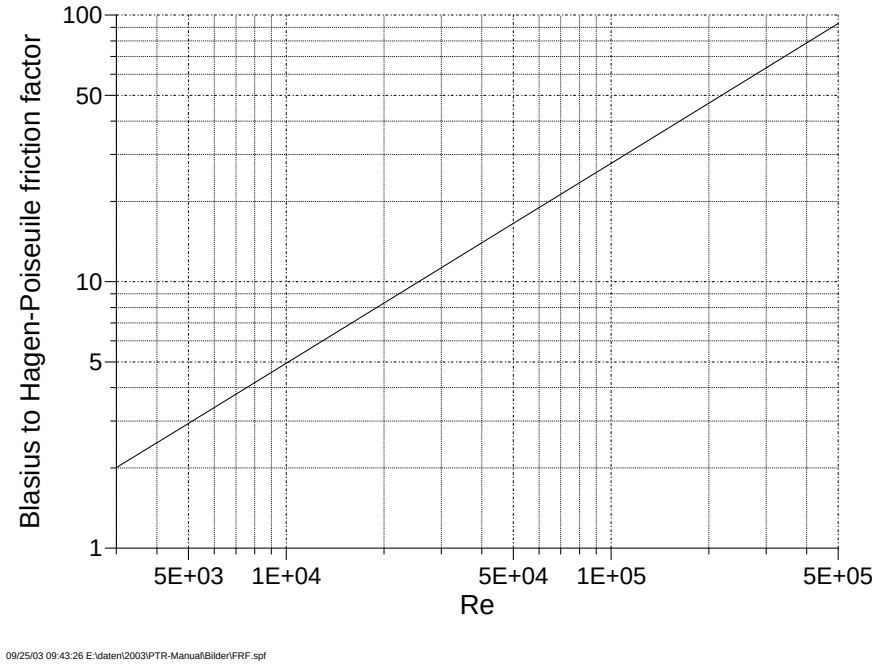

Fig. 9-7 Ratio of turbulent (Blasius) to laminar flow friction factors

9.2 Piston expander

The expander shown in Fig. 9-8 may be understood more easily. The piston with the swept volume V_{exp} must be moved so that the volume flow U_6 with constant temperature T_w is obtained at the hot end heat exchanger. The values of the volume floe U_6 and the pressure p_6 result from the previous calculation. Mass conservation at the expansion volume V_{exp} yields

$$\tilde{\rho}_6 \tilde{U}_6 = \frac{d}{dt}\left(\tilde{\rho}_6 \tilde{V}_{exp}\right) \tag{9.7}$$

For small amplitude oscillation of ideal gas we have

$$\rho = \frac{1}{RT_w}(p_0 + \hat{p}e^{j\omega t}), \qquad \tilde{U} = \hat{U}e^{j(\omega t+\varphi)}, \qquad \text{and} \qquad \tilde{V}_{exp} = \hat{V}_{exp}(1+e^{j(\omega t+\psi)}) \tag{9.8}$$

Neglecting terms with higher harmonics, Eq.(9.7) yields

$$j\omega\hat{V}_{exp} = \hat{U}_6 e^{j(\varphi-\psi)} \tag{9.9}$$

This yields amplitude and phase shift of the expander piston

$$\hat{V}_{exp} = \frac{\hat{U}_6}{\omega} \qquad \text{and} \qquad \psi = \varphi - \frac{\pi}{4}. \tag{9.10}$$

When the work flow W_6 is recovered and fed back to the compressor, the performance of will be better then that of the inertance system. Otherwise, both will have the same performance.

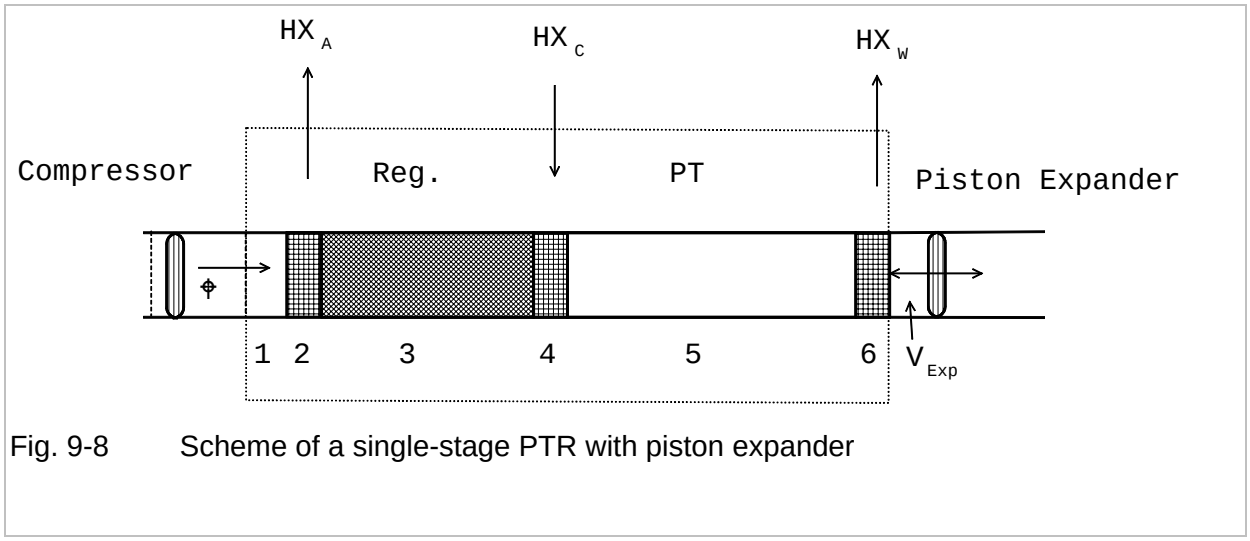

Fig. 9-8 Scheme of a single-stage PTR with piston expander

9.3 Double-inlet expander

The lay-out of a double-inlet system as shown in Fig. 9-9 can also be done by few 'hand calculations'. We may assume that both throttling devices, the by-pass BP and the orifice OR are simple resistances with flow rate proportional to the applied pressure difference. Hence the volume flow in the bypass is given by

$$\tilde{U}_{BP} = R_{BP}(p_2 - p_6) \tag{9.11}$$

and in the orifice

$$\tilde{U}_{OR} = R_{OR}(p_6 - p_B) \tag{9.12}$$

Where RBP and ROR are the flow resistances. For sufficiently large volume VB of the buffer canister, the pressure oscillations become very small, and the flow rate in the orifice throttle is given by

$$\tilde{U}_{OR} = \frac{\tilde{p}_6}{\left(R_{OR} - \frac{j}{\omega V_B}\right)} \tag{9.13}$$

Where R_{BP} is the flow resistance of the bypass. Both terms R_{BP} and R_{OR} must be chosen so that the equality

$$\tilde{U}_6 = \tilde{U}_{BP} + \tilde{U}_{OR} \tag{9.14}$$

Is achieved.

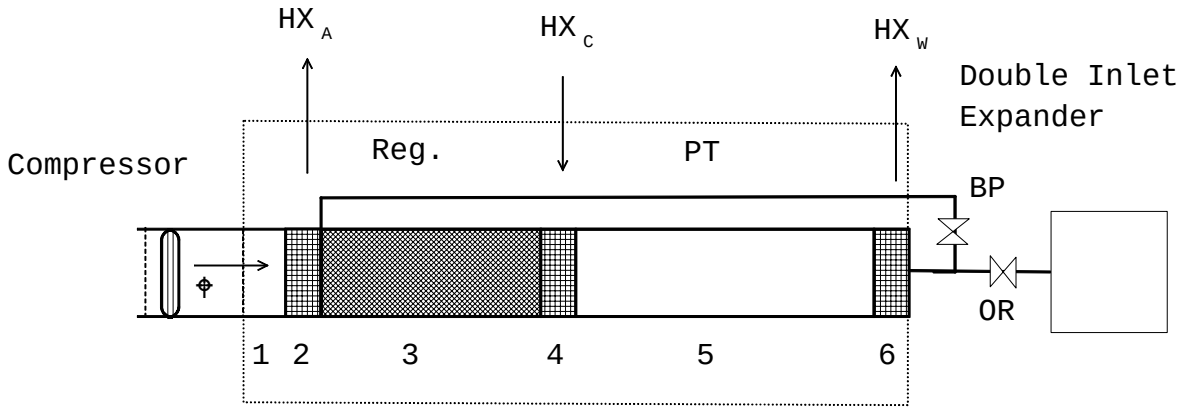

Fig. 9-9 Scheme of a single-stage PTR with double-inlet expander

10 Valved GM-type two-stage PTR

The numeric model is based on small amplitude approximations, and it does not include any non-linear effects and no higher harmonics. All those assumptions are not valid for GM-type coolers which are operated typically with pressure swings between about 10 bar and 24 bar. The situation is even worse when all flows are being controlled by open/close valves. The scheme of such a cooler is shown in Fig. 10-1. Is there any chance to get a reasonable prediction with such calculations? The answer can only be given by experiments.

The user of such coolers is only interested in final performance given by input power and refrigeration powers at both levels. Many other parameters may be considered for the validation of the calculations. Here we are restricted to those parameters which can be measured most easily. Those sensors are:

1. Pressure traces at the hot ends of
    - First stage regenerator, p(Reg)
    - First stage pulse tube, p(PT1)
    - Second stage pulse tube. P(PT2)
    - Exhaust and suction pressure of the compressor, p(H) and p(L)
2. Wall temperature along regenerators and pulse tubes, T_i
3. First and second stage refrigeration powers and temperatures, Q1, Q2, T1, T2
4. Mass flow supplied by the compressor, $\dot{M}_{Compr}$
5. Volume flow at the hot ends of the pulse tubes (evaluated from pressure drop at needle valves with given flow resistance)

With a properly chosen valve timing (Fig. 10-2) a rather good sinusoidal shape of the pressure swing is obtained. But the ratio of pressure amplitudes to mean pressure which should be small in the thermoacoustic model, is close to 0.3 in the experiment. Due to sudden switching of the valves, the volume flows (Fig. 10-3) are not smooth. But the mean values, which are a measure of the work flow, are close to those of the sinusoidal traces predicted with the thermoacoustic model. Additional losses will be produced by the higher harmonics of the flow rate.

Despite of those discrepancies, the prediction of the refrigeration power proves to be rather good. Typical 'ab initio' calculations (without any fit to experiments) will overestimate the first stage (50 K) cooling power by about 20 %, and the second stage (4 K) by about 50 %. This is not bad if one realises that the about 90 % of the 4 K acoustic work flow (Wx) is required for removing the parasitic losses of the second stage components. Details of this specific

calculation will not be given here, but the first example with the output given in Appendix A is a typical sample of a 4K-PTR. It can be seen there that more than 7 W of acoustic work flow is required to lift 0.54 W from 4 K to 300 K. This indicated that a 10 percent change of intrinsic losses will change the cooling power by more than 100 percent.

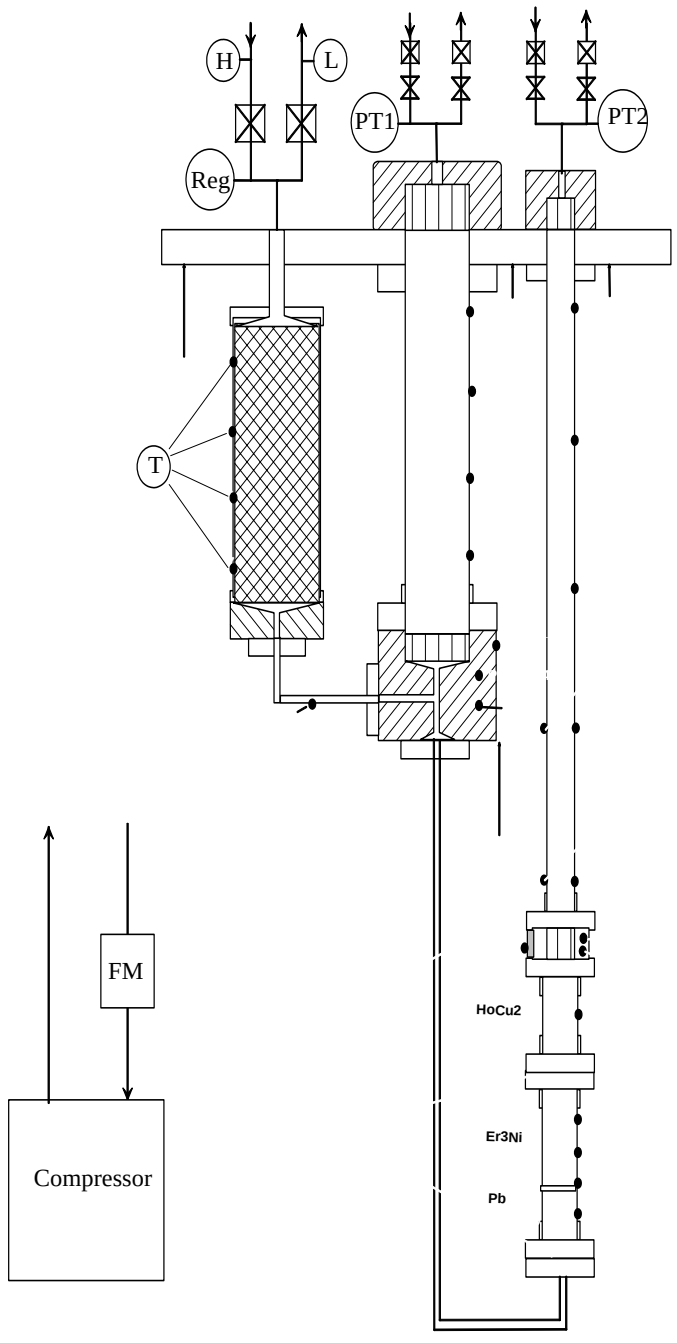

Fig. 10-1 Scheme of a 'valved' two-stage PTR with sensors for pressures (H, L, Reg, Pt1, PT2), temperatures (T) and the mass flow (FM))

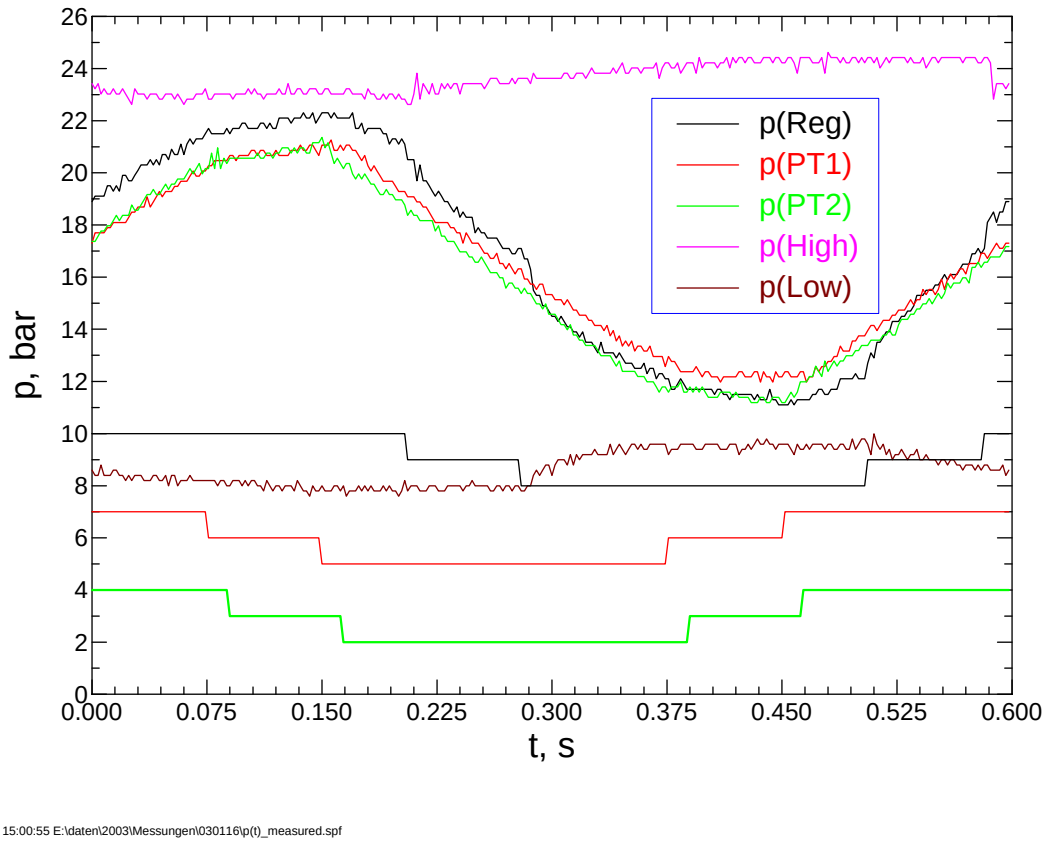

Fig. 10-2 Traces of pressures and valve timing

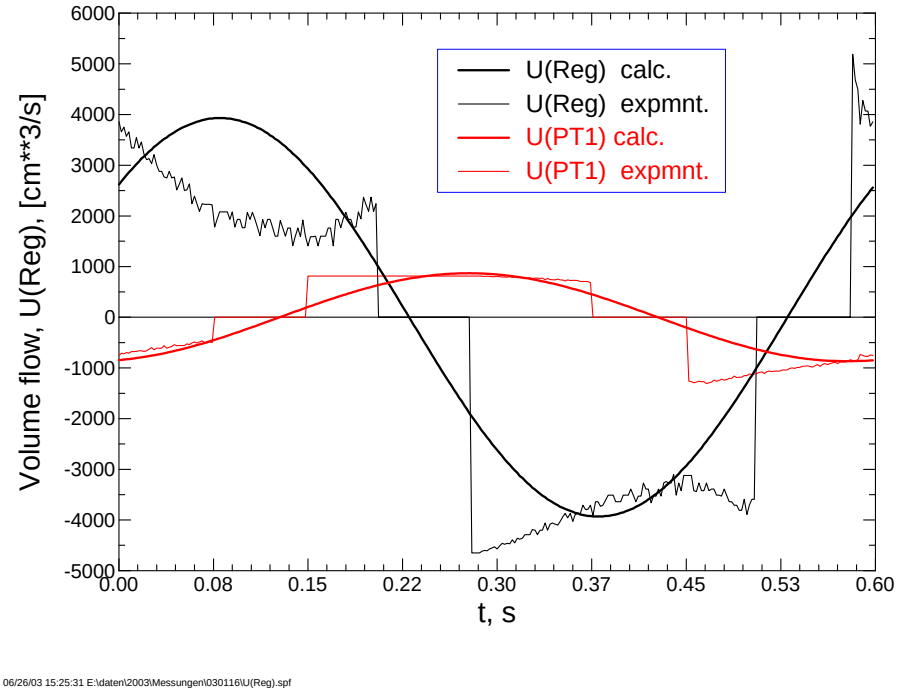

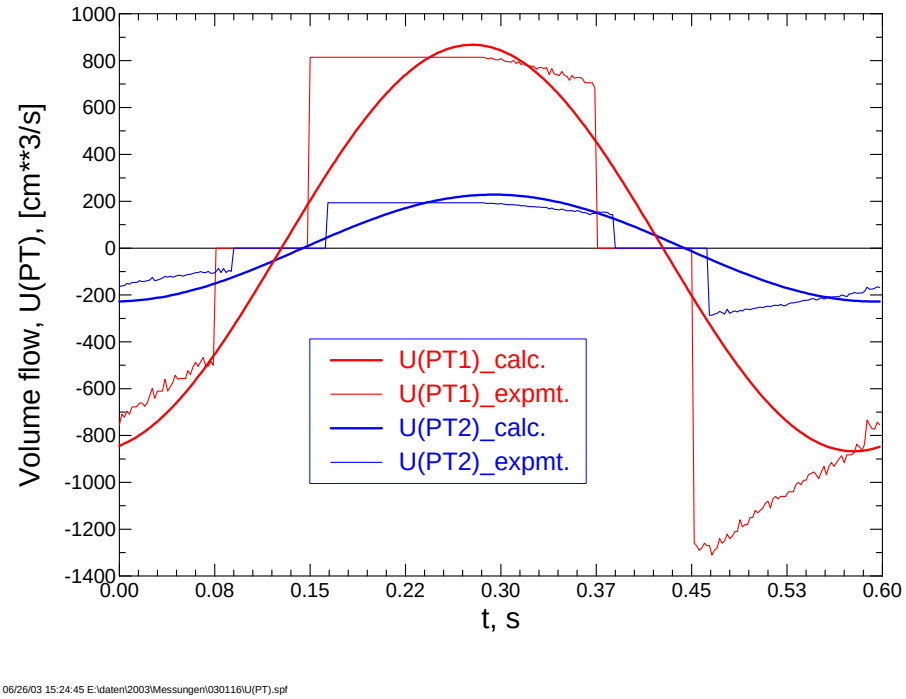

Fig. 10-3 Volume flows at the hot end of first stage regenerator and of first and second stage pulse tubes. Measurement on a valved PTR, calculation of theroacoustic model.

11 Thermally actuated drivers

So far we have seen that pulse tube coolers are operated so that large work flow is fed into the regenerator at the ambient temperature, and a relatively small work flow is available at its cold end. But this work flow will increase when the cold end temperature is increased by applying more power, and when the 'cold end' temperature becomes greater than the temperature at the compressor end, the work flow in the pulse tube may become greater than the work flow supplied by the compressor. In this case we will get a thermal amplifier, where the acoustic power supplied by the compressor is amplified by a heat flow applied at high temperature at the opposed end of the regenerator.

Now one can think to combine this kind of driver with a pulse tube cooler. The scheme of such a system is shown in Fig. 11-1. Two pulse tube systems are being operated in series. The temperatures in the different components will change as shown schematically in lower graph. In the first stage regenerator it will increase from ambient temperature (300 K) to an appreciably higher level of say 1000 K, and in the first stage pulse tube it will go back to 300 K. The second stage is a regular single-stage PTR. But the inlet impedance of the cooler section must be matched to the outlet impedance of the driver section. The performance of the cooler section will therefore be not as good as it was for the directly driven system as shown by example 1.

For treating such systems , the properties of stainless steel (jm=3), namely specific heat and thermal conductivity have been extended to 1100 K [Toul70] (only in the versions newer than 030623 of the code). A complete input file (**example 11**) of such a system is given in Fig. 11-2. The cooler section is mainly the same as in the previous example 2. where 111 W of 50 K cooling power have been achieved by using a 2 Hz compressor with 700 cm^3 swept volume. Here we has tried to get the same performance by using a half size compressor (300 cm3 swept volume). Its acoustic work flow will be amplified so that same 50 K cooling power can be achieved. It is found that this is achieved with 3100 W of heat power applied to the amplifier. The hot end temperature of its regenerator goes up to 1000 K. The output of this calculation will also show that the work flow entering into the second stage regenerator (the cooler) has increased from 1000 W to about 1100 W. The overall efficiency will not be much improved. But this process might be advantageous when bigger compressors are not available or when thermal power is much cheaper than electricity

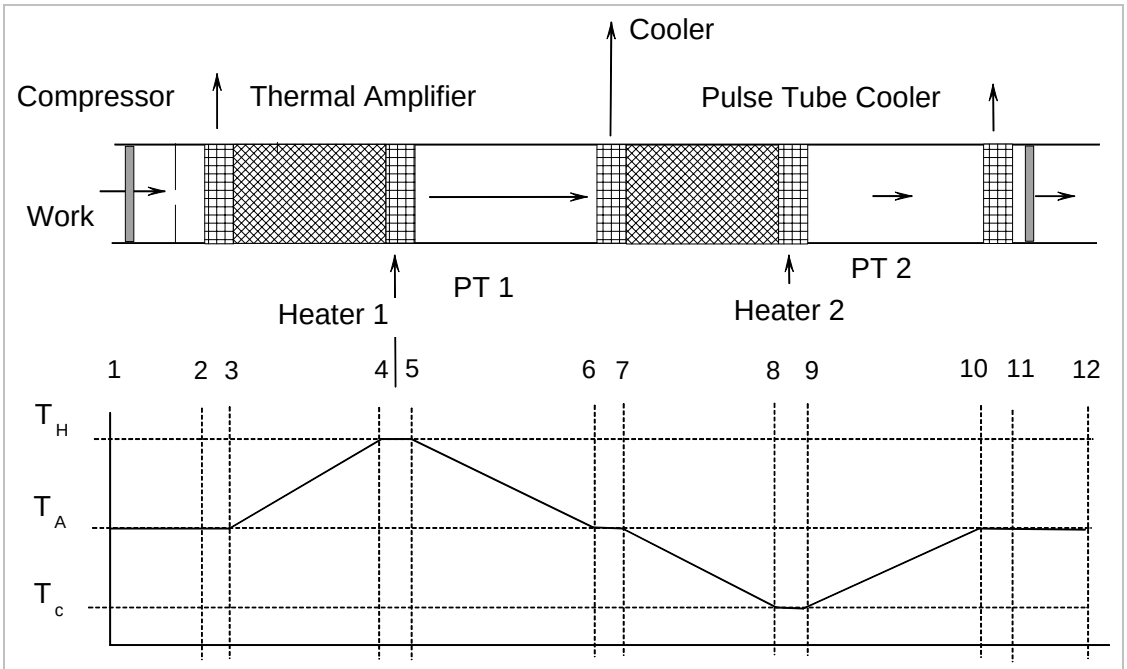

Fig. 11-1 Scheme of a pulse tube cooler combined with a 'thermal work flow amplifier'

e030916.txt - Editor

Datei Bearbeiten Suchen ?

```
30.09.03: Example 11: Single stage PTR with thermal amplifier
F       p0        p1/p0     SweptV   phi      TW       WREG1    WREG2       TOL
2       18E5      0.33      350e-6    45      300      0.001     0.001      1E-6

                          Length  TotalAr   b          bs         DeltaE    JMat  MSTEP   FRF      CDF   A/I
'1_ Tube Compr_Reg1 '     0.033   -1        29.0e-3     1.0e-3      0         3      1      1        1     'a'
'2_ Aftercooler     '     0.020   26.4E-4  103.0e-6    22.5e-6      0        1      1      1        1     'i'
'3_ Driver REG.     '     0.100   26.4E-4  49.21E-6    11.83E-6   -32        3     10      1        0.1   'a'
'4_ Heater          '     0.02    15.2e-4 103.0e-6    22.5e-6    3100       1      1      1        1     'i'
'5_ Branch st1/st2  '     1e-6      -1       2e-3       0.5e-3      0        3      1      1        1     'i'
'6_                 '     0         0        0          0           0        1      1      1        1     'a'
'7                  '     0         0        0          0           0        1      1      1        1     'a'
'8_                 '     0         0        0          0           0        1      1      1        1     'a'
'9_                 '     0         0        0          0           0        1      1      1        1     'i'
'10_                '     0         0        0          0           0        1      1      1        1     'a'
'11_                '     0         0        0          0           0        1      1      1        1     'a'
'12_                '     0         0        0          0           0        3      1      1        1     'a'
'13_                '     0         0        0          0           0        1      1      1        1     'a'
'14_                '     0         0        0          0           0        3      1      1        1     'a'
'15_ DriverPulseTube'     0.180     -1       22.0e-3     1.0e-3      0        3     10      1        1     'a'
'16_ WarmEnd HX1    '     0.02    15.2e-4 103.0e-6    22.5e-6   -3041       1      1      1        1     'i'
'17_ Cooler Reg.    '     0.130   15.20e-4 49.21e-6    11.83e-6     0        3     10      1        0.1   'a'
'18_ Cold End HX    '     0.02    15.2e-4 103.0e-6    22.5e-6      0        1      1      1        1     'i'
'19_CoolerPulseTube '     0.180     -1      22.0e-3      0.5e-3   112        3     10      1        1     'a'
'20_WarmEnd HX      '     0.02    15.2e-4 103.0e-6    22.5e-6      0        1      1      1        1     'i'
'Volumflow PT1/Reg2 '     0                 ! in percent (%)
'rel. dc-flow in PT1'     0.00
'rel. dc-flow in PT2'     0.000
'Compressor:        '
'Swept volume, m^3  '     50.0e-6
'Frequency of grid  '     50.0              ! in Hz
'He-Condensation    '     0.00    1.0e5     ! Low rate in kg/s,  Pressure in Pa,
'Zyklus,j=1, n=0    '     0
'List of suppl. var.'     1                 !ja=1, nein=0
'Variable in Col.10 '     21                !0 < integer < 23
'Variable in Col.11 '     22                !0 < integer < 23
*****************************************************************************************************
```

Fig. 11-2 Input data for calculation of a PTR combined with a 'thermal work flow amplifier'

12 Parallel tube regenerators and heat exchangers

In all previous examples the porous structures of regenerators and heat exchangers have been replaced by fictive arrays of parallel channels with inner radius b and wall thickness bs as derived in chapter 5.2. But the model can of cause also be applied structures which are really composed of real parallel tube structures. In the next example (**example 12**) it is assumed that the heat exchangers of the 60 Hz PTR as described by example 9 are composed of N circular channels with inner diameter 2b, wall thickness b_s, and the length L. The total cross sectional area is $\mathrm{totalAr} = N\pi(b + b_s)^2$.

The total cross sectional area of the pulse tube is about 1500 mm2. So it will be possible to replace the mesh type heat exchanger by 200 tubes with 1 mm i. d. and 0.5 mm wall. The total cross section area of this array is 628 mm^2. We assume that all heat exchangers, the aftercooler, CHX and WHX are made of identical units. It has not been intended to optimise the system. The main purpose is to find a consistent solution. The average gas temperature in the cold end heat exchanger has been set to 75 K. Further calculations of this heat exchanger must be done by hand. But some valuable parameters such as Reynolds number, depth of thermal penetration will be given when the key *'List of suppl. var.'* is actuated. Here we have the listing of Re and δ_s, the thermal penetration depth of the wall. The parallel tube heat exchangers are assumed to have 0.5 mm thick Cu walls. The thermal penetration length is about 0.75 mm for the room temperature heat exchangers, and it is 1.4 mm at 75 K. This indicates that the wall thickness should be reduced at least for the hot end HX. Also the loss work flow Wx in those heat exchangers (about 5 % for the aftercooler, as indicated in the output list) will give further advices for improving the heat exchangers.

Let us now consider the inertance tube. A total heat flow of about 300 W (the acoustic work flow extracted from the pulse tube) is to be rejected to ambient. The inner wetted surface is about 320 cm^2. The transversal heat flux with about 1 W/cm^2 could be transferred with a moderate temperature difference. The heat exchangers at both ends of the inertance tube would not be required in this case. But those calculations have been done with the flow resistance factor FRF=30. We do not yet know if this is a reasonable approach. If there are better arguments to use for a smaller flow resistance, the surface of the tube will become smaller so that the heat exchanger at the end facing the pulse tube will become advantageous.

It is not intended here to make a optimum design of such systems. The example should just show what kind of information can be obtained from such calculations.

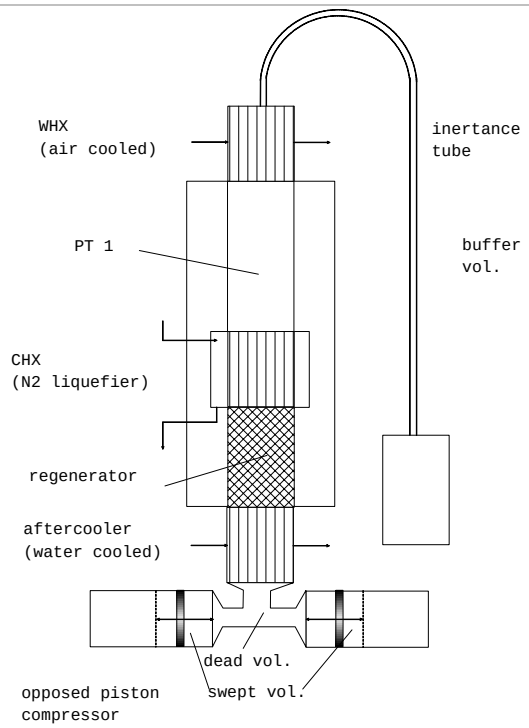

Fig. 12-1 Scheme of a PTR with parallel tube heat exchangers and inertance tube expander

e030916.txt - Editor

Datei Bearbeiten Suchen ?

```
30.09.03: Example 12: Single stage 60Hz-PTR with parallel tube HX and innertance tube phase shifter
F      p0       pl/p0    SweptV   phi     TW      WREG1   WREG2       TOL
60    17.0E5    0.2      88e-6    45      300     0.001    0.001      1E-6

                        Length  TotalAr   b         bs        DeltaE    JMat  MSTEP   FRF     CDF   A/I
'1_ Dead volume '       0.033   -1        29.0e-3    1.0e-3     0         3      1      1       1     'a'
'2_ Aftercooler     '   0.050   6.28E-4   0.5e-3     0.5e-3    61.        1      1      5       1     'a'
'3_ 1. REG.         '   0.065   26.4E-4   49.21E-6   11.83E-6   0         3     20      1       0.1   'a'
'4_                 '   0         0       0          0         0         1      1      1       1     'a'
'5_ Branch st1/st2  '   1e-6     -1        2e-3       0.5e-3    0         3      1      1       1     'a'
'6_                 '   0         0       0          0         0         3      1      1       1     'a'
'7_                 '   0         0       0          0         0         3      1      1       1     'a'
'8_                 '   0         0       0          0         0         1      1      1       1     'a'
'9_                 '   0         0       0          0         0         3      1      1       1     'a'
'10_                '   0         0       0          0         0         1      1      1       1     'a'
'11_                '   0         0       0          0         0         1      1      1       1     'a'
'12_                '   0         0       0          0         0         1      1      1       1     'a'
'13                 '   0         0       0          0         0         1      1      1       1     'a'
'14_                '   0         0       0          0         0         1      1      1       1     'a'
'15_Cold end HX     '   0.05     6.28e-4   0.5e-3     0.5e-3   234        1      1      5       1     'a'
'16_Pulse tube      '   0.120   -1        22.00e-3   0.5e-3     0         3     20      1       1     'a'
'17_WarmEnd HX      '   0.05     6.28e-4   0.5e-3     0.5e-3  -294        1      1      5       1     'a'
'18_Inertance Tube  '   1.445   -1        3.5e-3     0.5e-3     0.0       3     20     10       1     'a'
'19_Buffer HX       '   0         0       0          0         0         1      1      1       1     'a'
'20_Buffer volume   '   0.1855  -1       30.00e-3    1.0e-3     0         3     20      1       1     'a'
'Volumflow PT1/Reg2 '   0                ! in percent (%)
'rel. dc-flow in PT1'   0.00
'rel. dc-flow in PT2'   0.000
'Compressor:        '
'Swept volume, m^3  '   50.0e-6
'Frequency of grid  '   50.0             ! in Hz
'He-Condensation    '   0.00    1.0e5    ! Low rate in kg/s,  Pressure in Pa,
'Zyklus,j=1, n=0    '   0
'List of suppl. var.'   1                !ja=1, nein=0
'Variable in Col.10 '   21               !0 < integer < 23
'Variable in Col.11 '   13               !0 < integer < 23
*****************************************************************************************************
```

Fig. 12-2 Input data for a single stage PTR with parallel tube heat exchangers and inertance tube phase shifter.

13 Further options

The previous examples have shown that wide variety of thermoacoustic engines and refrigerators can be treated with the executable file primarily configured for 20 segments of a two-stage pulse tube cooler. Many other problems can be treated with this code just by modification of the input data file. If more segments are required, the source code, written in Fortran, can easily be modified.

For a later version of the code, it is planned to control the number of segments from the input list so that more segments can be added. The author has experienced that it is no problem to extend the calculations to 3 and more stages. Also other correlations for pressure drop and heat transfer can be implemented. Other regenerator materials can implemented by adding a table of specific heat and thermal conductivity data. Most of such modifications which are do be done in the Fortran source code, are rather simple. But they should be done by the author or at least in close contact with the author where the compilation is being done with the Lahey/Fujitsu Fortran 95 compiler. Earlier work had been done on a LINUX platform with IBM AIX XL Fortran Compiler/6000. The numeric results where somewhat different, and in some cases the input data had be modified to achieve convergence. This has negligible physical significance, but it might confuse the non-experienced user.

14 Conclusion

It has been shown, that the present code can be used to study many different types of pulse tube coolers. All examples discussed here can be treated just by modification of a simple list of input data. No modification of the source code is required. But one should always have in mind that the code is based on small amplitude approximations. So one should not expect too high accuracy of the prediction. The code will be very valuable for getting a prototype design as base for further empiric improvements. It will also be very valuable to improve the understanding of the complicated thermal processes running in such systems.

15 References

[CFIC] www.cficing.com, Qdrive Pressure Wave Generators (Brochure 7/01)

[CRYODAT] Cryodata, Inc., http://www.cryodata.com/partners

[Eck97] http:/www.cryodata.com, Copyright: Eckels Engineering, 3322 Ebenezer Chase Drive, Florence SC 29501, 1997

[Gar85] Gary, J., Daney, D.E., and Radebaugh, R, A Computational Model for a Regenerator, Prc. Third Cryocooler Conference, NIST Special Publication 689 (1985) 199

[Gar91] Gary, J. and Radebaugh, R., An improved numerical model for calculation of regenerator performance (REGEN3.1), Proc. Fourth Interagency Meeting on Cryocoolers,David Taylor Research Center, Report DTRC-91/003 (1991) 165

[Ged95] D. Gedeon, Sage: Object-Oriented Software for Cryocooler Design, Cryocoolers 8 (Ed. by R.G. Ross, Jr.) Plenum Press, New York 1995, p281-292

[Han75] B. A. Hands: A computer programme for the thermodynanic and thermophysical properties of helium - Second edition, Cryogenic Laboratory of University of Oxford, UK, Department Report 1121/75, June 1975

[HavBoe] Handbook of Haver & Boecker Wire weaving and Engineering Works, D.59282 OELDE, Germany

[Hof02] A. Hofmann, DC flow in pulse tube coolers, Adv. Cryog. Eng.: Proceedings of the Crygenic Engineering Conference, Vol. 47 (2002), p. 911-917

[Hof03] A. Hofmann, Liquefaction of Gases with Pulse Tube Coolers, Paper F-42 Subitted to 3rd Int Conf. on Cryogenics & Refrigeration, Hangzhou, China (The conference has been postponed from April 22-25, 2003 to the end of 2003)

[Hof99] A. Hofmann and H. Pan, Phase shifting in pulse tube refrigerators, Cryogenics 39 (1999) 529-537

[Kays84] W.M. Kays and A.L. London, Compact Heat Exchangers (Third Edition), McGraw-Hill Book Comp. NY 1984, ISBN 0.07-033418-8

[Luo03b] E. Luo, Inertance Tube Models and their Experimental Verification, CEC/ICMC 2003, Sept. 22-26, Anchorage, USA, Paper C2-G-03

[Lew98] M.A. Lewis, T. Kuriyama, F. Kuriyama, and R. Radebaugh, Measurement of heat conduction through stacked screens, Adv. Cryog. Eng, Vol 43 (1998), 1611

[Luo03] E. Luo, Inertance Tube Models and their Experimental Verification, CEC/ICMC 2003, Sept. 22-26, Anchorage, USA, paper C2-G-03

[Man55] E. Manegold: Kapillarsysteme, Bd. 1, Strassenbau, Chemie und Technik Verlags-GmbH, Heidelberg 1955, p. 422

[Merk75] Merkli, P. and Thomann, H., Transition to turbulence in oscillation pipe flow; J. Fluid Mech. Vol. 68 (1975) 567

[Nam02] K. Nam and S. Jeong, Experimental study on regenerators under actual operating conditions, Adv. Cryog. Eng., Vol. 47 (2002) 977

[Nam02b] Nam, K. and Jeong, S., Experimental study on regenerators under actual operating conditions, Adv. Cryog. Eng. , Vol. 47 (2002) 977

[PlotIT] Scientific Programming Enterprises, POB 669 Haslet, Mi 48840, spe@plotit.com

[Rad03] R. Radebaugh, M.A. Lewis, E. Luo, J.M. Pfotenhauer, G.F. Nellis, L.A. Schunk, Inertance Tube Optimization for Pulse Tube Refrigerators, CEC/ICMC 2003, Sept. 22-26, Ancharage, USA, paper C2-G-04

[Rott75] Rott, N. Thermally driven acoustic oscillations, Part III: Second order heat flux, ZAMP 26 (1975) 43

[Rott80] Rott, N. Thermoacoustics, Adv. Appl. Mech. 20 (1980) 135

[Schunk03] L.O. Schunk, J.M. Pfotenhauer, G.F. Nellis, Inertance Tubes for kW-Class Pulse Tubes, CEC/ICMC 2003, Sept. 22-26, Anchorage, USA , paper C1-B-02

[Sto90] P.J. Storch, R. Radebaugh, and J.E. Zimmermann, Analytic Model for the Refrigeration Power of an Orifice Pulse Tube Refrigerator, NIST Technical Note 1343 (1990)

[Swift97] G.W. Swift, Thermoacoustics, Encyclopedia of Applied Physics, Vol. 21 (1997) 245-264

[Toul70] Touloukian, Y.S. and Buyco, E.H., Thermophysical Properties of Matter, Vol.4 , p. 708 (Specific Heat) and Vol. 1, p 1174 (Thermal Conductivity of Metallic Elements and Alloys), Plenum, New York and Washington 1970)

[VDI77] VDI Wärmeatlas, VDI-Verlag Düsseldorf, 3. Auflage (1977) S. Le1

[War94] W.C. Ward and G.W. Swift, Design Environment for Low-amplitude Thermoacoustic Engines, J. Acoust Soc. Am., Vol 95 (1994) 3671
(http://www.lanl.gov/thermoacoustics/announce.html)

[Xiao95] J.H. Xiao
Thermoacoustic heat transportation and energy transformation
Part 1: Formulation of the problem, Cryogenics 35 (1995) 15

Appendix A Typical numeric output of a two-stage cooler

```
 Programm ptr030916
 --------------------------
 F      =   2.00     Hz
 P0     =   0.170E+07  Pa
 p1/p0  =  0.3300
 SweptV = 0.700E-03 m**3
 PHI    =   45.00
 TW     =   300.0      K
 Wreg1  =    0.0010  m
 Wreg2  =    0.0010  m
 TOL    =  0.1E-05
```

	x	TotalAr	b	bs	DeltaE	jMat	mstep	FRF	CDF	A/I
1_ Tube Compr_Reg1	1.000	-1.00	0.500E-02	0.100E-02	0.00	3	1	1.00	1.00	a
2_ Aftercooler	0.000	0.264E-02	0.540E-04	0.840E-05	0.00	1	1	1.00	1.00	a
3_ 1. REG. Part 1	0.130	0.264E-02	0.492E-04	0.118E-04	24.50	3	10	1.00	0.10	a
4_ 1. REG. Part2	0.000	0.264E-02	0.234E-04	0.225E-04	0.00	14	1	1.00	1.00	a
5_ Tube REG1/PT1	0.050	-1.00	0.250E-02	0.100E-02	40.00	1	1	1.00	1.00	a
6_ Flow Conditioner	0.018	0.152E-02	0.492E-04	0.118E-04	0.00	1	1	1.00	1.00	i
7_ 1.PulseTube	0.180	-1.00	0.225E-01	0.100E-02	0.00	3	10	1.00	1.00	a
8_ WARMEND HX1	0.020	0.152E-02	0.492E-04	0.118E-04	0.00	1	1	1.00	1.00	a
9_ Tube PT1 to Exp.	0.060	-1.00	0.200E-02	0.500E-03	0.00	3	1	1.00	1.00	a
10_Tube PT1/Reg2	0.010	-1.00	0.250E-02	0.500E-03	5.22	1	1	1.00	1.00	a
11_2. Reg. spacer 1	0.002	0.452E-03	0.492E-04	0.118E-04	0.00	1	1	1.00	1.00	a
12_2. Reg. Pb	0.050	0.452E-03	0.234E-04	0.225E-04	0.00	14	10	1.00	0.10	a
13_2. REG. spacer 2	0.002	0.452E-03	0.492E-04	0.118E-04	0.00	1	1	1.00	1.00	a
14_2. Reg. Er3Ni	0.070	0.452E-03	0.234E-04	0.225E-04	0.00	62	10	1.00	1.00	a
15_2. Reg. Spacer 3	0.002	0.452E-03	0.492E-04	0.118E-04	0.00	1	1	1.00	1.00	a
16_2. TubeReg2PT2	0.050	-1.00	0.100E-02	0.500E-03	0.00	3	1	1.00	1.00	a
17_ColdEnd HX2	0.020	0.254E-03	0.540E-04	0.840E-05	0.54	3	10	1.00	1.00	i
18_2.Pulse Tube	0.300	-1.00	0.900E-02	0.500E-03	0.00	3	10	1.00	1.00	a
19_Warmend HX2	0.020	0.254E-03	0.540E-04	0.840E-05	0.00	1	1	1.00	1.00	i
20_Tube PT2/Exp.2	0.000	-1.00	0.300E-02	0.100E-02	0.00	3	1	1.00	1.00	a

```
  mdot =  3.788E-03 (kg/s)     approx. mass flow into first stage regenerator

 Working Gas: Helium
 Volume Flow in PR 1, % :    ,   7.0E+01
 rel. dc-flow in PT 1, % :     0.000
 rel. dc-flow in PT 2, % :    1.8000E-03
```

(A)

1_ Tube Compr_Reg1

x m	T K	p bar	Ph(p) °	U cm**3/s	Ph(U) °	Wx W	Qx W	Ex W	Val(12) SI	Val(21) SI
0.0000	300.00	5.61000	1.000	4398.230	45.000	887.452	0.000	887.452		
1.0000	303.84	5.62124	0.795	4228.052	42.921	881.360	5.956	887.316		

2_ Aftercooler

x m	T K	p bar	Ph(p) °	U cm**3/s	Ph(U) °	Wx W	Qx W	Ex W	Val(12) SI	Val(21) SI
0.0000	303.84	5.62124	0.795	4228.052	42.921	881.360	-881.496	-0.136		
0.0000	303.84	5.62123	0.795	4228.047	42.921	881.359	-881.495	-0.136		

3_ 1. REG. Part 1

x m	T K	p bar	Ph(p) °	U cm**3/s	Ph(U) °	Wx W	Qx W	Ex W	Val(12) SI	Val(21) SI
0.0000	303.84	5.62123	0.795	4228.048	42.921	881.359	-856.995	24.364		
0.0130	277.82	5.56691	0.295	3815.966	41.954	793.556	-768.271	25.286		
0.0260	248.99	5.52038	-0.129	3373.703	40.874	702.767	-676.460	26.307		
0.0390	216.40	5.48186	-0.473	2890.314	39.631	605.949	-578.488	27.461		
0.0520	179.42	5.45156	-0.735	2361.113	38.138	501.055	-472.283	28.772		
0.0650	137.66	5.42946	-0.918	1785.722	36.224	386.437	-356.184	30.253		
0.0780	90.37	5.41526	-1.027	1162.807	33.476	259.463	-227.529	31.934		
0.0910	46.01	5.40802	-1.077	609.293	28.668	143.046	-109.518	33.528		
0.1040	40.42	5.40374	-1.099	517.716	21.406	129.228	-95.495	33.733		
0.1170	40.37	5.39969	-1.114	493.117	13.203	128.999	-95.264	33.735		
0.1300	40.34	5.39571	-1.121	479.646	4.362	128.809	-95.073	33.736		

(B)

5_ Tube REG1/PT1

x m	T K	p bar	Ph(p) °	U cm**3/s	Ph(U) °	Wx W	Qx W	Ex W	Val(12) SI	Val(21) SI
0.0000	40.34	5.39571	-1.121	479.646	4.362	128.809	-95.073	33.736		
0.0500	41.37	5.39572	-1.156	479.963	3.998	128.964	-95.266	33.698		

6_ Flow Conditioner

x m	T K	p bar	Ph(p) °	U cm**3/s	Ph(U) °	Wx W	Qx W	Ex W	Val(12) SI	Val(21) SI
0.0000	41.37	5.39572	-1.156	335.974	3.998	90.275	-16.577	73.698		

```
  0.0180  41.37  5.38836    -1.156   336.083    -6.558    90.145   -16.447    73.698

7_ 1.PulseTube

     x       T     p       Ph(p)    U          Ph(U)       Wx      Qx         Ex       Val(12)     Val(21)
     m       K    bar       °       cm**3/s     °          W       W          W         SI          SI
  0.0000  41.37  5.38836    -1.156   336.083    -6.558    90.145   -16.447    73.698
  0.0180 116.60  5.38836    -1.156   351.698   -18.125    90.628   -16.930    73.698
  0.0360 177.99  5.38836    -1.156   379.130   -28.642    90.615   -16.917    73.698
  0.0540 226.01  5.38836    -1.156   416.652   -37.615    90.283   -16.586    73.698
  0.0720 261.44  5.38836    -1.156   461.970   -45.020    89.736   -16.038    73.698
  0.0900 286.00  5.38836    -1.156   513.051   -51.042    89.060   -15.362    73.698
  0.1080 301.76  5.38836    -1.156   568.314   -55.929    88.318   -14.620    73.698
  0.1260 310.72  5.38835    -1.156   626.598   -59.914    87.556   -13.858    73.698
  0.1440 314.57  5.38835    -1.156   687.079   -63.192    86.802   -13.104    73.698
  0.1620 314.71  5.38835    -1.156   749.172   -65.914    86.073   -12.375    73.698
  0.1800 312.23  5.38835    -1.156   812.468   -68.199    85.378   -11.680    73.698

8_ WARMEND HX1

     x       T     p       Ph(p)    U          Ph(U)       Wx      Qx         Ex       Val(12)     Val(21)
     m       K    bar       °       cm**3/s     °          W       W          W         SI          SI
  0.0000 312.23  5.38835    -1.156   812.468   -68.199    85.378   -11.680    73.698
  0.0200 305.44  5.37572    -0.819   866.712   -70.171    82.150    -8.452    73.698

9_ Tube PT1 to Exp.

     x       T     p       Ph(p)    U          Ph(U)       Wx      Qx         Ex       Val(12)     Val(21)
     m       K    bar       °       cm**3/s     °          W       W          W         SI          SI
  0.0000 305.44  5.37572    -0.819   866.712   -70.171    82.150    -8.452    73.698
  0.0600 305.01  5.37340    -0.809   868.292   -70.223    82.025    -8.327    73.698

10_Tube PT1/Reg2

     x       T     p       Ph(p)    U          Ph(U)       Wx      Qx         Ex       Val(12)     Val(21)
     m       K    bar       °       cm**3/s     °          W       W          W         SI          SI
  0.0000  41.37  5.39572    -1.156   143.989     3.998    38.689   -33.467     5.222
  0.0100  42.18  5.39571    -1.158   144.076     3.748    38.727   -33.535     5.193

11_2. Reg. spacer 1

     x       T     p       Ph(p)    U          Ph(U)       Wx      Qx         Ex       Val(12)     Val(21)
     m       K    bar       °       cm**3/s     °          W       W          W         SI          SI
  0.0000  42.18  5.39571    -1.158   144.076     3.748    38.727   -33.535     5.193
  0.0020  42.20  5.39425    -1.159   143.974     2.933    38.733   -33.541     5.192

12_2. Reg. Pb

     x       T     p       Ph(p)    U          Ph(U)       Wx      Qx         Ex       Val(12)     Val(21)
     m       K    bar       °       cm**3/s     °          W       W          W         SI          SI
  0.0000  42.20  5.39425    -1.159   143.974     2.933    38.733   -33.541     5.192
  0.0050  30.41  5.35526    -1.186   104.147     1.929    27.846   -22.216     5.630
  0.0100  12.81  5.33356    -1.196    40.643     0.287    10.835    -4.489     6.346
  0.0150   8.64  5.32197    -1.198    31.930    -1.164     8.497    -1.957     6.539
  0.0200   8.54  5.31003    -1.197    31.856    -2.297     8.456    -1.913     6.543
  0.0250   8.52  5.29805    -1.193    31.856    -3.413     8.432    -1.888     6.544
  0.0300   8.50  5.28606    -1.187    31.869    -4.518     8.409    -1.864     6.545
  0.0350   8.47  5.27403    -1.179    31.894    -5.611     8.385    -1.839     6.546
  0.0400   8.45  5.26197    -1.168    31.929    -6.691     8.361    -1.814     6.547
  0.0450   8.43  5.24988    -1.154    31.975    -7.758     8.338    -1.790     6.548
  0.0500   8.40  5.23776    -1.138    32.032    -8.811     8.314    -1.765     6.549

13_2. REG. spacer 2

     x       T     p       Ph(p)    U          Ph(U)       Wx      Qx         Ex       Val(12)     Val(21)
     m       K    bar       °       cm**3/s     °          W       W          W         SI          SI
  0.0500   8.40  5.23776    -1.138    32.032    -8.811     8.314    -1.765     6.549
  0.0520   8.41  5.23737    -1.137    32.098    -9.639     8.313    -1.764     6.549

14_2. Reg. Er3Ni

     x       T     p       Ph(p)    U          Ph(U)       Wx      Qx         Ex       Val(12)     Val(21)
     m       K    bar       °       cm**3/s     °          W       W          W         SI          SI
  0.0520   8.41  5.23737    -1.137    32.098    -9.639     8.313    -1.764     6.549
  0.0590   4.62  5.21865    -1.105    29.313   -10.478     7.547    -0.887     6.659
  0.0660   4.57  5.19949    -1.069    29.368   -11.201     7.516    -0.855     6.660
  0.0730   4.51  5.18025    -1.031    29.427   -11.910     7.485    -0.823     6.662
  0.0800   4.45  5.16092    -0.989    29.490   -12.604     7.454    -0.791     6.663
  0.0870   4.39  5.14150    -0.943    29.556   -13.284     7.423    -0.759     6.664
  0.0940   4.33  5.12200    -0.895    29.626   -13.949     7.391    -0.726     6.665
  0.1010   4.26  5.10240    -0.843    29.698   -14.600     7.359    -0.693     6.666
  0.1080   4.19  5.08270    -0.788    29.774   -15.237     7.327    -0.660     6.667
  0.1150   4.13  5.06291    -0.729    29.853   -15.860     7.295    -0.627     6.669
  0.1220   4.05  5.04302    -0.667    29.934   -16.469     7.263    -0.593     6.670

15_2. Reg. Spacer 3

     x       T     p       Ph(p)    U          Ph(U)       Wx      Qx         Ex       Val(12)     Val(21)
     m       K    bar       °       cm**3/s     °          W       W          W         SI          SI
  0.1220   4.05  5.04302    -0.667    29.934   -16.469     7.263    -0.593     6.670
  0.1240   4.06  5.04257    -0.666    29.990   -16.847     7.262    -0.592     6.670

16_2. TubeReg2PT2

     x       T     p       Ph(p)    U          Ph(U)       Wx      Qx         Ex       Val(12)     Val(21)
     m       K    bar       °       cm**3/s     °          W       W          W         SI          SI
```

```
  0.1240   4.06  5.04257    -0.666    29.990   -16.847     7.262    -0.592     6.670
  0.1740   4.20  5.03887    -0.777    30.006   -16.950     7.261    -0.593     6.667

17_ColdEnd HX2

     x       T     p       Ph(p)    U          Ph(U)       Wx      Qx         Ex       Val(12)     Val(21)
     m       K   bar       °       cm**3/s     °          W        W          W         SI          SI
  0.0000   4.20  5.03887    -0.777    30.006   -16.950     7.261    -0.058     7.202
  0.0020   4.20  5.03798    -0.774    30.044   -17.198     7.259    -0.057     7.202
  0.0040   4.20  5.03710    -0.771    30.083   -17.445     7.258    -0.056     7.202
  0.0060   4.20  5.03621    -0.768    30.122   -17.691     7.257    -0.054     7.202
  0.0080   4.20  5.03532    -0.765    30.162   -17.937     7.255    -0.053     7.202
  0.0100   4.20  5.03444    -0.762    30.202   -18.182     7.254    -0.052     7.202
  0.0120   4.20  5.03355    -0.759    30.243   -18.427     7.252    -0.050     7.202
  0.0140   4.20  5.03266    -0.756    30.284   -18.670     7.251    -0.049     7.202
  0.0160   4.20  5.03176    -0.753    30.326   -18.913     7.250    -0.047     7.202
  0.0180   4.20  5.03087    -0.750    30.368   -19.155     7.248    -0.046     7.202
  0.0200   4.20  5.02998    -0.746    30.411   -19.397     7.247    -0.044     7.202

18_2.Pulse Tube

     x       T     p       Ph(p)    U          Ph(U)       Wx      Qx         Ex       Val(12)     Val(21)
     m       K   bar       °       cm**3/s     °          W        W          W         SI          SI
  0.0000   4.20  5.02998    -0.746    30.411   -19.397     7.247    -0.044     7.202
  0.0300   16.20  5.02996    -0.747    33.055   -29.836     7.265    -0.534     6.731
  0.0600   65.15  5.02995    -0.747    43.634   -49.537     7.230    -2.334     4.895
  0.0900  133.59  5.02994    -0.747    58.607   -62.459     6.985    -4.528     2.457
  0.1200  196.77  5.02994    -0.747    75.710   -70.574     6.567    -6.350     0.216
  0.1500  244.48  5.02993    -0.747    93.797   -75.879     6.053    -7.527    -1.474
  0.1800  276.52  5.02993    -0.747   112.291   -79.486     5.515    -8.124    -2.609
  0.2100  296.12  5.02992    -0.747   130.910   -82.023     4.994    -8.297    -3.303
  0.2400  306.70  5.02992    -0.747   149.518   -83.860     4.509    -8.187    -3.678
  0.2700  311.02  5.02991    -0.747   168.053   -85.225     4.067    -7.898    -3.831
  0.3000  311.07  5.02990    -0.747   186.488   -86.262     3.668    -7.501    -3.833

19_Warmend HX2

     x       T     p       Ph(p)    U          Ph(U)       Wx      Qx         Ex       Val(12)     Val(21)
     m       K   bar       °       cm**3/s     °          W        W          W         SI          SI
  0.0000  311.07  5.02990    -0.747   186.488   -86.262     3.668    -7.501    -3.833
  0.0200  311.07  5.02736    -0.347   200.431   -86.561     3.327    -7.160    -3.833

20_Tube PT2/Exp.2

     x       T     p       Ph(p)    U          Ph(U)       Wx      Qx         Ex       Val(12)     Val(21)
     m       K   bar       °       cm**3/s     °          W        W          W         SI          SI
  0.0000  311.07  5.02736    -0.347   200.431   -86.561     3.327    -7.160    -3.833
  0.0000  311.07  5.02736    -0.347   200.431   -86.561     3.327    -7.160    -3.833

 Pressure drop           (Re(p), Imag(p) in bar:
 p(Reg1) - p(PT1) =,      0.25      0.15
 p(PT1)  - p(PT2) =,      0.35     -0.01

 Rate of Helium condensation  =    0.0000  g/s

 Check of compatibility between mass flow supplied by the compressor and the requirement of the cold head:
Mass flow supplied by compressor,     MFComp  =        4.545 g/s
Mass flow demanded at the cold head,  MFtotal =        4.524 g/s
Difference,                    MFKomp-MFtotal =        0.021 g/s
 In case of unacceptable difference, either the compression ratio p1/p0
 or the initial volume flow given by SweptV must be modified!
```

(B)

Appendix B Friction and heat transfer of porous beds

FZK/ITP, 18.10.02

Internal Report 0210, part 2

by A. Hofmann, FZK/ITP

Improved correlations for pressure drop and heat transfer in regenerators

Summary

The computer code used so far is based on the model that the porous regenerator is described by an array of long parallel channels with hydraulic diameter and with the length equal to the length of the regenerator. The inlet and outlet effects which contribute much to friction loss and to heat transfer have been neglected first. Later, an empirical factor for taking account of the enlarged friction factor had been introduced in the computer code. But this did not take account of heat transfer. Now the code has been improved by implementation of more realistic correlations for pressure drop and heat transfer as they are given in literature for porous beds of woven wires and of packed spheres.

Pressure drop

The code PTRyymmdd describes primarily the laminar flow (Hagen-Poiseuille) of compressible gas in circular channels. The inlet and outlet effects are neglected. In this case, the friction factor is

(1) $$f_D = \frac{64}{Re_D} \qquad or \qquad f_F = \frac{16}{Re_F}$$

with the Reynolds number

(2) $$Re = \frac{\rho u l}{\eta}$$

The difference by a factor of 4 in both expressions in Eq(1) can cause much confusion in literature. In the terminology of the Fanning friction factor as used in most US literature characteristic length of hydraulic diameter given by

(3) $$D_h = \frac{4 A_F L}{A_{HT}}$$

where A_F is the area of the flow cross section and A_{HT} is the heat transfer area (friction area). In the Darcy terminology as mostly used in non US literature the Reynolds number is based on the hydraulic radius given by

(4) $$r_h = \frac{A_F L}{A_{HT}}$$

Hence

(5) $$D_h = 4 r_h$$

In the frequently referenced book of Kays&London [1] the Reynolds number is normally based on the hydraulic diameter, but this is not always done consequently. Very careful examination is recommended. Data on pressure drop of randomly stacked sphere matrices are also given the 'VDI Wärmeatlas' [2]. Both results will be compared here. The hydraulic diameter for randomly packed spheres is given by [2]

(6) $$D_h = \frac{2}{3}\frac{\varepsilon}{1-\varepsilon} D_K$$

with porosity ε and sphere diameter D_K. The pressure drop is

(7) $$\Delta p = f_D \frac{\rho}{2}\left(\frac{U}{\varepsilon A_c}\right)^2 \frac{L}{D_h}$$

with

(8) $$f_D = 2.2\left(\frac{64}{Re_D} + \frac{1.8}{Re_D^{0.1}}\right) \qquad for \quad 2 < Re_D < 10^5$$

This numeric value is 4 times the value given by Kays&London [1] (Fig. 7-19 and Tab. 10-13). Both friction factors and also the laminar flow friction factor are plotted in Fig. 1. They do not differ significantly. Obviously the pressure drop is underestimated appreciably by using Eq(1). In the codes PTRyymmdd with 020625 < yymmdd < 021007 the enhanced pressure has been treated by multiplication with empirical factors FRF (friction resistance factor). The enhancement factor based on the present results is shown in **Fig. 2**. The Reynolds numbers in the regenerators of a typical 4 K cooler are plotted in **Fig. 3**. They are calculated for peak values of sinusoidal volume flow. (It might be more reasonable to consider the time averaged effective values which are reduced by a factor of 0.7). The plotted Reynolds numbers are in the range of 20 < Re < 100 in the first stage 200 mesh regenerator operated at 50 < T < 300 and they become close to 300 in the second stage regenerators. Hence the FRF factor can range up to 15. Newer PTR codes will be modified such that the factor f/f_{lam} is adapted continuously.

Sharp edge powders such as the Chinese rare earth materials can also be described with the given definitions. But the friction factor is higher than that of sphere packages. It cannot be predicted precisely a reasonable estimate is a factor of 1.3 to 2.0

above the sphere package. In the new codes yymmdd>021009 the FRF factor will describe this enhancement.

For mesh type regenerators the hydraulic diameter is given by

(9) $$D_{h,mesh} = D_{wire}\frac{\varepsilon}{1-\varepsilon}$$

The Fanning friction factor measured for steady flow is also given in [2]. In the range $Re_D < 150$ the 4 times higher Darcy friction factor is given by [3]

(10) $$f_{D,mesh} = 4*\left(\frac{51}{Re}+\frac{0.86}{Re^{0.12}}\right) \qquad for\ Re < 150$$

This factor is plotted in **Fig. 4** together with the friction factor for spheres. The difference of less than 20% in the range 10<Re<100, the range where mesh type regenerators are used, is not significant. In order to make the PTR code not too complicated all regenerators will be calculated with the sphere type friction factor given by Eq(10).

Conventional data [1,2] have been obtained for steady flow measurements. Recently it has been verified that Eq(10) is also valid for the mesh type regenerators operated at frequencies up to about 10 Hz [3]. But at 60 Hz, the ratio of oscillating to steady flow friction factor can become appreciably higher.

Heat transfer

It is known that the heat transfer will be improved with increasing friction factor. It is common practise to describe the heat transfer coefficient, *h*, by the Nusselt number

(11) $$Nu = \frac{hD_h}{k}$$

or by the equivalent Stanton number

(12) $$St = \frac{h}{Gc_p}$$

Both are functions of the Reynolds number. The correlation between both may be written as

(13) $$Nu = \frac{\eta c_p}{k} Re\, St = Pr\, Re\, St$$

For gas flow in randomly stacked sphere matrix Kays and London give

(14) $$St_{sphere} = 0.23\, Pr^{-2/3}\, Re^{-0.3}$$

and the respective Nusselt number becomes

(15) $$Nu_{sphere} = 0.23\,Pr^{1/3}\,Re^{0.7}$$

For randomly stacked woven screen matrix with a porosity of 0.602 the corresponding correlation is

(16) $$St_{mesh} = 0.49\,Pr^{-2/3}\,Re^{-0.39}$$

or $$Nu_{mesh} = 0.49\,Pr^{1/3}\,Re^{0.61}$$

(17)

The Nusselt number and hence the heat transfer coefficient will increase with the Reynolds number. For small Reynolds numbers it proves to be smaller than that of fully developed laminar flow in circular ducts, Nu_{lam}=3.66, and it is greater for higher Reynolds numbers. In **Fig. 5** the ratio of both is plotted for spheres and for mesh packages.

Further references on those topics have also been discussed by S. Wild [5].

Implementation of enhanced friction and heat transfer factors into the PTR code

The numeric code has been derived gas flow in very long circular channels. This means that fully developed laminar flow is assumed for calculating both the friction loss and the heat transfer from the gas to the matrix. The respective governing equations are [4]

(18a) $$\frac{d\tilde{p}}{dx} = -Z_F U$$

(18b) $$\frac{d\tilde{U}}{dx} = -\frac{1}{Z_C} + \beta_0 f_{WT}\,\frac{dT_0}{dx}\,\tilde{U}$$

(18c) $$\frac{dT_0}{dx} = \frac{\frac{1}{2}Re[\tilde{U}\tilde{p}^{*}(1 - T_0\beta_0 f_{qx})] - E_0}{A_f K_e}$$

(18d) $$\frac{dE}{dx} = h_w U_w (T_c - T_0)$$

Details on the significance of the different terms should be taken from [4]. Now it is the question how those equations are to be modified for taking account of the enhanced friction and heat transfer factors. The friction factor is embedded in the com-

plex impedance Z_F . The most simple way for taking account of the enhanced pressure drop is done by multiplication with the factor f/f_{lam} . This had been done in previous codes. On the other hand the heat transfer coefficient which is hidden in the terms f_{WT} and f_{qx} should also be increased with increasing friction factor. But those term do not only depend on the heat transfer from the wall to the solid matrix. They also describe in very complicated manner the heat flow within the matrix material. So they cannot be simply multiplied with factor Nu/Nu_{lam} for describing the non constant heat transfer coefficient of the gas.

Previous calculations have been done by using an empirical enhancement factor for increasing Z_F. Reasonable results are obtained with the factors FRF=4 for the first stage regenerator and with FRF<8 for the second stage. But too small refrigeration power is obtained by increasing the second stage FRF to 12 as it would result from Fig. 2 and Fig. 3. This shows that the modification of the heat transfer is also necessary.

Now another way is considered, namely to modify both the viscosity and the thermal conductivity of the gas for obtaining the correction terms for pressure drop and for heat transfer. The Reynolds numbers for gas flow in regenerator of low frequency pulse tube coolers are typically in the range 30<Re<300. And both quantities, the scaled friction factor, f/f_{lam}, and the scaled Nusselt number, Nu/Nu_{lam}, increase linearly by a factor of 5 in this range. For taking account of those effects, the viscosity and the thermal conductivity will be scaled with the factors

(19) $$F_\eta = \frac{f}{f_{lam}} = 2.62 + 0.033\,Re$$

and

(20) $$F_k = \frac{Nu}{Nu_{lam}} = 0.0845\,Re^{0.65}$$

Those correlation result from linear curve fits of the plots in Fig. 2 and Fig. 5, and Fk has been evaluated from the average spheres and mesh. With those terms, the friction factor can be written as

(21) $$f = f_{lam} F_\eta = \frac{64}{D_h G}\,\eta\, F_\eta$$

and the heat transfer coefficient becomes

(22) $$h = \frac{Nu}{D_h} k = \frac{Nu_{lam}}{D_h}\, k\, F_k$$

Hence the enhancement of those quantities is obtained by substitutions of viscosity η by ηF_η and the thermal conductivity k of the gas by kF_k.

Those correlations have been derived for porous packages operated at low frequencies (below 10 Hz). But for taking account of other packages such as sharp edge powders or for taking account of enhanced factors at higher operational frequencies, the factors F_η and F_k may be multiplied by an additional empirical enhancement fac-

tor. The parameter FRF in the input file of the computer code will be used for that purpose. The new code ptr021010.f results from the earlier code ptr020626.f just by adding the following lines in the subroutine FCN.

```
c 16.10.02: Regenerator an Werte von Kays&London angepasst
c ---------------------------------------------------------------------
      Re=DSQRT(y(3)*y(3)+y(4)*y(4))/Af*2*b/vis0*rho0
c Nur bei kleinem hydraulischen Durchmesser:
      if(b .lt. 0.1e-3) then
        k0=(k0*0.0845*Re**0.65)*flowres      !flowres ist äquivalent zu FRF
        vis0=vis0*(2.62+0.033*Re)*flowres
      else
        continue
      endif
c -------------------------------------------------------
```

Calculated results

The refrigeration power predicted with the new code is some what smaller than the prediction with ptr020625 when the empirical flow resistance factor FRF=5 was assumed. But the new code seems to be more realistic. The prediction for the 4K-Mark II, vers. 29.09.02 becomes 40W at 42 K + 0.62 W at 4.3 K for 200 mesh in the first stage regenerator and it is expected to become increased to 40W at 41K + 0.68 W when 170 mesh material is used. The improvement is less than predicted earlier (Report 0209, part 2).The respective list of input parameters e021010.txt is attached together with the compiled file ptr021010.exe. The so calculated pressure drop is about 2 bar peak to peak in the first stage and 0.5 bar peak to peak in the second stage. It proves to be close to measured values (see Monthly report June 2002).

REFERENCES

1) W.M. Kays and A.L. London, Compact Heat Exchangers (Third Edition), McGraw-Hill Book Comp. 1984, ISBN 0-07-033418-8

2) VDI Wärmeatlas , VDI-Verlag Düsseldorf 3. Auflage (1977) , Seite Le1

3) K. Nam and S. Jeong, Experimental study on the regenerators under actual operating conditions, Adv. Cryog. Eng. Vol.47(2002)977

4) J.H. Xiao, Thermoacoustic heat transportation and energy transformation, Part 1, Cryogenics 35(1995),15

5) S. Wild, Untersuchungen ein- und zweistufiger Pulsrohrkühler, Dissertation Universität Karlsruhe 1997

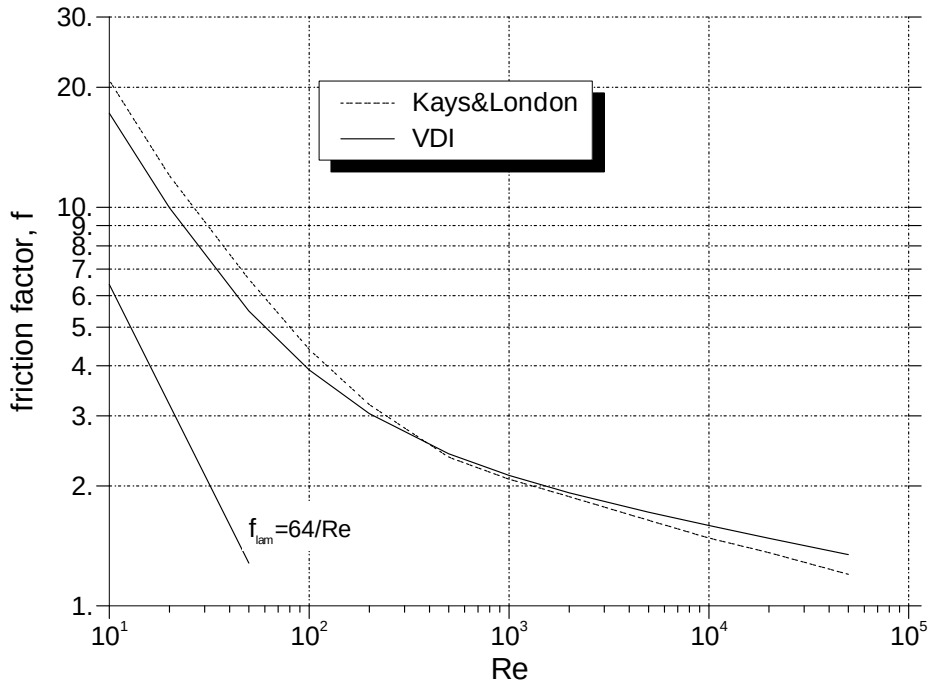

Fig. 1: Friction factor for randomly packed spheres given in [1] and in [2] and laminar flow friction factor plotted versus $Re_D=(\rho U D_h)/(\varepsilon A_c \eta)$, (U=volume flow rate)

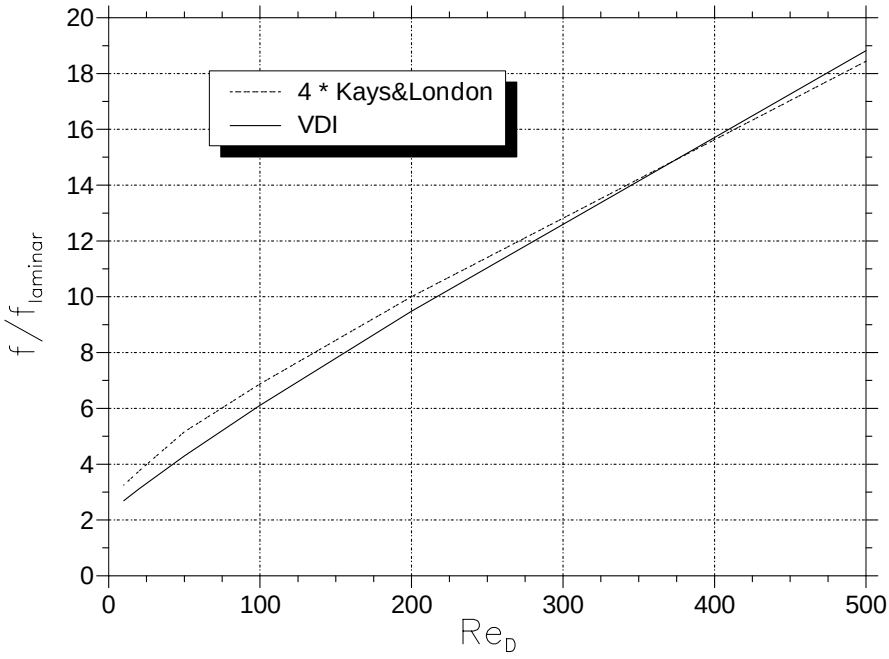

Fig. 2: Ratio of random sphere bed to laminar flow friction factor

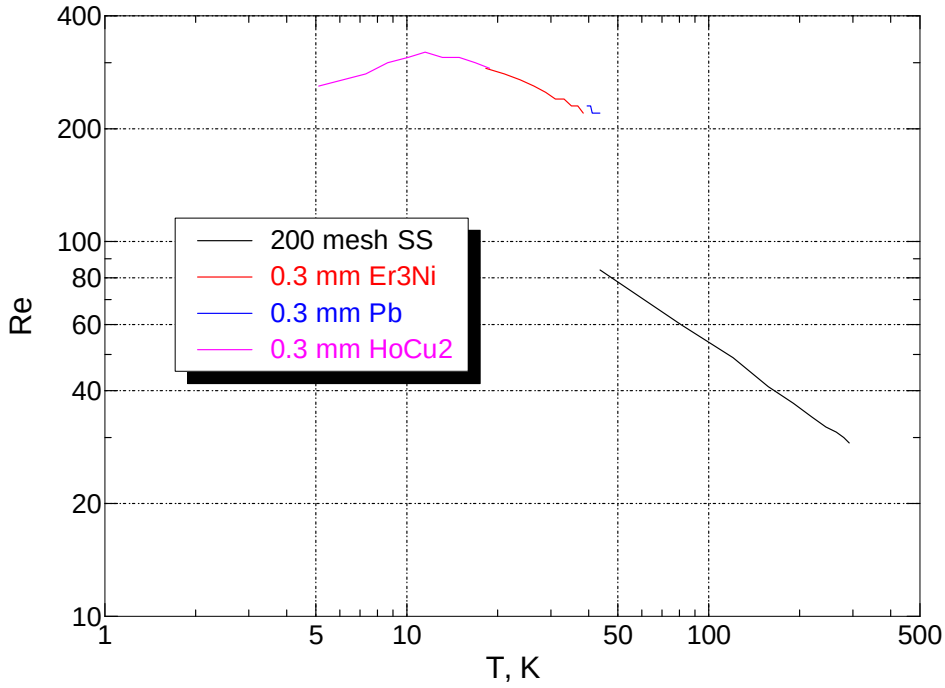

Fig. 3: Reynolds number in the regenerators of a 4 K PTR

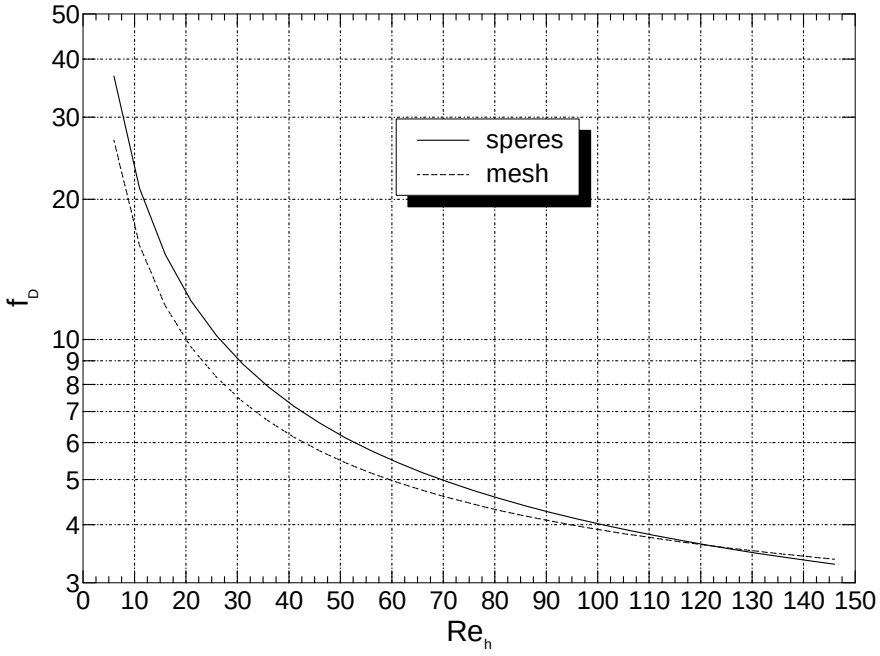

Fig. 4: Friction factors of randomly stacked woven screen [1,3] and of randomly stacked spheres matrices [2].

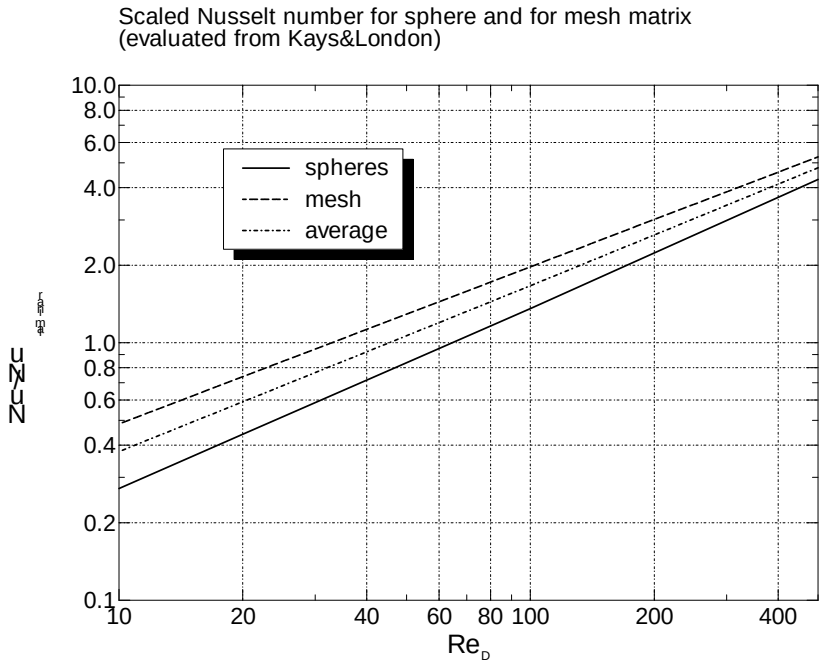

Fig. 5: Nusselt numbers of randomly stacked sphere of woven screen matrix [1] scaled with Nu_{lam} of fully developed laminar flow in circular channels.

Appendix C List of materials to be selected by the parameter 'jmat'

Pick a material by number from the following list.

a) Materials evaluated from CRYOPROP, Vers.3.01 (0< jm < 61)

jmat: description

1: Copper (specified by RRR and magnetic field, B)
2: Aluminum (specified by RRR and magnetic field, B)
3: 304 Stainless Steel
4: G-10 (fiberglass-epoxy), parallel to warp fibers
5: G-10 (fiberglass-epoxy), parallel to fill fibers
6: G-10 (fiberglass-epoxy), normal to cloth layer
7: Beryllium
8: Niobium
9: Inconel 718, annealed
10: Inconel 718, cold worked
11: Titanium
12: Epoxy
13: YBCO
14: Pb-Sn soft solder
15: Polyamide (Nylon 6), PA6
16: Pyrex Glass
17: Silver
18: Gold
19: Quartz (Single Crystal [100])
20: Sapphire, polycrystalline
21: 6061-T6 Aluminum
22: Indium
23: Teflon (Polytetrafluoroethylene, PTFE)
24: Invar-36
25: Polyethylene, parallel to sheet
26: Polyethylene, normal to sheet
27: Quartz glass
28: Manganin (84%Cu 12%Mn 4%Ni weight basis)
29: Beryllium copper (2 % Be)
30: Titanium alloy (Ti-6Al-4V)
31: Phosphor bronze (A alloy, 94Cu, 5Sn, .2P, ...)
32: Nickel, 4N5
33: Lead
34: Carbon Fiber Reinforced Plastic, CRFP parallel (T300)

35: Carbon Reinforced Plastic, CRFP normal to fiber (T300)
36: Copper Nickel, 90-10
37: Copper Nickel, 70-30
38: Constantan, Cu-Ni, 57-43%
39: Brass, 90-10% Cu-Zn, Commercial Bronze, CDA 22000
40: Brass, 80-20% Cu-Zn, Low Brass, CDA 24000
41: Brass, 70-30% Cu-Zn, Cartridge Brass, CDA 26000
42: Brass, 65-35% Cu-Zn, Yellow Brass, CDA 27000
43: Mylar, PET, amorphous, partly crystalline, typical MLI
44: Mylar, PET, semicrystalline, approximately 50%
45: Apiezon "N" Grease
46: Styrofoam, SpGr = 0.05
47: Styrofoam, SpGr = 0.1
48: Polystyrene, PS, unmodified, general purpose, SpGr = 1.04
49: Polycarbonate, PC, Amorphous extruded plate
50: 5083-T0 Aluminum Alloy (Annealed)
51: HDPE, High Density Polyethylene, SpGr.=0.94
52: Micarta, CE, Cotton Phenolic Composite, parallel to fiber
53: 1020 Steel
54: 9Ni Steel, 2800, ASTM A353
55: GE 7031 Lacquer, well dried in application
56: K Monel, annealed, 67Ni-30Cu-1.4Fe-1Mn
57: PCTFE, Kel-F, 50% crystallinity
58: NbTi Alloy
59: 7075-T6 Aluminum Alloy
60: 4340 Steel
61: Nb3Sn

b) Additional materials (61< jm < 67), only specific heat

62: Er3Ni, Interpolation G. Thummes (3.3.98), 2 < T< 20 K
63: ErNi, (Beijing University, China), interpolation for 2 < T< 20 K
64: ErNi0.8Co0.2, ((Beijing University, China), interpolation for 2 < T< 20 K
65: ErNi0.9Co0.1, Interpolation G. Thummes (3.3.98), 2 < T< 20 K
66: HoCu2 (Beijing University, China)
67: HoCu2 Toshiba

Appendix D Comments to the File of Input Data

Line 1 an2:	Comments
Line 3:	
F	fequency, 1/s
p0	mean gas pressure, Pa
p1/p0	pressure ration (amplitude/mean pressure)
SweptV	swept volume of (fictive) piston compressor
phi	Phase angle of volume flow at compressor related to pressure (in degrees)
TW	warm end temperature (dummy in present version)
WREG1	wall thickness of first stage regenerator tube
WREG2	wall thickness of second stage regenerator tube
TOL	accuracy parameter for solving the differential equations with DIVPAG
Line 4 and 5:	Comments
Line 6 to 25:	
'……'	Name of segment (must be filled up to 20 spaces)
Length	length of the section
totalAr	total cross sectional area (input or calculated from radius b and wall thickness bs for circular ducts if totalAr= - 1)
b	hydraulic radius of tubes or of porous material segments
bs	wall thickness of " " "
DeltaE	Change of gas enthalpy flow at the inlet of a segment
JMAT	parameter of material from CRYOCOMP and/or evaluated from additional sub-routines (see Appendix C)
MSTEP	number of lines in output
FRF	Flow Resistance Factor (enhancement compared to laminar flow) (in later codes (from 021010) this is an empirical correction factor)
CDF	Conductivity Degradation Factor
A/I	Switch for setting the section either to 'adiabatic' (a) or to 'isothermal' (i) condition.

Lines 26 to 28:	
'Volumflow st1/st2 '	Fraction of volume flow branching into PT 1
'rel. dc-flow in PT1'	Ratio of DC volume flow in PT1 to amplitude of flow at inlet of segment 1
'rel. dc-flow in PT1'	Ratio of DC volume flow in PT2 to amplitude of flow at inlet of segment 1

Line 29:	Comment
Line 30 and 31:	Parameters of GM type compressor
'Swept volume, m^3 '	Swept volume of capsule
'Frequency of grid '	Rotational frequency of capsule (Hz)
Line 32:	
'He-Condensation '	Mass flow of Helium gas to be condensed by thermal contact to

	regenerators and both cold stages
Line 33:	
'Zyklus,j=1, n=0 '	Calculates pressure, p(t), volume flow, U(t), and work flow, p*U, at the hot ends of regenerator and both pulse tubes
Line 34 to 36:	
'List of suppl. var.':	1 (yes) means that the temperature swing in regenerators are calculated and, and additional variable are written into Matrix V(i) (see Table 8.2.1)
'Variable in col. 10 ':	Number(0<I<23) of variable Vi) written in column 10
'Variable in col. 11 ':	Number (0<I<23) of variable V(i) written in column 11
Lines > 36:	Comments, copies of other input files